ADA 286281

[illegible] study of recently deposited organic matter in sediments of the Santa Barbara Basin

[illegible] Hedges, Katherine H. Freeman and Timothy R. Filley

Department of Geosciences
The Pennsylvania State University

Final report submitted to the Naval Research Laboratories for work performed under Grant No. N00014-92-1-G906

PENNSTATE

College of Earth and Mineral Sciences

REPORT DOCUMENTATION PAGE

Form Approved
OBM No. 0704-0188

1. Agency Use Only *(Leave blank).*	2. Report Date.	3. Report Type and Dates Covered.
	September 1993	Contractor Report

4. Title and Subtitle.
Results from a Study of Recently Deposited Organic Matter in Sediments of the Santa Barbara Basin

5. Funding Numbers.

Program Element No.	061153N
Project No.	3204, 3205
Task No.	030, 0101
Accession No.	DN252108
Work Unit No.	(74) 5140

6. Author(s).
Patrick G. Hatcher, Kathering H. Freeman and Tiimothy R.Filley

7. Performing Organization Name(s) and Address(es).
Pennsylvania State University
Department of Geosciences
201 Willard Building
University Park, Pa 16802-2801

8. Performing Organization Report Number.

9. Sponsoring/Monitoring Agency Name(s) and Address(es).
Naval Research Laboratory
Marine Geosciences Division
Stennis Space Center, MS 39529-5004.

10. Sponsoring/Monitoring Agency Report Number.
NRL/CR/7430--94-0014

11. Supplementary Notes.

12a. Distribution/Availability Statement.
Approved for public release; distribution is unlimited.

12b. Distribution Code.

13. Abstract *(Maximum 200 words).*

Presents a detailed organic geochemical investigation of the core sections which involves analysis of both the bulk sediment and the lipid extracts of the sediment. To date, these are the most comprehensive analyses performed on sediments from the Santa Barbara Basin.

14. Subject Terms.
Marine Sediment Diagenesis, Microstructure, Clays, Physical Properties

15. Number of Pages.
72

16. Price Code.

17. Security Classification of Report.	18. Security Classification of This Page.	19. Security Classification of Abstract.	20. Limitation of Abstract.
Unclassified	Unclassified	Unclassified	SAR

Results from a study of recently deposited organic matter in sediments of the Santa Barbara Basin

Patrick G. Hatcher, Katherine H. Freeman and Timothy R. Filley

Department of Geosciences
The Pennsylvania State University

Final report submitted to the Naval Research Laboratories for work performed under Grant No. N00014-93-1-G906

Introduction

A small diameter subcore of a larger box core collected from the Santa Barbara Basin (Lat. 34° 13.53' N, Long. 120° 03.51' W) yielded samples from which organic geochemical studies were conducted. The samples were obtained under a blanket of nitrogen at approximate intervals of 2 cm. The intervals were 0-2, 2-4, 4-6, 8-10, 10-12, and 14-18.5 cm. The isolated samples were subjected to a detailed analytical scheme shown in Figure 1 to characterize the organic matter in the upper sedimentary layers of the basin. The explicit goal of this project was to examine downcore changes in the nature of the organic matter in order to delineate changes which might be ascribed to early diagenesis and to relate these diagenetic changes to sediment physical properties and clay microfabric. The results presented below demonstrate a detailed organic geochemical investigation of the core sections which involves analysis of both the bulk sediment and the lipid extracts of the sediment. To date, these are the most comprehensive analyses performed on sediments from the Santa Barabara Basin. We herein describe and interpret the results of our study with the eventual goal of combining the conclusions obtained with the sediment physical properties being obtained by Dr. Richard Bennett of the Naval Research Laboratories. The eventual product will be a joint paper or papers detailing the results of this interdisciplinary study.

Carbon analysis

The dried sediment samples were subjected to total and organic carbon analysis and the results are presented in Table 1. The difference between total and organic carbon represents the inorganic carbon or carbonate carbon, mostly calcium carbonate listed in Table 1 as a % calcium carbonate carbon. One can immediately observe that the sediments from the Santa Barbara Basin are rich in organic carbon with values ranging from 2.88 to 3.88%. There doesn't appear to be a definite trend with increasing depth in the core, probably due to the fact that most of the carbon is fairly refractory or that diagenesis is occurring at too slow a rate to induce significant changes over the entire depth of core studied. One might expect at least a 50% decrease in carbon content if diagenetic alteration of freshly deposited material were substantial. Based on the data presented below, it is clear that the former explanation-that most of the carbon is refractory terrestrially-derived carbon-is the more valid conclusion. Accordingly, the variations one might observe in carbon content or the concentration of individual compounds will be mostly due to variations in source inputs. Schimmelmann and Tegner (1991) have alternatively suggested on the basis of carbon isotope data that the California margin receives significant input from phytoplankton biomass and that this may be the dominant source of carbon to the sediment in the Santa Barbara Basin. We are at odds with this conclusion and suggest that the dominant source of carbon is from refractory terrestrial runoff.

NMR data

Figures 2 and 3 show the solid-state ^{13}C NMR spectra of raw extracted and dried sediment samples listed as a function of increasing depth. All spectra appear to be very similar, indicative of the fact that the bulk of the organic matter is rather uniform with depth over the interval examined (0-18.5 cm). This is very surprising for a sediment having such a high input of organic matter. We know that anoxic conditions are established at or near the sediment/water interface due to the fact that bottom waters are nearly anoxic themselves. Thus, one might argue that the invariant nature of the NMR data would be consistent with there being little or no degradation of the organic matter over the interval studied. However, the lack of significantly intense peaks for carbohydrates in the region between 60 and 100

ppm indicates that the organic matter has undergone a substantial amount of degradation, perhaps prior to sedimentation.

The poor signal-to-noise and the broad overlap of signals precludes accurate quantification of the various regions. However, several qualitative observations can be made. The most striking and significant aspects of the NMR data are the intense signals between 100 and 160 ppm. These are due to aromatic carbons. The most like source of aromatic carbon in modern sediments is from lignin and degraded lignin as would be found in soils and other terrestrial deposits such as peat. Thus, the intense signals betray a significant and perhaps dominant contribution from terrestrial carbon sources. That lignin is a major contributor is also substantiated by the presence of a peak at 55 ppm, the peak attributable almost exclusively to methoxyl carbons in lignin, and from the pyrolysis data discussed below showing the presence of lignin-derived compounds. Such a large contribution from terrestrial carbon is unexpected for these sediments, where others have proposed a predominantly marine source based on lipid extracts and stable carbon isotopes of the total organic matter (Schimmelmann and Tegner, 1991). Had there been a predominant source of marine carbon, the NMR spectra would have shown much more aliphatic alkyl carbon (0-50 ppm).

The presence of a peak at 175 ppm indicates that these samples contain a significant amount of carboxyl functionality, perhaps inherited from oxidized lignin components as would be found in peat or soil. This bit of information, combined with the fact noted above that carbohydrate carbons are minor components suggests that the major portion of the organic matter in these sediments was derived from vascular plant material, oxidatively degraded in the water column or subaerially, and transported and deposited within the anoxic sedimentary regime. Once buried under anaerobic conditions, degradation of the terrestrial organic matter generally ceased, thereby accounting for the invariant NMR signature in the vertical profile.

Terrestrial materials present in such large amounts in a marine sediment are unusual in the modern environment where one might expect the dominant contributors to be planktonic algae. From studies of numerous algal-dominated marine sediments by NMR, the predominant chemical structures of the bulk carbon are clearly aliphatic. It is only deposits of terrestrial plants, usually nonmarine, which provide such clear predominances of aromatic carbons. Once buried and subjected to maturation over extended periods of geological time, the highly aromatic organic matter will likely be transformed to a type III kerogen.

Flash pyrolysis/gc/ms

Whole sediment samples were subjected to flash pyrolysis/gc/ms to examine molecular components of the macromolecular organic matter. Pyrolyzed fragments of larger macromolecules provide information regarding the monmeric units comprising the bulk organic matter and allows reconstruction of the macromolecular framework.

Figures 4-10 show the seven total ion chromatograms (TIC) obtained from the raw sediment samples along with specific ion chromatograms (SIC) representing lignin-derived compounds (m/z 94, 108, 122, 124, 138). The complexities of each pyrogram reveal that a significant amount of effort will be required to unravel the structure of the material. Most of the peaks appear to be present in the early eluting part of the pyrogram. Benzene and its alkylated homologs as well as phenol and its alkylated homologs constitute a significant fraction of the total intensity. Lignin-derived pyrolysis fragments could be detected, but only as small contributors, surprising considering the observation of a peak for methoxyl carbons in the NMR spectra. It is possible that the lignin phenols are highly oxidized and do not yield pyrolysis fragments other than the simple phenols. The presence of phenols and alkylated homologs could be the only remnants of lignin-derived structures, perhaps from grass lignins known to be enriched in *p*-hydroxyphenols as monomeric units. The alkyl benzenes are possible from multiple sources but have been detected in soil organic

matter and kerogen or coal. Pyridine, pyrroles and indoles are also detected. These are probably derived from chlorophyll pigments and other nitrogen-containing substances of a likely dual source-aquatic and terrestrial. A single ion chromatogram trace for alkanes (m/z 57) shows only alkanes in the carbon number range less than 20 with no clear pattern. Both normal and branched homologs are present. There appears to be a general lack of long chain polymethylenic material as evidenced by the lack of an homologous series of n-alkanes and n-alkenes extending to n-C32. These substances are usually characteristic of contributions from leaf epicuticular material or algae.

There appear to be few significant changes in the pyrolysis data as a function of depth in the core. It is difficult to ascertain whether some small changes in relative intensities of some peaks are significant. Based on this observation of invariance with depth, we can conclude that the sedimentary organic matter does not show a great deal of change which might betray diagenetic changes. Alternatively, the pyrolysis data are insensitive to diagenetic alteration of the small magnitude encountered in this core. A similar observation was made above with the NMR data.

Extractable Lipids

Methods

Sediment samples were extracted by standard methods. Specifically, the sediment was Soxhlet extracted for 24-36 hours using a 2:1 azeotrope of methanol and dichloromethane. The extracted residue was preserved for NMR and Py-GCMS analysis discussed above. The extract was saponified under basic conditions, and then partitioned into acid and neutral fractions. Four fractions were isolated from the neutral fraction by column chromatography using 8 g silica gel, deactivated by 5% (by weight) with water. Hydrocarbons were eluted with 40 mL hexane, ketones were eluted with 20 mL 5% + 20 mL 10% ethylacetate in hexane and 20 mL 15% + 20 mL 20% ethylacetate in hexane was used to elute the sterol fraction. More polar components were removed with 100% methanol, and saved for future analyses.

Quantitation of the components in these three neutral fractions was accomplished (via co-injected standards) using a Hewlett-Packard GC equipped with an on-column injector, an HP Ultra-1 column (50 m x 0.21mm i.d.) with a cross-linked silicone phase, and a flame ionization detector (FID). Select samples were also run on a Kratos GC-MS for compound identification. Identifications were determined by comparison of our mass spectra with previously published spectra and by comparisons with the NIST/Wiley library of mass spectra. Isotopic analyses of select individual compounds were made using a Finnigan MAT 251 isotope-ratio-monitoring mass spectrometer equipped with a GC-combustion interface.

Results

Saturated hydrocarbon fraction- Chromatograms for each interval analyzed for saturated hydrocarbons are presented in Figures 11-17 and the concentrations of individual hydrocarbons are given in Table 2. In all compound classes, qualitative and quantitative differences are observed down the depth of the core. In the hydrocarbon fractions, the n-alkanes range from n-C22 to n-C32 and are dominated by n-C29 and n-C31. These compounds are generally considered indicators of terrestrial organic matter, since they are abundant components of leaf epicuticular waxes. Also apparent in the chromatograms are two broad unresolved regions in the retention time ranges of 28-40 min. and 40-55 min. containing a complex mixture of peaks which co-elute. Oil-contaminated sediments even from nearby basins of the southern California Bight typically show intense unresolved regions (Venkatesan, et al., 1980). No doubt oil contamination from spillage and natural seeps in the area could contribute to the hydrocarbons observed. The extent of such

contamination is not great however in comparison with well-known oil-contaminated sediments.

Examination of the down-core distributions of each individual n-alkane indicates significant variations (Figures 18-28). Most notable is a persistent increase in the concentration of all n-alkanes from the 0-2 cm interval down to the 4-6 cm interval, following which a dramatic decrease in concentration is observed. Another increase is observed at the 10-12 cm interval. The observed large fluctuations are highly indicative of varying inputs of terrestrial material, considering the fact that the n-alkane distributions are predominantly of a terrestrial nature. Thus we can conclude that fluctuations in the n-alkanes are controlled primarily by varying inputs of terrestrial material which overshadow changes in alkane distributions due to diagenesis.

Perhaps the one most distinguishing feature of terrestrially-derived n-alkanes is the predominance of odd-carbon number alkanes over the even ones. The "odd-carbon" dominance of the n-alkanes is typically quantified using a simplified carbon-preference index (CPI) or abundance ratio, which is defined as the ratio of the sum of odd n-alkanes divided by the sum of all even n-alkanes. Figure 29 shows the down-core trend in CPI. Aside from the low CPI value observed at the 2-4 cm interval, a gradually decreasing trend is observed. At the surface a high CPI is typical of terrestrially-derived material whereas at deeper intervals in the core the CPI is more typical of microbially-derived material or petroleum-derived material having CPI values approaching 1.

Fatty acids- The fatty acid fractions were analyzed and the chromatograms are shown in Figures 30 through 35 and concentrations listed in Table 3. All fractions appear to have a similar series of fatty acid methyl esters (FAME) with palmitic acid methyl ester (C16:0) as the dominant FAME. This FAME is fairly ubiquitous in all sedimentary systems. Lesser quantities of the other saturated FAMES ranging from C14 to C28 are present. The even carbon-numbered fatty acids dominate over the odd carbon-numbered ones. Also apparent are the unsaturated FAMES, notably the C18:1 and C16:1. Branched-chain FAMES, notably the C15 ones are indicative of microbial inputs.

Down-core distributions of individual FAMES are shown in Figures 36-40. The microbially-derived branched-chain C15 FAMES, iso and anteiso C15, show a similar profile, increasing to a depth of 2-4 cm, remaining constant to a depth of 8-10 cm, and then dramatically decreasing. This distribution is perhaps indicative of the increased microbiological activity at mid-depth in the core. The C16:0 and C16:1 FAMES show a similar trend. The terrestrially-derived FAMES, notably the C24:0 (Figure 40) and higher homologs, show a different distribution which is more indicative of varying source inputs and parallels the distribution observed for terrestrial n-alkanes discussed above. Peaks in the concentrations at the 4-6 cm interval and the 8-10 cm interval are perhaps indicative of greater inputs of terrestrial materials at the point in time of deposition. A ratio of the concentration of C24 FAME to C16 FAME (Figure 41) also appears to parallel the trend observed for alkanes. This ratio can be used to reflect the relative contribution of terrestrial material.

It is clear that the FAME distributions within the core are reflecting the varying inputs of terrestrial material, overshadowing diagenetic transitions. Since we might expect diagenetic trends to mainly involve loss of unsaturated FAMES relative to the saturated ones, we calculated the ratio of C16:0 to C16:1 and found the value to be invariant with depth. This is perhaps indicative of the fact that diagenetic alteration of FAMES is not occurring over the intervals analyzed.

Alcohols- The alcohols represent the most abundant lipid class within the core. The most striking observation from this fraction is the variation in dominance between phytoplankton derived sterols and phytol and terrestrial derived higher molecular weight straight chain alcohols (Figures 42-48). Phytol, derived from the hydrolysis of the chlorophyl side chain, is the alcohol of greatest concentration for each depth (Table 4). The

intervals of 4-6 cm and 10-12 cm are however, devoid of all steroidal compounds except the dinoflagellate derived dinosterol. High molecular weight, straight chain alcohols dominate the chromatograms from these depths. C24 through C30 alcohols are thought to be sourced in terrestrially derived cuticular waxes. Cholesterol and brassicasterol are major components in 6-8 cm, 8-10 cm and 14-18 cm. The selective preservation of dinosterol within the intervals dominated by terrestrial based alcohols is not surprising as the 4-methyl sterol is known to be a highly refractory moiety as it has been shown to be quite resistant to ingestion by copepods.

Ketones- Ketone fractions (Figures 49-55 , Table 5) from samples from 0-2 cm, 2-4 cm, 6-8 cm, 8-10 cm and 14-18 cm contain abundant long-chain, unsaturated methylketones ("alkenones"). These compounds are derived from prymnesiophyte algae (such as *Emiliani huxleyi*) and the relative abundance of the tri- and diunsaturated C37 alkenones can be used to reconstruct ancient sea-surface temperatures. A high-resolution study of alkenones in Santa Barbara basin sediments was recently completed by J. Kennedy (currently a post-doctoral associate working with Simon Brassell).

Alkenones abundances are low (or not detected) in samples from 4-6 cm and 10-12 cm, indicating prymnesiophytes were not major contributors to the sedimentary organic matter at these depths. All ketonic moieties, in fact, are absent from these intervals. Notably, steroidal ketones, the diagenetically oxidized analogues of sterols, do not exist in these intervals. The sterol concentrations are also significantly lower and, in general, preservation of phytoplankton-derived organic matter is apparently reduced at these horizons. The complete absence of these compounds suggests that environmental conditions may heve been such that the more labile species were completely mineralized from these depths. These horizons may then represent times of more oxidative conditions, a change that should be accompanied by decreased sulfur and organic carbon content. It is interesting to note that proxies for bacterial input, iso and and anteiso C15:0 FAMES as well as those for terrestrial input, C24 and C26 alcohols, C29 and C31 n-alkanes and C24 FAMES, all increase dramatically as the ketones and sterols are removed. Such an inverse relationship in the molecular markers for phytoplankton and terrestrial matter may suggest a dilution of the normal basin sediments with extrabasinal sediments, rich in terrestrial matter.

Compound-Specific Isotopic Abundances

The alcohol fractions contained the greatest abundance, and all of these samples were analyzed for the $\delta^{13}C$ of individual components. The fractions containing sterols were also isotopically analyzed, but because chromatographic difficulties (co-elution limits our ability to attain accurate and precise isotopic values), we are only presenting data for cholesterol and its unsaturated isomer, cholestanol. In addition, normal-alkanes from the sample from 2-4 cm were isolated from the hydrocarbon fraction by clathration with urea crystals. Straight chain compounds are adducted within the crystals and branched and cyclic compounds are removed in the solvent phase. The n-alkanes are subsequently released when the urea is dissolved in methanol. This procedure removes the unresolved complex mixture of compounds in the hydrocarbon fraction, and the $\delta^{13}C$ values are readily determined for the remaining alkanes which are free from co-eluting constituents. The results of the analyses of alkanes are presented in Table 6.

The aliphatic alcohols n-C24 and n-C26, cholesterol and phytol were analyzed for isotopic abundance in all sample horizons. In order to prepare alcohols for separation by gas chromatography, they were first derivatized by replacing the proton on the alcohol

group with trimethyl siloxane (TMS). As a result, three carbon atoms are added to each structure and the measured $\delta^{13}C$ value must be corrected for their isotopic abundance. To evaluate the $\delta^{13}C$ of the added carbons, we determined the isotopic composition of androstanol and androstanol-TMS, and then used the isotopic mass balance equation to estimate the $\delta^{13}C$ of the TMS carbon atoms:

$$\delta_{total} n_{total} = n_{TMS}\,\delta_{TMS} + n_{andr}\,\delta_{andr}$$

Where δ_{total} represents the isotopic composition (expressed relative to the standard PDB) measured for androstanol-TMS and δ_{andr} represents the $\delta^{13}C$ of androstanol. The number of carbons are represented by n, and $n_{TMS} = 3$, $n_{andro} = 20$ and $n_{total} = 23$. The value for TMS is then used to correct the measured values for the sample alcohols, and it is these values that included in this report (Table 7). Estimates of error are propagated for these calculations using standard methods and are reported along with the isotopic values.

Algal inputs to the sedimentary organic matter are represented by phytol, the major constituent in the alcohol fractions. The isotopic composition of this compound is consistent with an algal origin, and ranges from -21 to -22.2 per mil. The $\delta^{13}C$ values vary with depth, with the highest values in the surface and 8-10 cm fractions (Figure 56). Slightly lower values are found in the 2-4, 4-6 and 6-8 cm samples. Likewise, the isotopic composition of cholesterol tracks that of phytol, indicating that cholesterol which is ubiquitous in marine organisms is dominated by phytoplankton sources.

The variations of about 1 permil in cholesterol and phytol may derive from several possible processes related to the conditions under which primary photosynthate was produced. Because of the draw-down of CO_2(aq) in seawater during very high rates of phytoplankton growth, isotopic enrichment in algal biomass is associated with high levels of productivity. Thus the enrichment in the upper and lower samples may represent times of increased algal productivity, consistent with the changes in % organic carbon over these intervals. Alternatively, the $\delta^{13}C$ of CO_2(aq) can decrease as a result of inputs of isotopically depleted inorganic carbon during upwelling events, which may account for the depletion in phytol in the 2 to 8 cm section of the core (Table 4). A shift in the dominant phytoplankton population from organisms which can assimilate HCO_3^- to those that do not, will also produce a decrease the $\delta^{13}C$ in algal biomass.

We note that the abundance of brassicasterol is high in the surface samples and in the 6-8 and 8-10 cm horizons (Table 4), approximately the same depths in which isotopic enrichment is observed. Although brassicasterol can come from prymnesiophytes, it is usually considered a marker for inputs from diatoms. Many diatoms are capable of HCO_3^- assimilation, and thus the association of higher $\delta^{13}C$ for phytol with increased brassicasterol abundances points to a phytoplankton population shift as the underlying cause for the enrichment. However, since the % organic carbon and other phytoplankton biomarkers such as alkenones (markers for prymnesiophytes), cholesterol and dinosterol (a marker for dinoflagellates) also increase in the same samples as does brassicasterol (Table 4), we suggest the isotopic enrichment in phytol represents an increase in paleoproductivity.

The isotopic composition of the terrestrial inputs to the Santa Barbara Basin sediment can be determine from high molecular weight, odd-carbon numbered normal-

alkanes (Figure 57). In the 2-4 cm fraction the n-alkanes C27 and C29 are isotopic depleted relative to the shorter chain compounds (C20 through C26), and their $\delta^{13}C$ values are consistent with the lower values observed for waxes from modern tree leaves (i.e., Reiley et al., 1991). These isotopic data are largely consistent with the odd/even abundances discussed above, and indicate a terrestrial origin for n-C27 and n-C29. However, the isotopic composition of n-C25 is greater than that of C27 and C29, and is similar to the lower molecular weight compounds (both odd and even). Since its isotopic composition indicates a non-terrestrial origin, n-C25 apparently is not a good marker for terrestrial inputs to sedimentary organic matter.

The isotopic composition of the long-chain alcohols (Figure 58) indicate disparate origins for the 24 and 26-carbon alcohols. They both have values about 10 per mil lower than phytol and cholesterol (-31 vs. -21 per mil) and clearly are not derived from algal sources. The low $\delta^{13}C$ of the C26 alcohol is similar to that of the long-chain odd n-alkanes (C27 and C29), and derives from a terrestrial source. In contrast, the $\delta^{13}C$ of the C24 alcohol increases over 3 per mil with depth. The origin of this compound is not readily apparent from this data, but it may represent a mixture of terrestrial and bacterial contributions.

In summary, the compound-specific isotope data indicate both terrestrial and algal components are important constituent of the neutral lipid fraction. The isotopic variations of phytoplankton derived compounds varies about 1 per mil throughout the sampled interval, indicating the changes in lipid abundances represent variations in productivity, and not changes in the phytoplankton populations. The isotopic compositions of both alcohols and alkanes are largely consistent with their respective algal or terrestrial sources. Exceptions include n-C25 alkane and C24 alcohol, both of which appear to derive at least in part from a non-terrestrial, possibly bacterial source.

Conclusions

The organic geochemical data presented for the seven intervals of the core taken from the Santa Barbara Basin all seem to present a consistent picture of a sediment dominated by inputs of organic matter derived chiefly from terrestrial sources. The bulk analyses (NMR and pyrolysis/gc/ms) show a dominant input from terrestrial carbon which contrasts greatly with the belief that marine phytoplankton is the dominant source. This view proposed by Schimmelmann and Tegner (1991) is based on carbon isotope compositions of the total organic matter which shows $\delta^{13}C$ values of about -23 per mil. Our data clearly indicate a terrestrial source for the bulk organic carbon. The lipid extract data are consistent with this conclusion, even though some markers for phytoplankton can be discerned (e.g., phytol, dinosterol, cholesterol, etc.). However, the dominant lipid components appear to be from terrestrial carbon sources, a finding which justifies publication. A paper is currently being prepared for publication of this information in the scientific literature.

Our attempts to discern diagenetic changes which might be correlated with physical properties of the sediments being performed by Dr. Richard Bennett, Naval Research Laboratories, Stennis Space Center, were unsuccessful. This is due in large part to the large variations observed in the types of terrestrial carbon being supplied to the sediment and to the fact that it is likely that terrestrial carbon being supplied to the sediment has probably experienced multiple cycles of deposition and is thus fairly refractory to diagenetic alteration which can be detected by the methods used. Schimmelman and Kastner (1993) similarly observed large fluctuations in bulk chemical properties indicative of fluctuations caused by water column productivity, particle flux to the sediment and bottom water

oxygenation. In addition, turbidite units present within the core appear at irregular intervals and deposit predominantly terrestrial material.

Another interesting finding is the excellent correlation of the isotopic composition of phytol and cholesterol. The covariation is indicative of these two compounds having a similar source. The excursions in the values as a function of depth are indicative of changes in paleoproductivity of algae.

Suggestions for Future Work

Numerous studies have shown that sulfides interact with functionalized lipids in recent sediments to form sulfur-bound lipids during early diagenesis (see Figure 59). It has been hypothesized that during early diagenesis, in sulfide-rich sedimentary environments, an increasing amount of macromolecular organic matter can be generated by the crosslinking of reactive lipids within the sediments by sulfides (Sinninghe Damste et al., 1989; Kohnen et al, 1991). Such a process, if it could amount to an appreciable sink for what would normally be easily biodegraded matter, might alter the bulk physical properties of the sediment, i.e. shear strength, plasticity, long term preservation capacity, etc. The sediments from Santa Barbara Basin have been shown to contain large amounts of organically-bound sulfides (Schimmelmann and Kastner, 1993) and offers an ideal site to test the role of sulfide vulcanization. As the results from the lipids, pyrolysis and NMR studies failed to yield obvious indications of early diagenetic alterations that might affect the bulk geotechnical properties of the Santa Barbara sediments within the upper 20 cm., we engaged in additional preliminary work to define the possible role of organic sulfides in the vulcanization of the sediments.

Figure 60 shows the protocol employed in the analysis of sulfide-bound lipids within the total lipid extract. A split of the TLE was separated into neutrals and polars by column chromatography. The macromolecular polars were then reacted with Raney nickel catalyst to cleave all carbon-sulfur linkages. This procedure removes the crosslinking sulfides and releases the previously bound lipid for analysis. Three representative chromatograms are shown in Figure 61, depicting released hydrocarbons from 0-2 cm., 6-8 cm., and 10-12 cm. Phytane and phytenes are the dominant components released. With increasing depth the sediments also yield a suite of n-alkanes and steranes. The released phytane and phytenes are derived from interaction of diagenetically altered phytol with pore water sulfides. Recall that phytol was the dominant lipid present within the sediments from the Santa Barbara Basin core. Figures 62 and 63 show the concentration profile with depth of Raney nickel released phytane and free phytol from the total lipid extract, respectively. It is interesting to note that phytol shows a maximum where phytane is at a minimum. This suggests that the conditions that resulted in the anomalous behavior for the lipids at depths 4-6 and 10-12 cm., evidenced by the increase in terrestrial sourced lipids and loss of marine molecular markers, also affected the vulcanization process in a negative fashion.

It is obvious that vulcanization is an important process which binds lipids to the sedimentary organic matter. Future studies should be directed towards a more comprehensive understanding of this vulcanizations process, one that very likely plays a major role in modifying the distributions of lipids in sedimentary profiles but also could play a huge role in modulating sediment physical characteristics. Other than identifying lipids bound to a macromolecular phase of the sediment, emphasis should be placed in identifying sulfur-linked macromolecules in more complex macromolecular materials extracted by more severe extraction techniques as proposed by Kohnen et al. (1991).

References

Kohnen, M.E.L., Sinninghe Damste, J.S., Kock-Van Dalen, JA.C., de Leeuw, J.W., (1991), Di- or poylsulfide-bound biomarkers in sulfur-rich geomacromolecules as revealed by selective chemolysis, *Geochim. Cosmochim. Acta*, v. 55, p. 1375-1394.

Schimmelmann, A. and Kastner, M. (1993) Evolutionary changes over the last 1000 years of reduced sulfur phases and organic carbon in varied sediments of the Santa Barbara Basin, California., *Geochim .Cosmochim. Acta*, v. 57, p. 67-78

Schimmelmann, A. and Tegner, M. J. (1991) Historical oceanographic events reflected in the $^{13}C/^{12}C$ ratio of total organic carbon in laminated Santa Barbara Basin sediment. *Global Biogeochemical Cycles*, v. 5, p. 173-188.

Sinninghe Damste, J.S., Rijpstra, W.I.C., Kock-Van Dalen, A.C., de Leeuw, J.W. and Schenk, P.A., (1989), Quenching of labile functionalized lipids by inorganic sulfur species: Evidence for the formation of sedimentary organic sulfur compounds at the early stages of diagenesis, *Geochim. jCosmochim. Acta*, v. 53, p. 1443-1455.

Venkatesan, M. I., Brenner, S., Ruth, E., Bonilla, J. and Kaplan, I. R. (1980) Hydrocarbons in age-dated sediment cores from two basins in the Southern California Bight. *Geochim. Cosmochim. Acta*, v. 44, p. 789-802.

Table 1. Total carbon, carbonate and organic carbon concentrations in the Santa Barbara Basin sediment core.

Depth (cm)	% Total carbon	%$CaCO_3$-carbon	% Organic Carbon
0-2	4.86	1.03	3.83
2-4	4.79	0.97	3.82
4-6	4.20	0.92	3.28
6-8	4.87	1.11	3.76
8-10	4.54	1.06	3.48
10-12	4.64	1.13	2.88
12-14	4.36	1.07	3.29
14-18.5	4.36	1.10	3.35

Table 2. Concentrations of n-alkanes in the total lipid extract (TLE) also reported as ng/gram of wet sediment from various intervals in the Santa Barbara Basin core.

Hydrocarbons Quantified in SBB sediment	n-Alkane	ng in TLE	ng/ gram wet sed. wt
0-2 cm	C22	1.25	0.19
	C23	1.53	0.23
	C24	1.36	0.20
	C25	1.93	0.29
	C26	1.55	0.23
	C27	5.42	0.80
	C28	2.42	0.36
	C29	13.43	1.99
	C30	1.93	0.29
	C31	13.33	1.97
	C32	1.54	0.23
2-4 cm.	C22	16.33	0.58
	C23	20.79	0.73
	C24	19.67	0.69
	C25	20.47	0.72
	C26	13.91	0.49
	C27	21.10	0.74
	C28	14.21	0.50
	C29	45.91	1.62
	C30	12.54	0.44
	C31	38.45	1.35
	C32	8.03	0.28
4-6 cm.	C22	74.34	2.61
	C23	82.59	2.90
	C24	67.22	2.36
	C25	76.04	2.67
	C26	39.12	1.38
	C27	90.86	3.20
	C28	31.07	1.09
	C29	237.17	8.34
	C30	21.60	0.76
	C31	183.72	6.46
	C32	19.52	0.69
6-8 cm.	C22	5.33	0.15
	C23	7.88	0.23
	C24	5.48	0.16
	C25	10.02	0.29
	C26	8.08	0.23
	C27	18.09	0.52
	C28	17.33	0.50
	C29	65.89	1.91
	C30	17.92	0.52
	C31	51.01	1.48
	C32	7.57	0.22

Hydrocarbons Quantified in SBB sediment	n-Alkane	ng in TLE	ng/ gram wet sed. wt
8-10 cm	C22	4.84	0.14
	C23	6.15	0.17
	C24	5.57	0.16
	C25	7.23	0.20
	C26	5.09	0.14
	C27	12.00	0.34
	C28	13.78	0.39
	C29	29.45	0.83
	C30	7.21	0.20
	C31	33.17	0.94
	C32	4.88	0.14
10-12 cm.	C22	24.89	0.67
	C23	42.53	1.15
	C24	45.56	1.23
	C25	63.53	1.71
	C26	62.79	1.69
	C27	115.87	3.12
	C28	118.60	3.20
	C29	273.19	7.37
	C30	86.11	2.32
	C31	245.76	6.63
	C32	66.20	1.78
14-18 cm.	C22	4.77	0.07
	C23	6.73	0.10
	C24	7.40	0.11
	C25	8.42	0.12
	C26	6.74	0.10
	C27	6.13	0.09
	C28	4.29	0.06
	C29	8.55	0.13
	C30	1.98	0.03
	C31	6.05	0.09
	C32	1.34	0.02

Table 3. Concentrations of fatty acid methyl esters (FAMES) in the total lipid extract (TLE) also reported as ng/gram of wet sediment from various intervals in the Santa Barbara Basin core.

FAMES in SBB Sediments		ng in T.L.E.	ng/ gram wet sed. wt
0-2cm	IsoC15:0	43.49	6.43
	AnteisoC15:0	28.36	4.20
	C16:1	144.10	21.31
	C16:0	393.33	58.18
	C24:0	87.88	13.00
2-4cm	IsoC15:0	100.00	3.52
	anteisoC15:0	55.52	1.96
	C16:1	180.97	6.37
	C16:0	673.27	23.71
	C24:0	101.79	3.59
4-6cm	IsoC15:0	101.29	3.56
	anteisoC15:0	59.98	2.11
	C16:1	205.34	7.22
	C16:0	869.92	30.59
	C24:0	336.15	11.82
6-8cm	Iso C15:0	99.08	2.87
	anteiso C15:0	54.60	1.58
	C16:1	213.35	6.19
	C16:0	677.67	19.65
	C24:0	131.92	3.83
8-10cm	Iso C15:0	117.17	3.32
	anteiso C15:0	62.22	1.76
	C16:1	247.35	7.01
	C16:0	1072.03	30.39
	C24:0	305.76	8.67
10-12cm	Iso C15:0	38.03	1.03
	anteiso C15:0	19.78	0.53
	C16:1	132.77	3.58
	C16:0	568.17	15.32
	C24:0	211.03	5.69
14-18cm	Iso C15:0	41.91	0.62
	anteiso C15:0	16.06	0.24
	C16:1	66.45	0.98
	C16:0	178.63	2.63
	C24:0	50.12	0.74

Table 4. Concentrations of selected alcohols in the total lipid extract (TLE) also reported as ng/gram of wet sediment from various intervals in the Santa Barbara Basin core.

Dominant Alcohols in SBB Sediment		ng in T.L.E.	ng/ gram wet sed. wt.
0-2cm	phytol	410.57	60.73
	n-C24-ol	59.61	8.82
	n-C26-ol	34.58	5.11
	cholesterol	112.05	16.57
	cholestanol	54.43	8.05
	brassicasterol	89.48	13.24
	brassicastanol	60.26	8.91
	dinosterol	86.69	12.82
2-4cm	phytol	500.47	17.63
	n-C24-ol	78.02	2.75
	n-C26-ol	47.73	1.68
	cholesterol	127.65	4.50
	cholestanol	60.85	2.14
	brassicasterol	111.56	3.93
	brassicastanol	62.23	2.19
	dinosterol	109.46	3.86
4-6cm	phytol	1514.03	53.24
	n-C24-ol	160.11	5.63
	n-C26-ol	84.79	2.98
	cholesterol	TRACE	TRACE
	cholestanol	TRACE	TRACE
	brassicasterol	TRACE	TRACE
	brassicastanol	TRACE	TRACE
	dinosterol	283.98	9.99
6-8cm	phytol	999.62	28.99
	n-C24-ol	43.57	1.26
	n-C26-ol	40.11	1.16
	cholesterol	191.63	5.56
	cholestanol	79.65	2.31
	brassicasterol	179.27	5.20
	brassicastanol	69.60	2.02
	dinosterol	157.05	4.55
8-10cm	phytol	830.34	23.54
	n-C24-ol	56.30	1.60
	n-C26-ol	31.32	0.89
	cholesterol	252.22	7.15
	cholestanol	102.51	2.91
	brassicasterol	209.74	5.95
	brassicastanol	87.62	2.48
	dinosterol	203.03	5.75
10-12cm	phytol	500.86	13.50
	n-C24-ol	54.65	1.47
	n-C26-ol	24.46	0.66
	cholesterol	4.61	0.12
	cholestanol	12.21	0.33
	brassicasterol	0.98	0.03
	brassicastanol	2.18	0.06
	dinosterol	118.59	3.20
14-18cm	phytol	234.51	3.45
	n-C24-ol	25.40	0.37
	n-C26-ol	11.95	0.18
	cholesterol	81.46	1.20
	cholestanol	47.71	0.70
	brassicasterol	75.65	1.11
	brassicastanol	36.54	0.54
	dinosterol	89.77	1.32

Table 5. Concentrations of alkenones in the total lipid extract (TLE) also reported as ng/gram of wet sediment from various intervals in the Santa Barbara Basin core.

	Alkenones quantified in SBB sediments	ng in TLE	ng/gram wet sed. wt
0-2cm	C37:3 one	14.81	2.19
	C37:2 one	20.88	3.09
2-4cm	C37:3 one	40.91	1.44
	C37:2 one	41.36	1.46
4-6cm	C37:3 one	0.00	0.00
	C37:2 one	0.00	0.00
6-8cm	C37:3 one	24.84	0.72
	C37:2 one	29.53	0.86
8-10cm	C37:3 one	50.68	1.44
	C37:2 one	55.51	1.57
10-12cm	C37:3 one	0.00	0.00
	C37:2 one	0.00	0.00
14-18cm	C37:3 one	42.98	0.63
	C37:2 one	34.78	0.51

Table 6. Carbon isotopic compositions ($\delta\ ^{13}C$) for the various n-alkanes from the 2-4 cm interval of the core from the Santa Barbara Basin.

n-alkane	δ
C20	-29.54 ± 0.007
C22	-29.54 ± 0.28
C23	-29.12 ± 0.455
C24	-29.82 ± 0.015
C25	-29.5 ± 0.41
C26	-28.88 ± 0.015
C27	-31.14 ± 0.12
C29	-31.4 ± 0.1
C30	-31.0 ± 0.5

Table 7. Carbon isotopic composition of selected lipids

depth	phytol	cholesterol	cholestanol	tetradecanol	hexadecanol
0-2	-21.25±0.016	-21.08±0.401	-25.31±0.215	-31.92±0.108	-31.09±0.218
2-4	-21.72±0.085				
4-6	-21.8±0.068			-31.56±0.105	
6-8	-22.07±0.018	-21.61±0.204	-24.07±0.144		-30.85±0.295
8-10	-21±0.126	-20.38±0.14	-23.4±0.027		
10-12	-21.19±0.021			-28.5±0.478	-30.35±0.136
14-18	-21.49±0.023	-22.67±0.85	-23.75±0.036	-29.29±0.089	

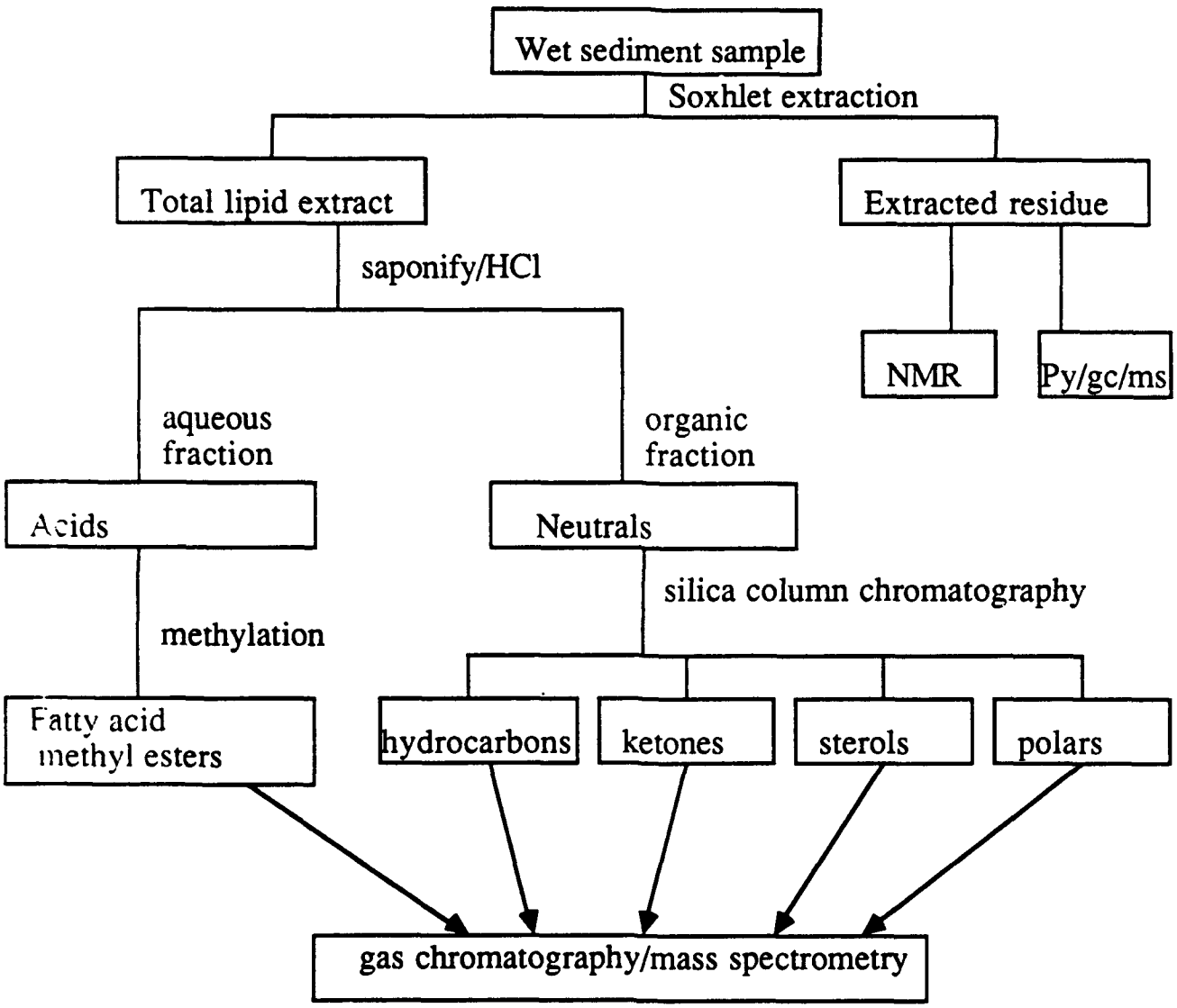

Figure 1. Analytical protocol for analysis of Santa Barbara Basin core samples.

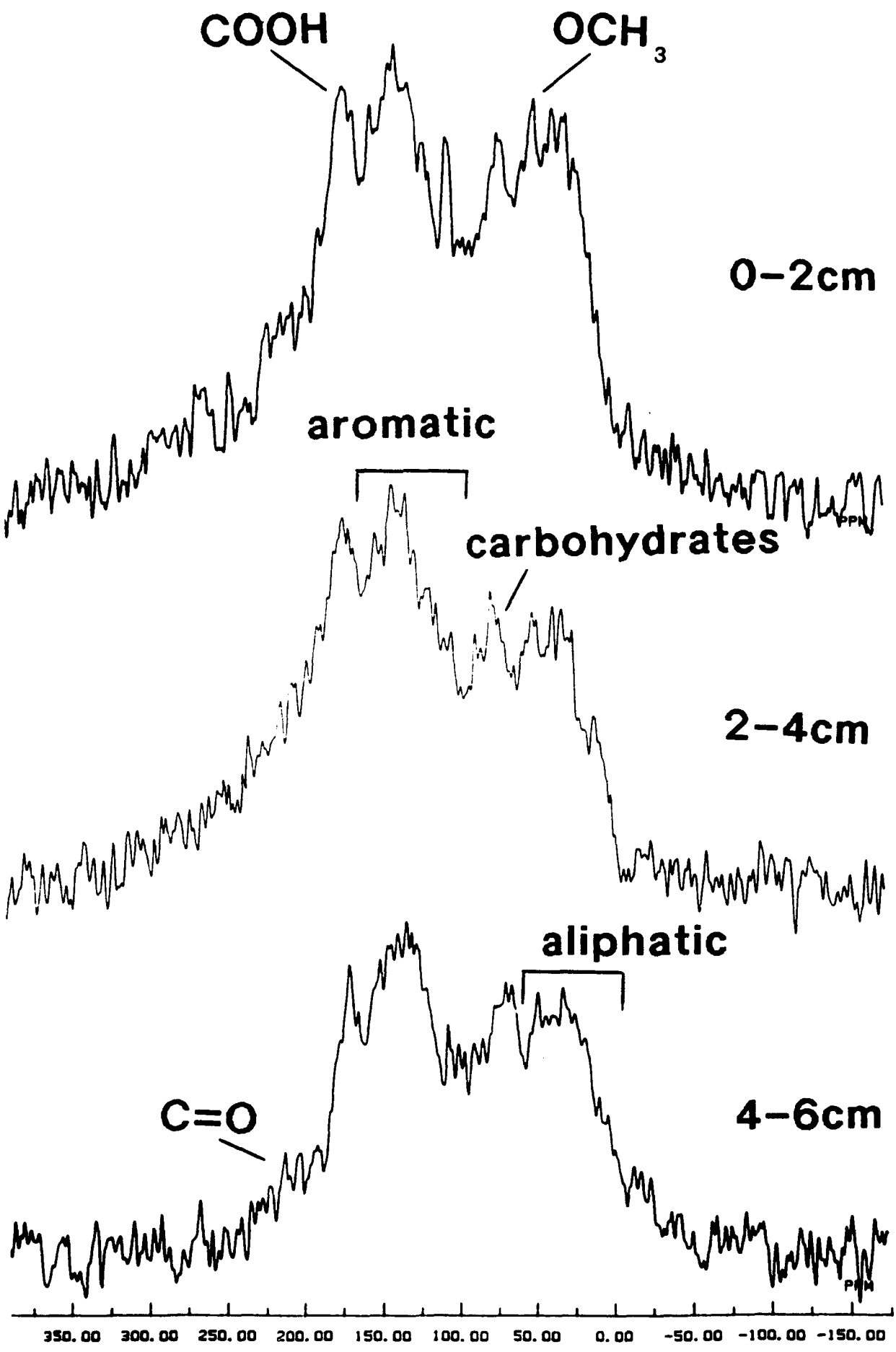

Figure 2. Solid-state ^{13}C NMR spectra for the various intervals in the top 6 cm of core. Peaks for various functional groups are denoted. The abscissa is chemical shifts in ppm relative to tetramethylsilane.

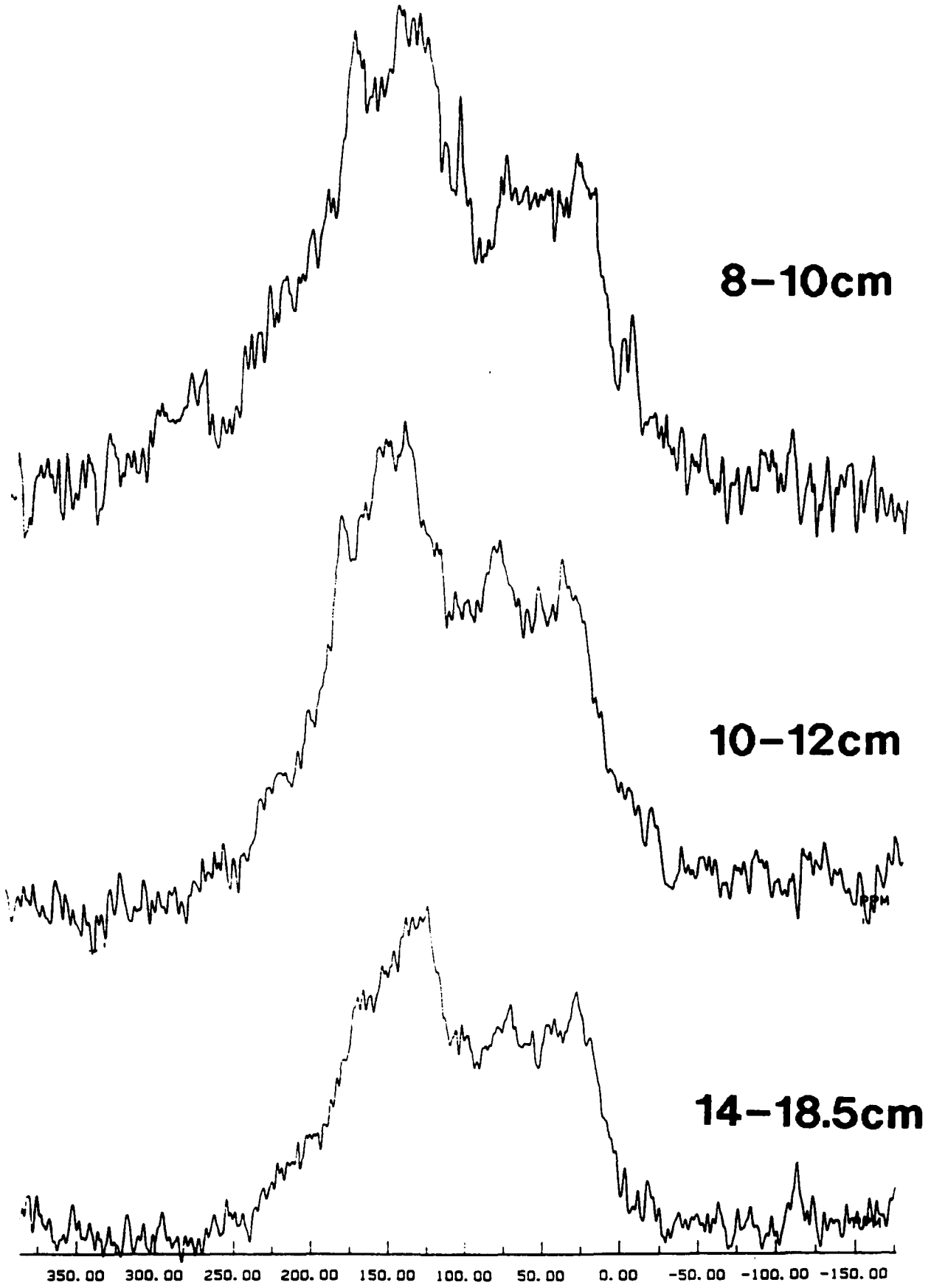

Figure 3. Solid-state ^{13}C NMR spectra for intervals below 8 cm depth in the core.

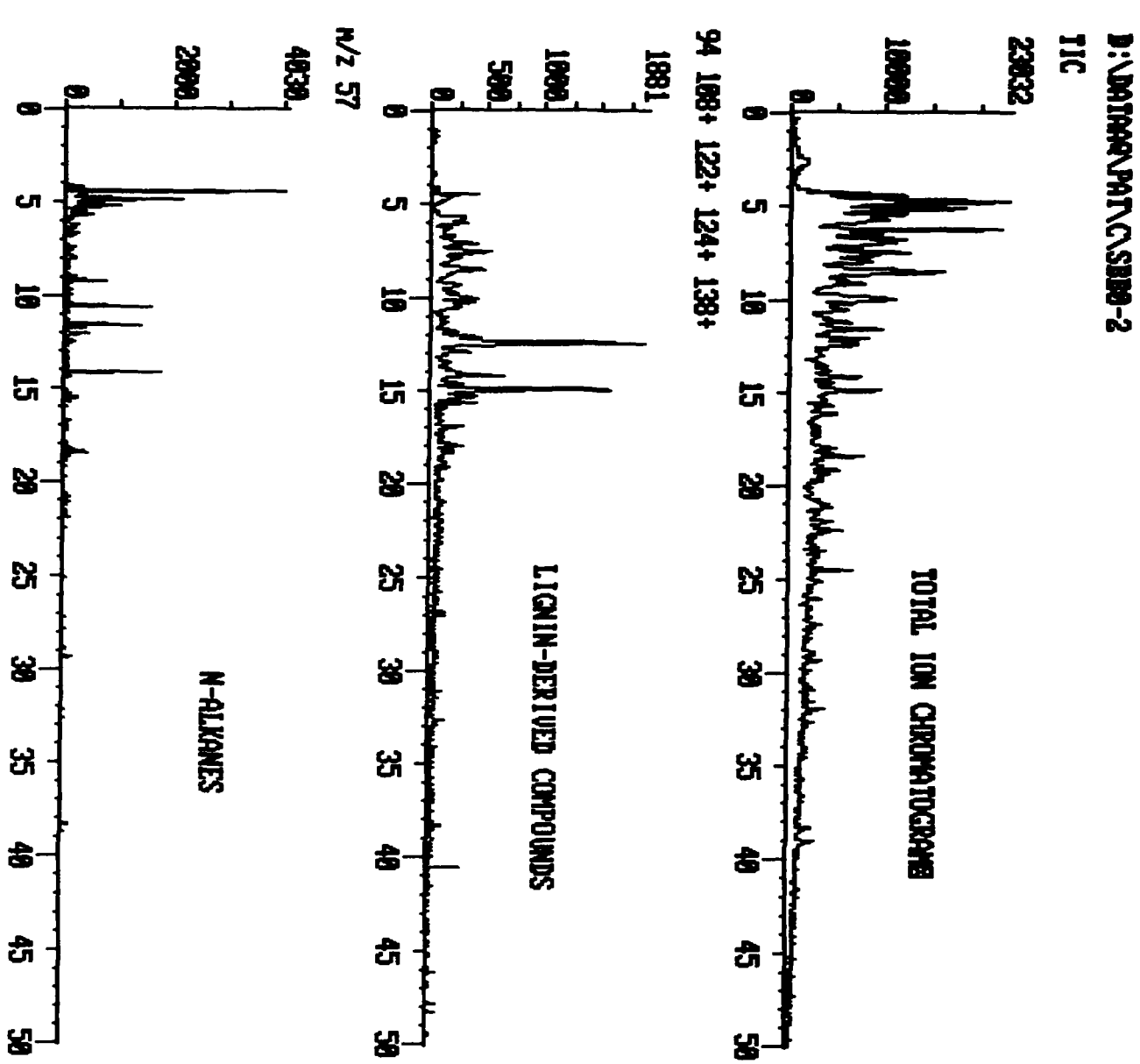

Figure 4. Flash pyrolysis/gc/ms data for Santa Barbara Basin core interval 0-2 cm. The uppermost trace is the total ion chromatogram and the two lower traces are specific ion chromatograms for ions characteristic of lignin-derived aromatic compounds (the sum of m/z 94,108,122,124, and 138) and for n-alkanes (m/z 57).

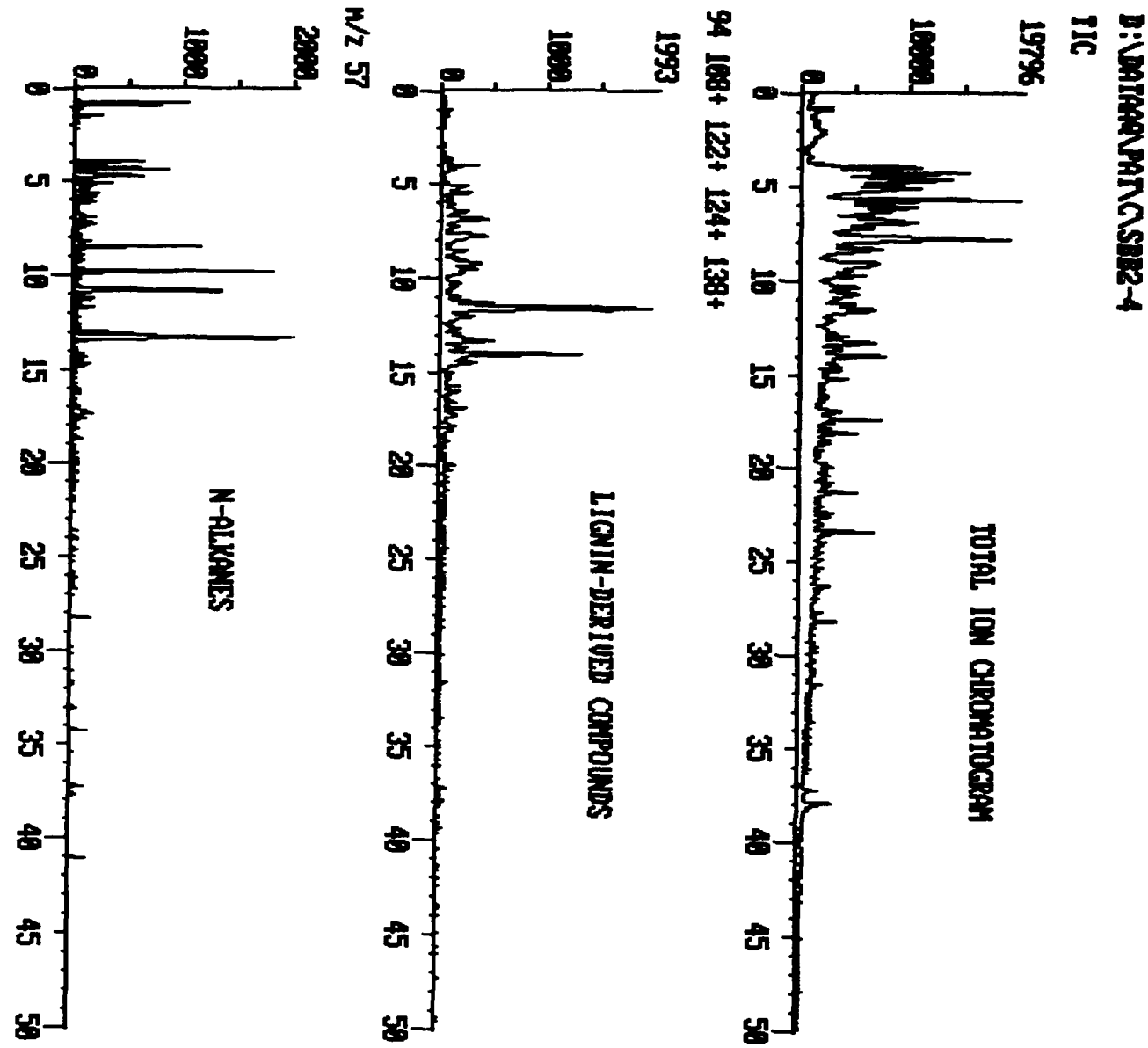

Figure 5. Flash pyrolysis/gc/ms data for Santa Barbara Basin core interval 2-4 cm. The uppermost trace is the total ion chromatogram and the two lower traces are specific ion chromatograms for ions characteristic of lignin-derived aromatic compounds (the sum of m/z 94,108,122,124, and 138) and for n-alkanes (m/z 57).

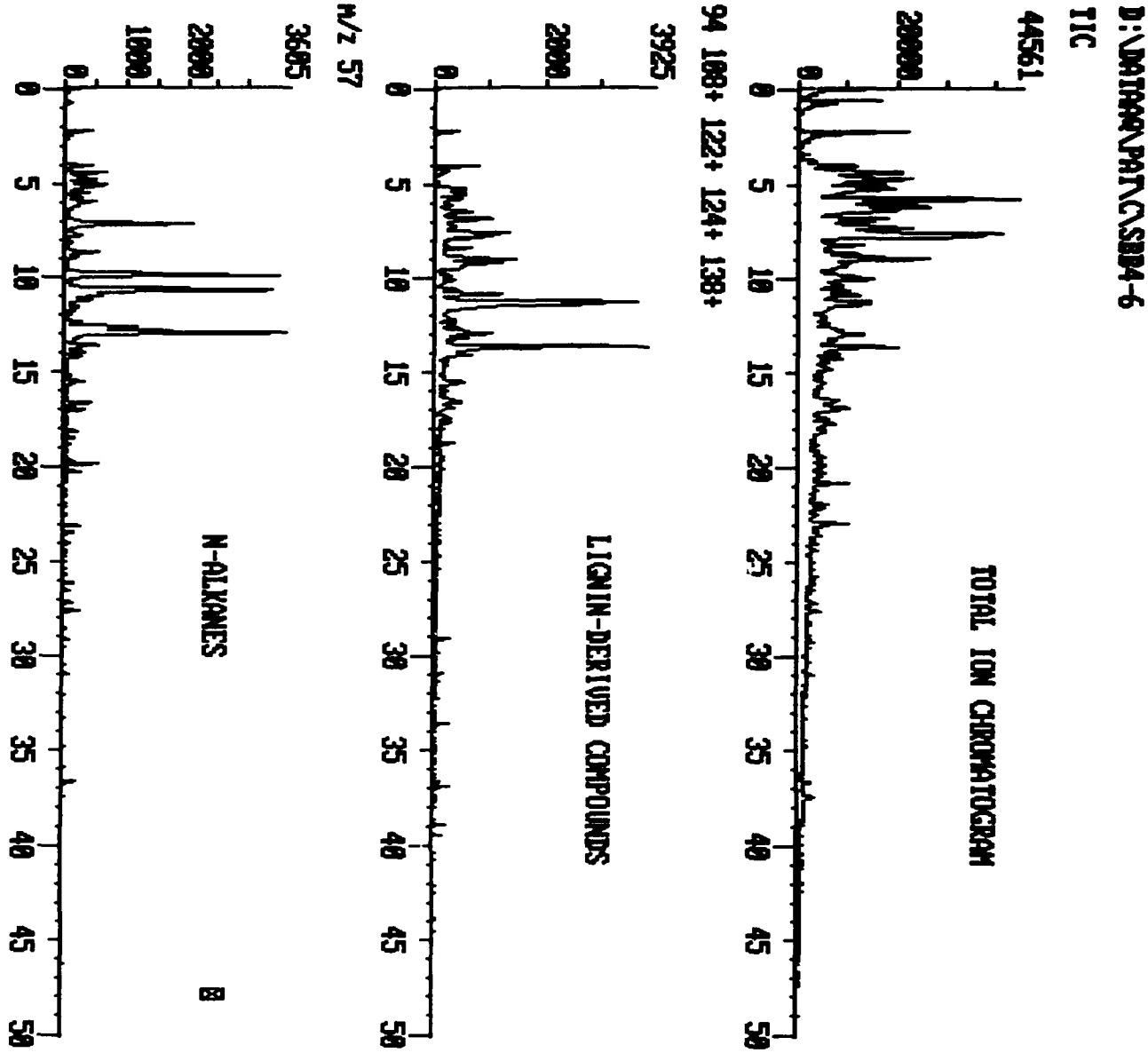

Figure 6. Flash pyrolysis/gc/ms data for Santa Barbara Basin core interval 4-6 cm. The uppermost trace is the total ion chromatogram and the two lower traces are specific ion chromatograms for ions characteristic of lignin-derived aromatic compounds (the sum of m/z 94,108,122,124, and 138) and for n-alkanes (m/z 57).

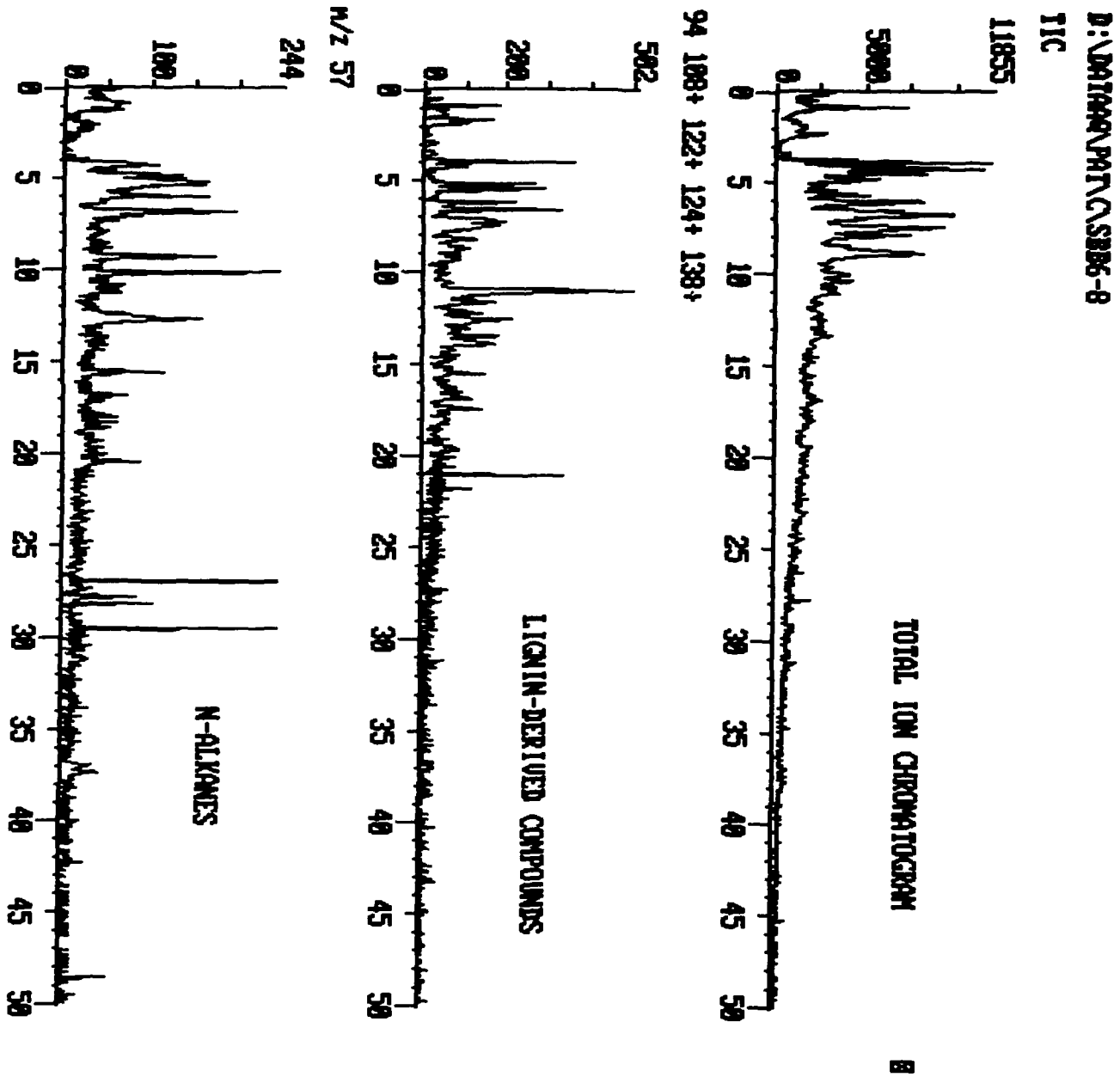

Figure 7. Flash pyrolysis/gc/ms data for Santa Barbara Basin core interval 6-8 cm. The uppermost trace is the total ion chromatogram and the two lower traces are specific ion chromatograms for ions characteristic of lignin-derived aromatic compounds (the sum of m/z 94,108,122,124, and 138) and for n-alkanes (m/z 57).

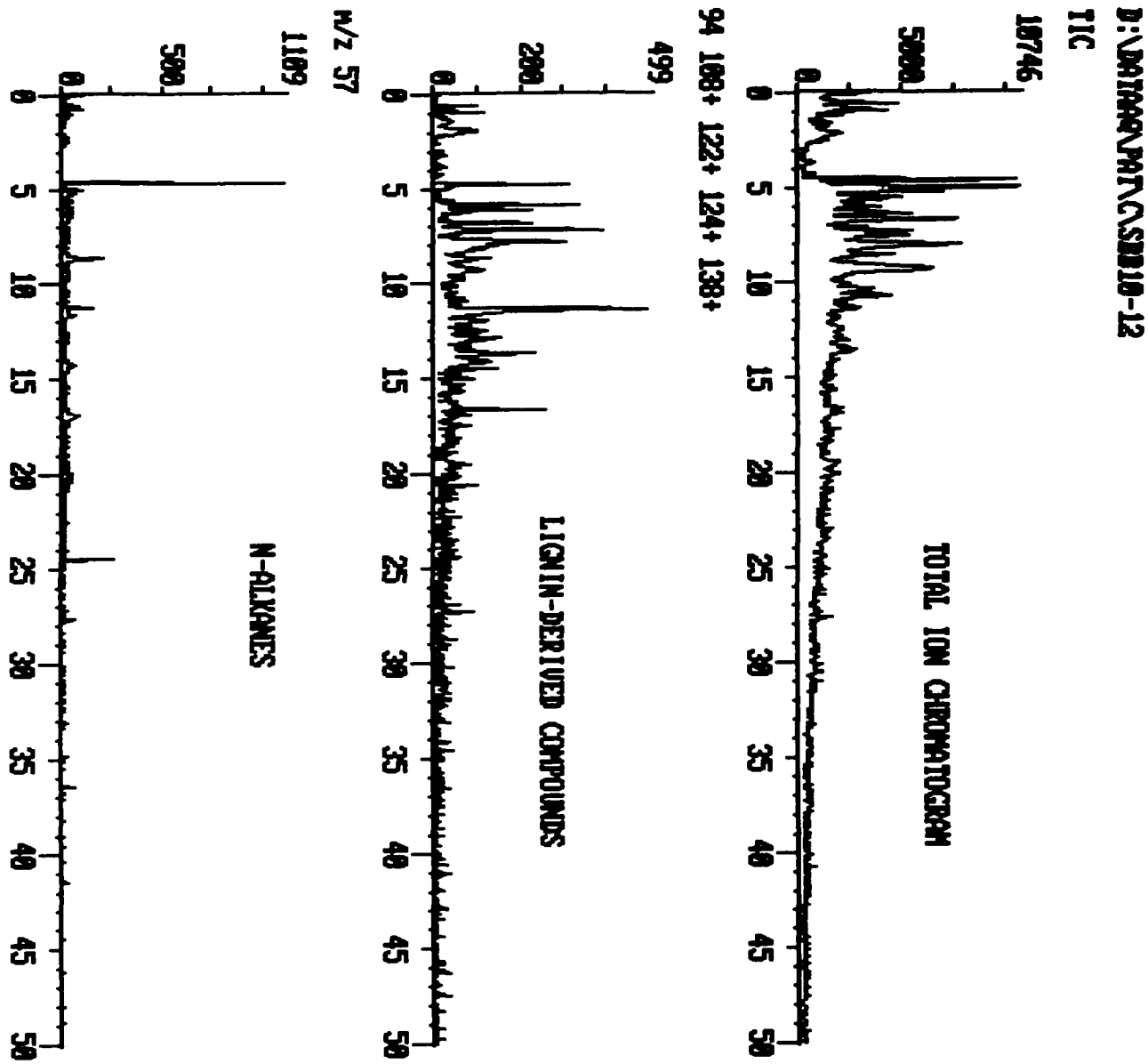

Figure 8. Flash pyrolysis/gc/ms data for Santa Barbara Basin core interval 10-12 cm. The uppermost trace is the total ion chromatogram and the two lower traces are specific ion chromatograms for ions characteristic of lignin-derived aromatic compounds (the sum of m/z 94,108,122,124, and 138) and for n-alkanes (m/z 57).

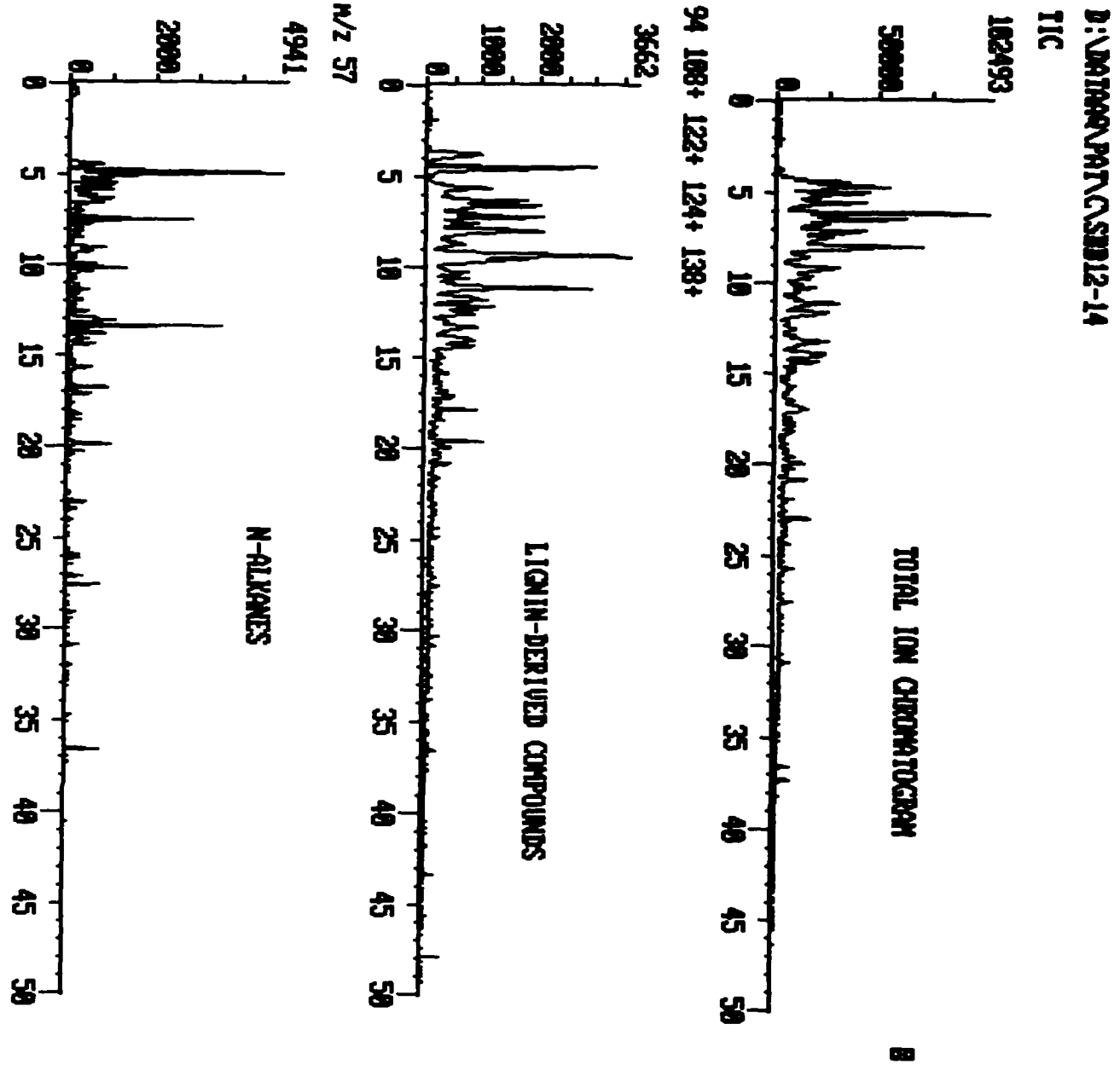

Figure 9. Flash pyrolysis/gc/ms data for Santa Barbara Basin core interval 12-14 cm. The uppermost trace is the total ion chromatogram and the two lower traces are specific ion chromatograms for ions characteristic of lignin-derived aromatic compounds (the sum of m/z 94,108,122,124, and 138) and for n-alkanes (m/z 57).

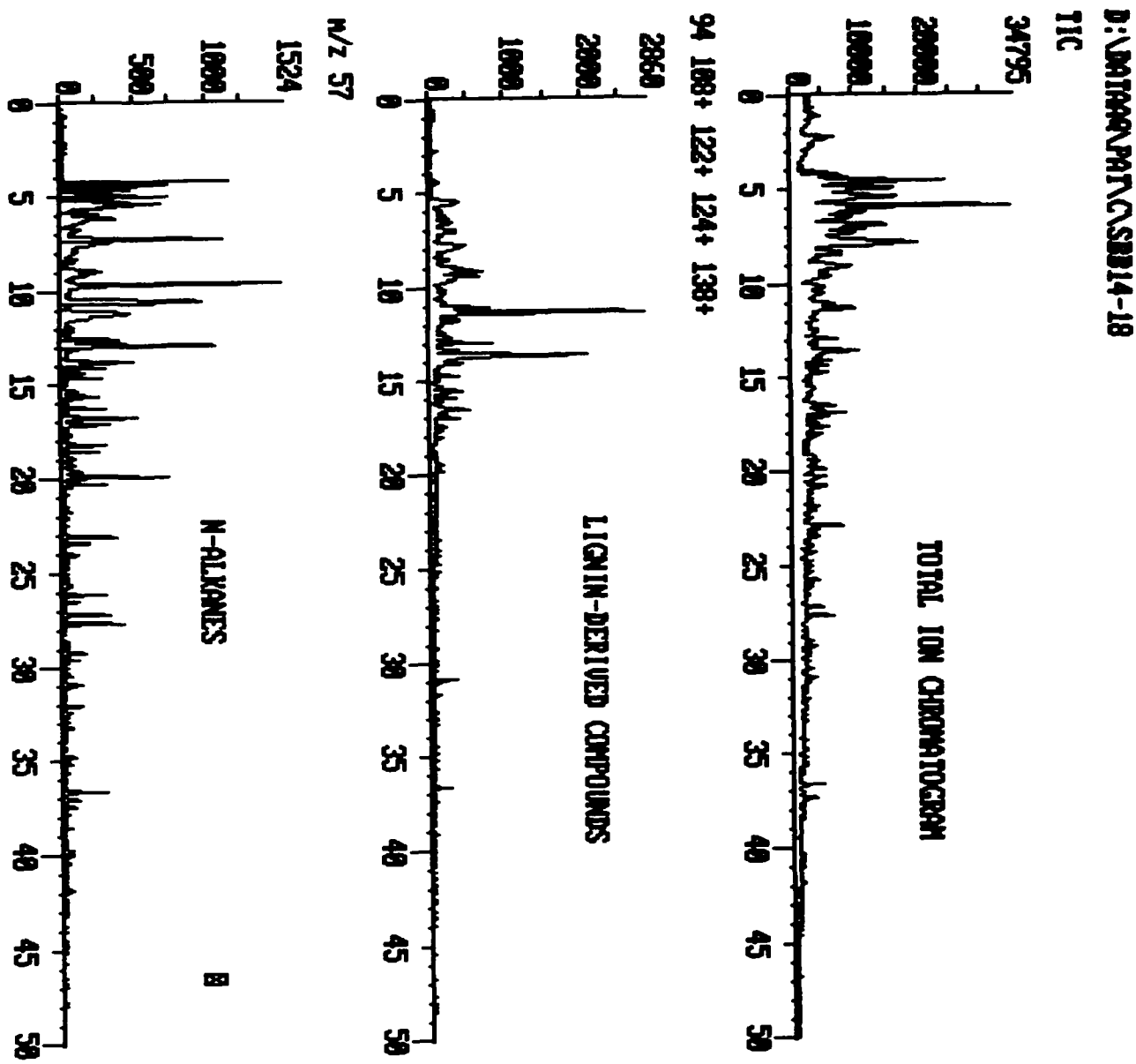

Figure 10. Flash pyrolysis/gc/ms data for Santa Barbara Basin core interval 14-18 cm. The uppermost trace is the total ion chromatogram and the two lower traces are specific ion chromatograms for ions characteristic of lignin-derived aromatic compounds (the sum of m/z 94,108,122,124, and 138) and for n-alkanes (m/z 57).

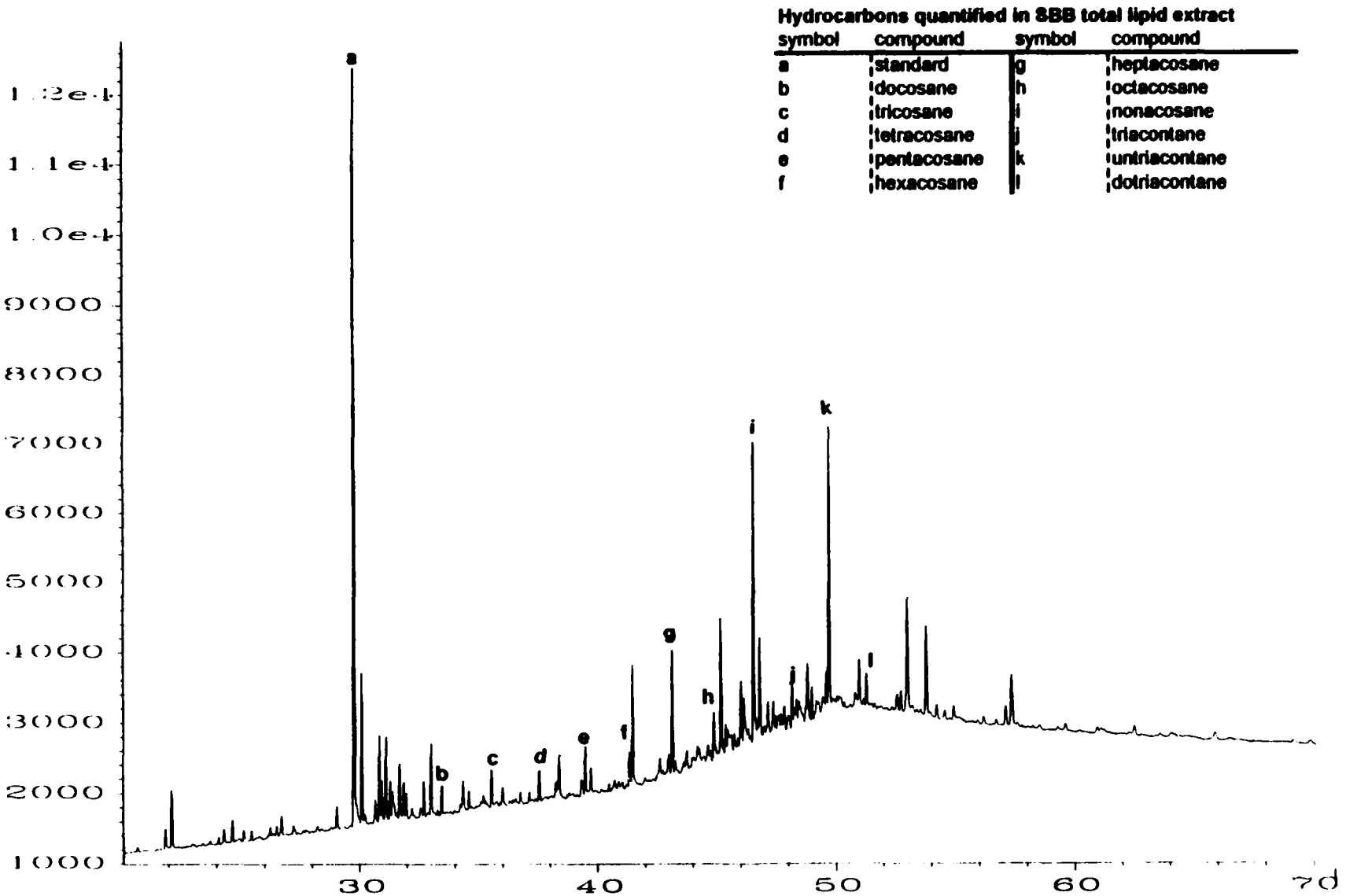

Figure 11. Partial GC chromatogram of the hydrocarbon fraction from liquid chromatography of total lipid extract neutrals (0-2 cm depth).

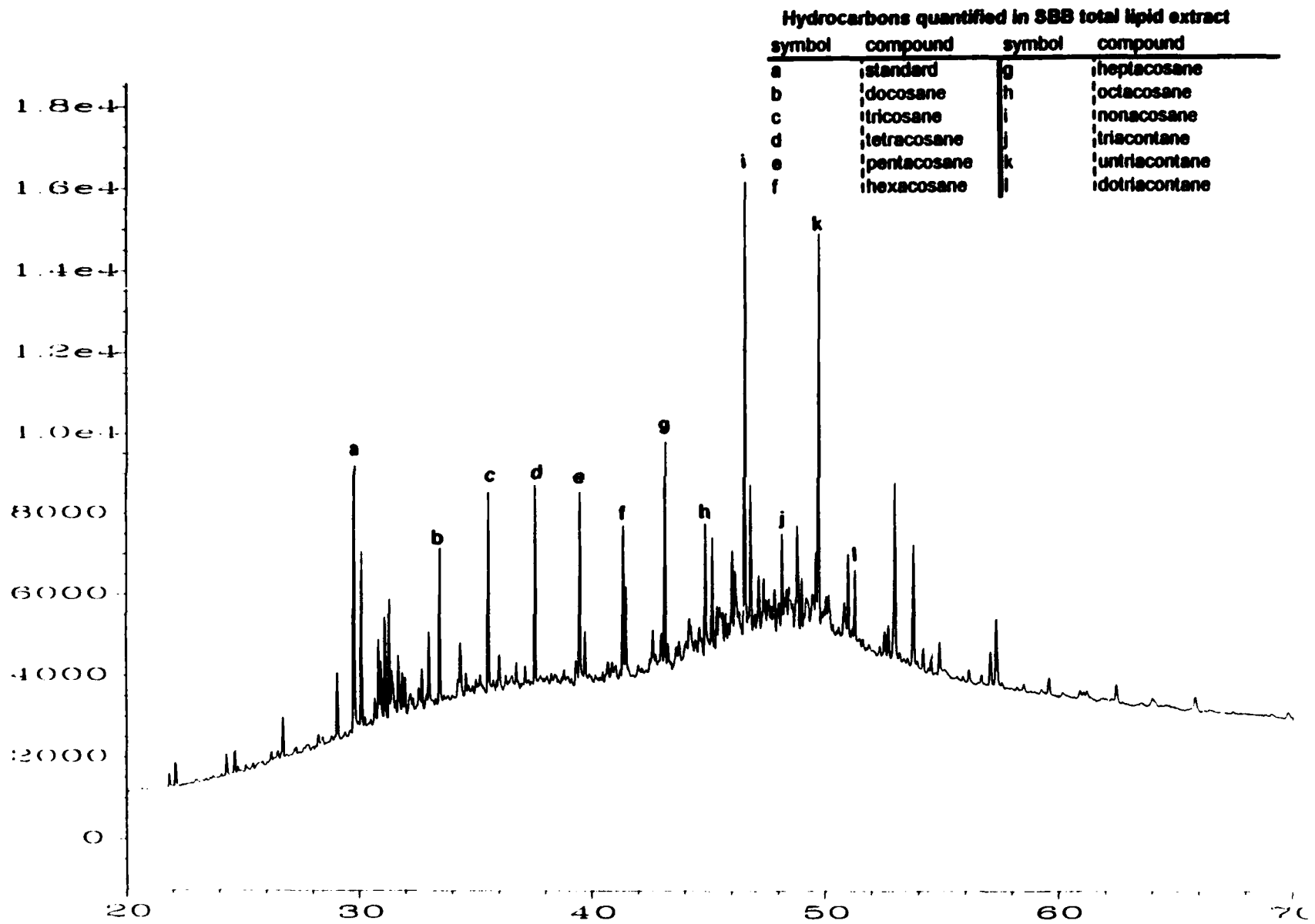

Figure 12. Partial GC chromatogram of the hydrocarbon fraction from liquid chromatography of total lipid extract neutrals (2-4 cm depth).

Hydrocarbons quantified in SBB total lipid extract

symbol	compound	symbol	compound
a	standard	g	heptacosane
b	docosane	h	octacosane
c	tricosane	i	nonacosane
d	tetracosane	j	triacontane
e	pentacosane	k	untriacontane
f	hexacosane	l	dotriacontane

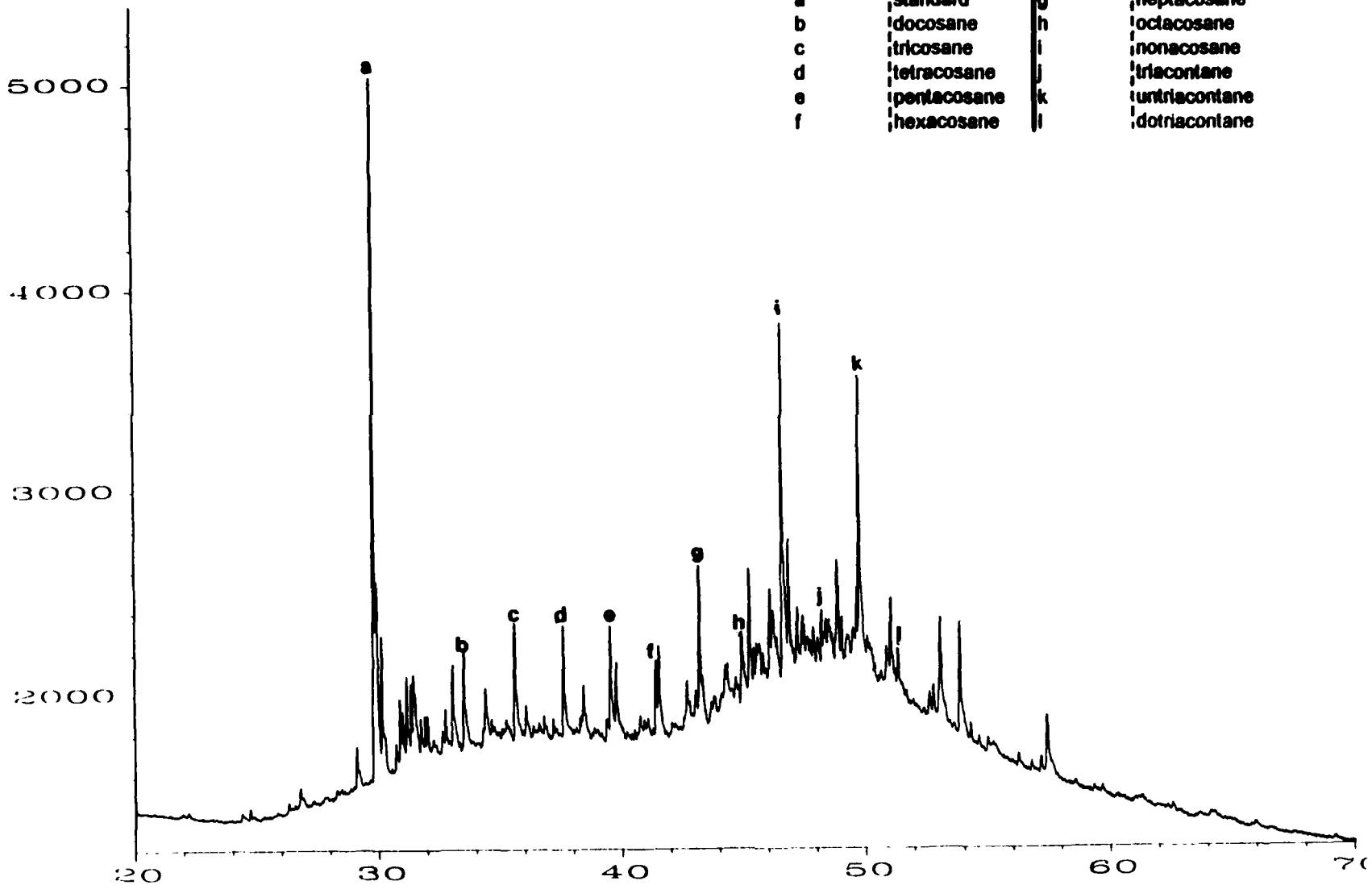

Figure 13. Partial GC chromatogram of the hydrocarbon fraction from liquid chromatography of total lipid extract neutrals (4-6 cm depth).

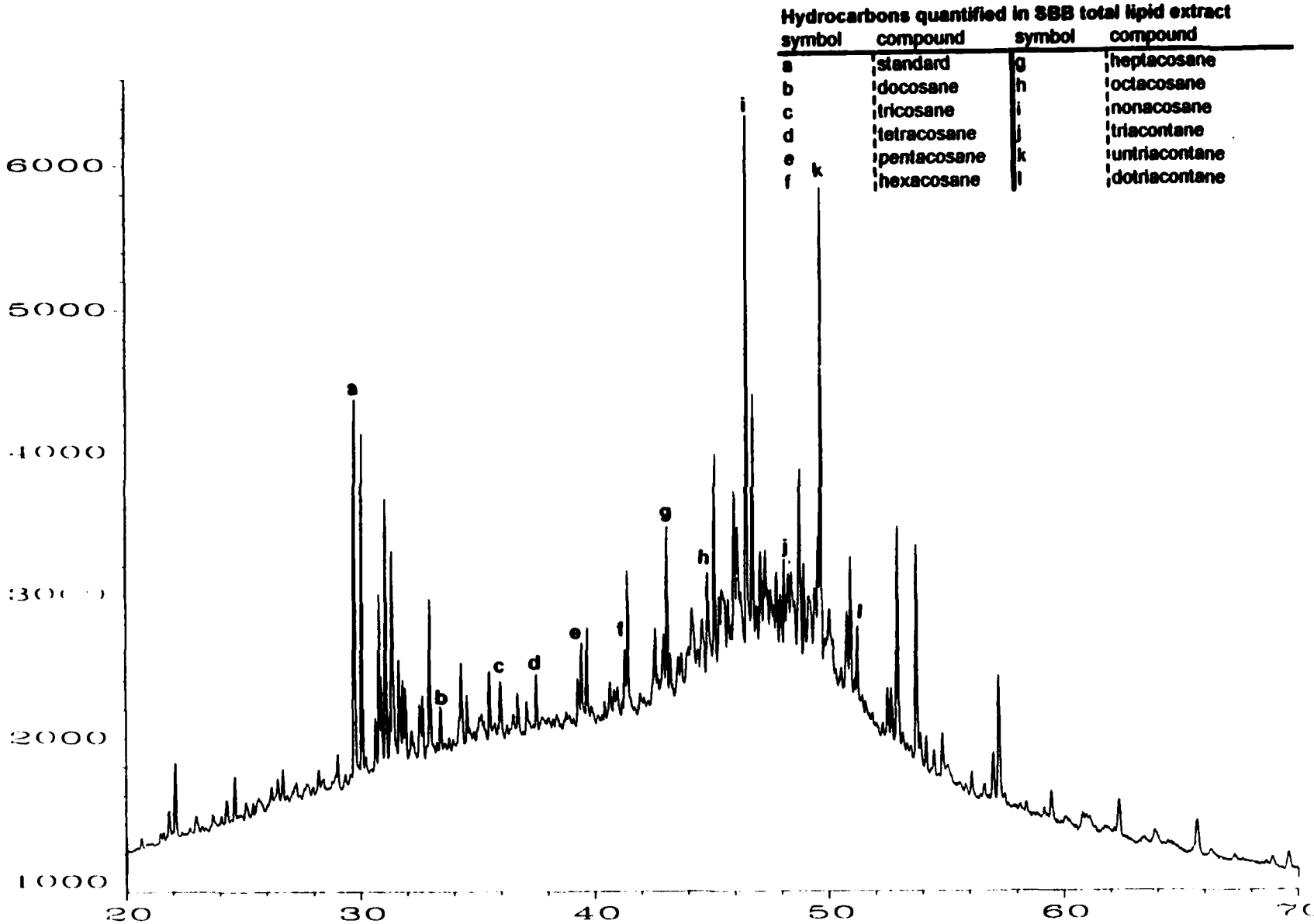

Figure 14. Partial GC chromatogram of the hydrocarbon fraction from liquid chromatography of total lipid extract neutrals (6-8 cm depth).

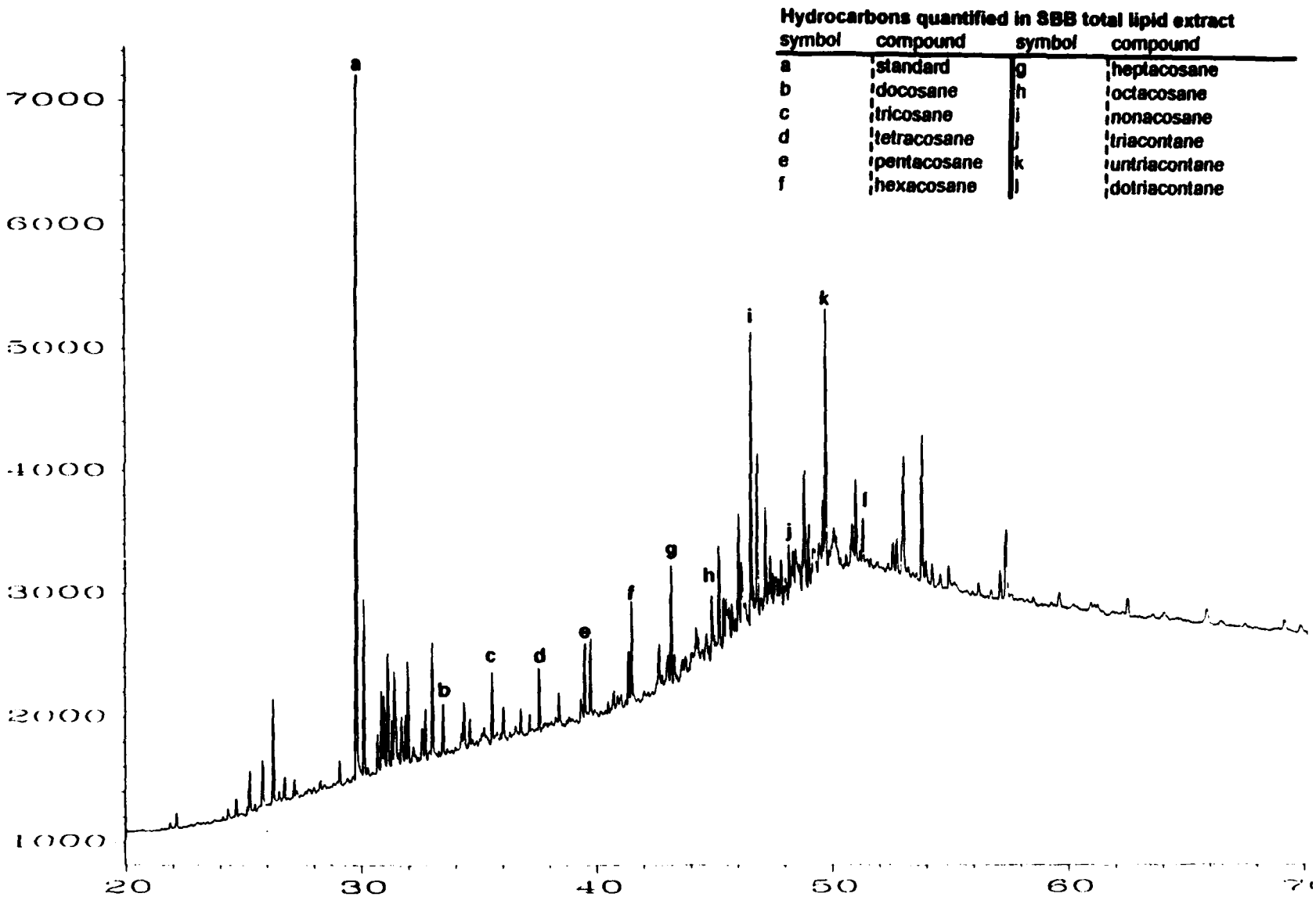

Figure 15. Partial GC chromatogram of the hydrocarbon fraction from liquid chromatography of total lipid extract neutrals (8-10 cm depth).

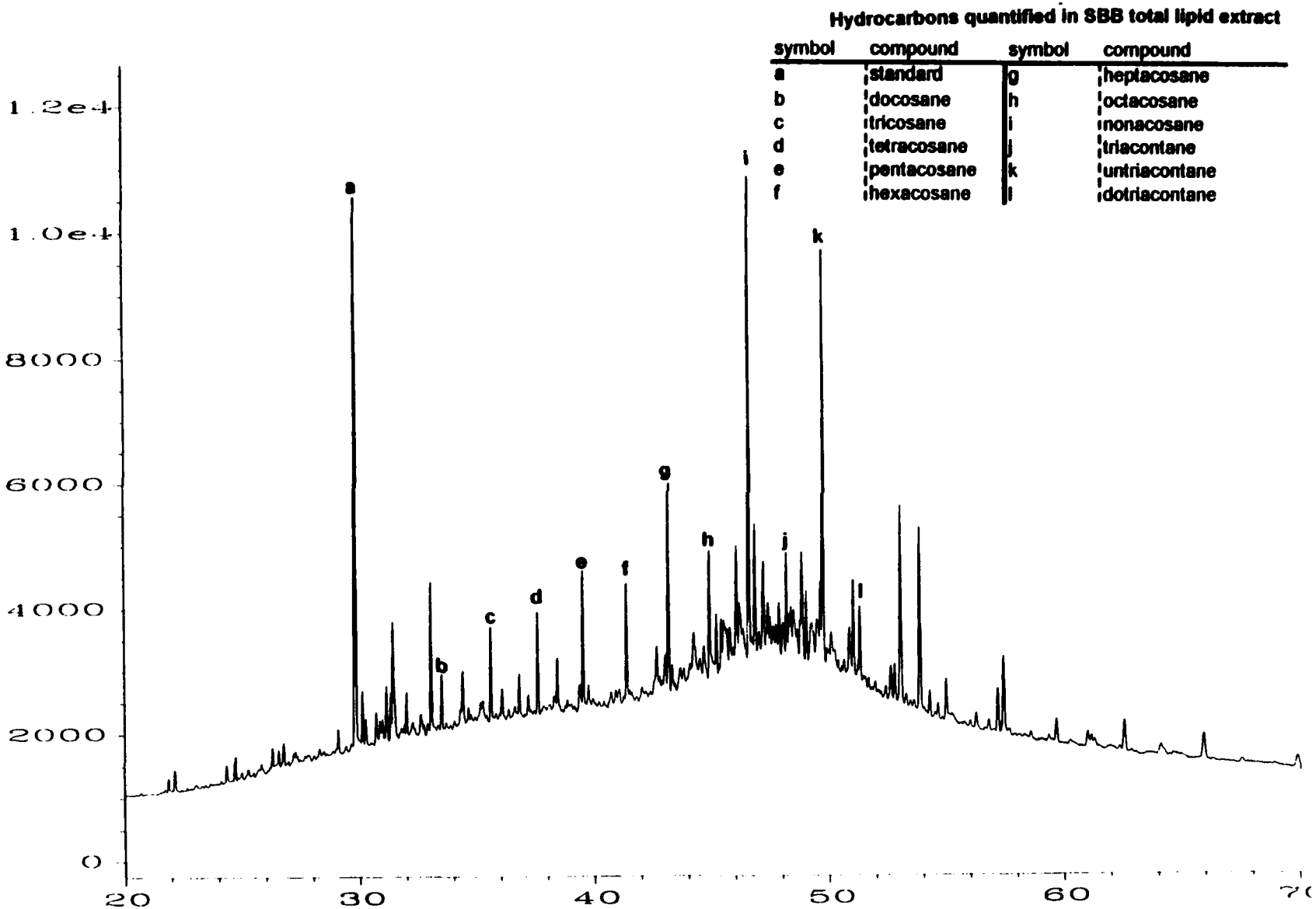

Figure 16. Partial GC chromatogram of the hydrocarbon fraction from liquid chromatography of total lipid extract neutrals (10-12 cm depth).

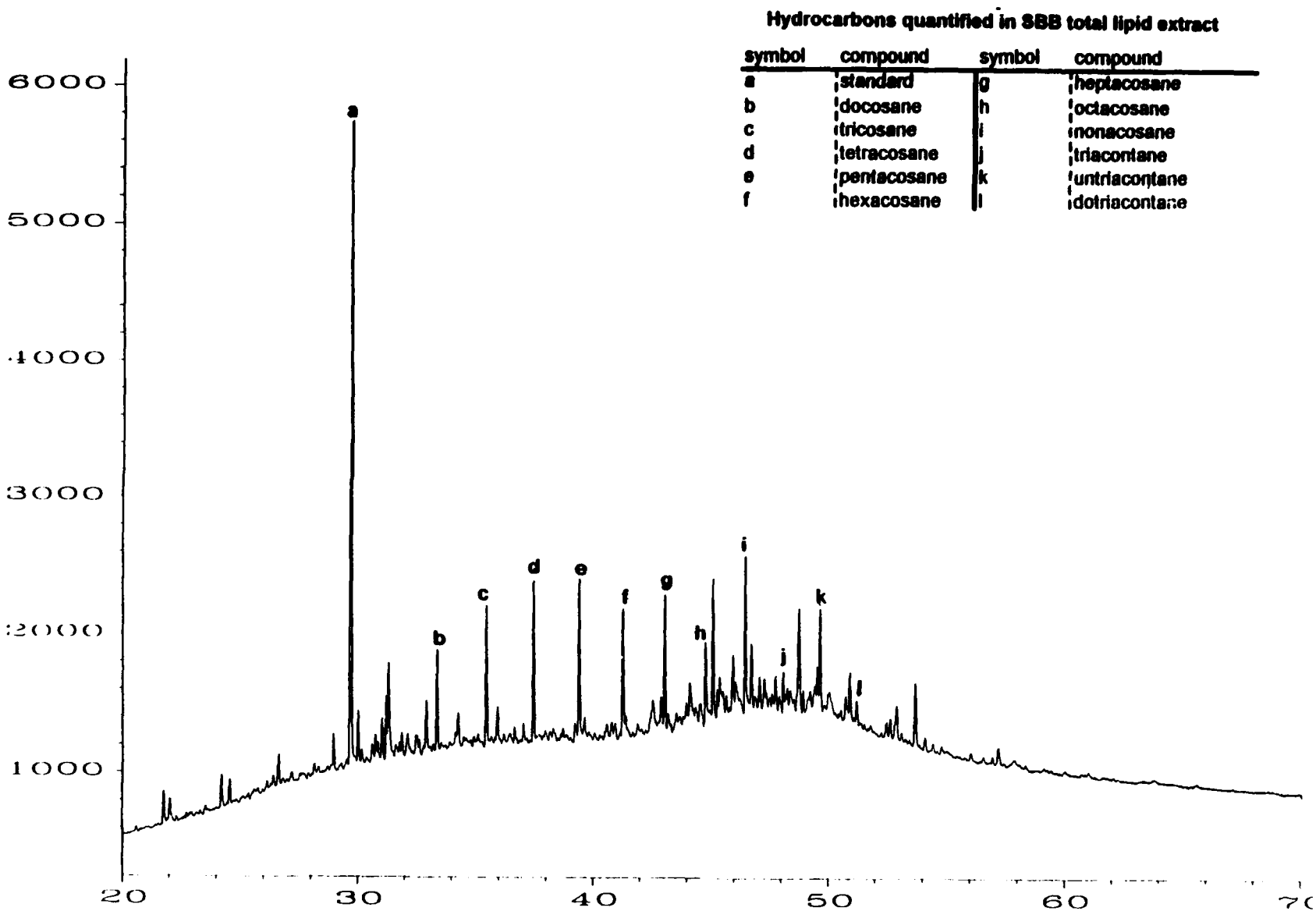

Figure 17. Partial GC chromatogram of the hydrocarbon fraction from liquid chromatography of total lipid extract neutrals (14-18 cm depth).

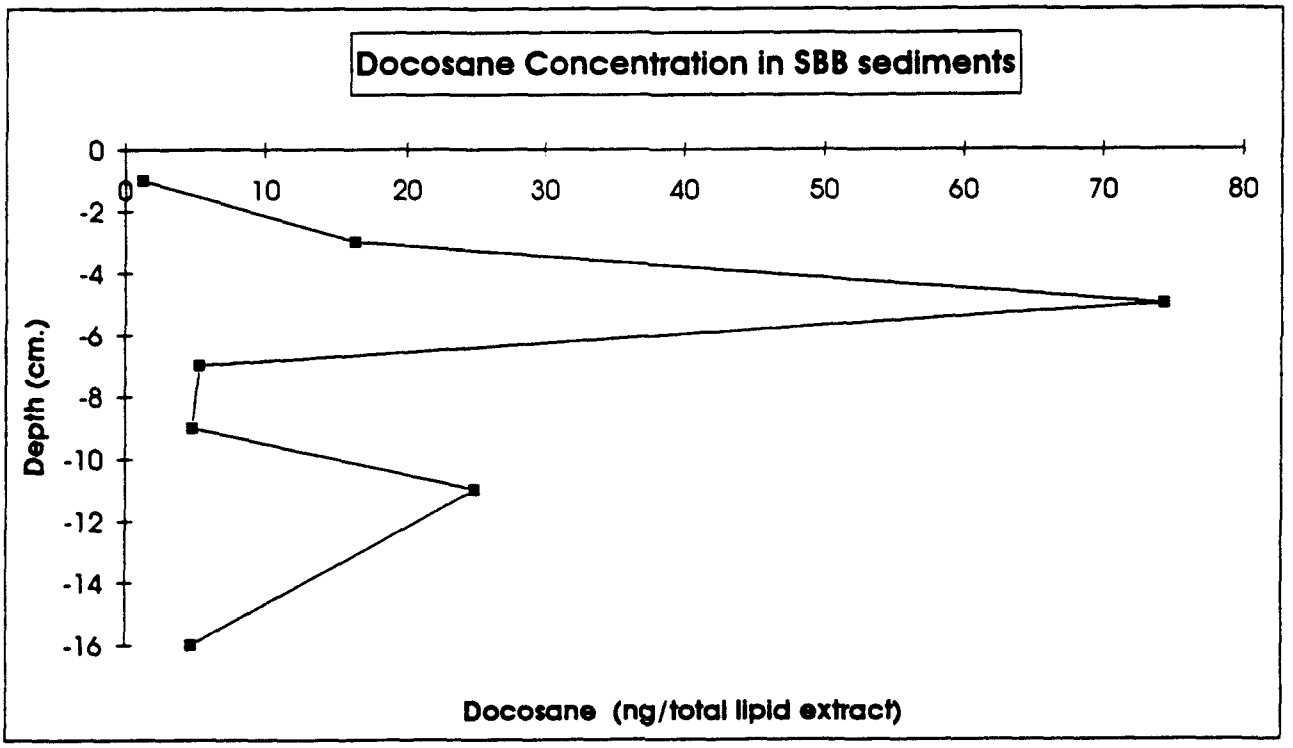

Figure 18. Depth profile for the concentration of docosane (C22) in the core of Santa Barbara Basin.

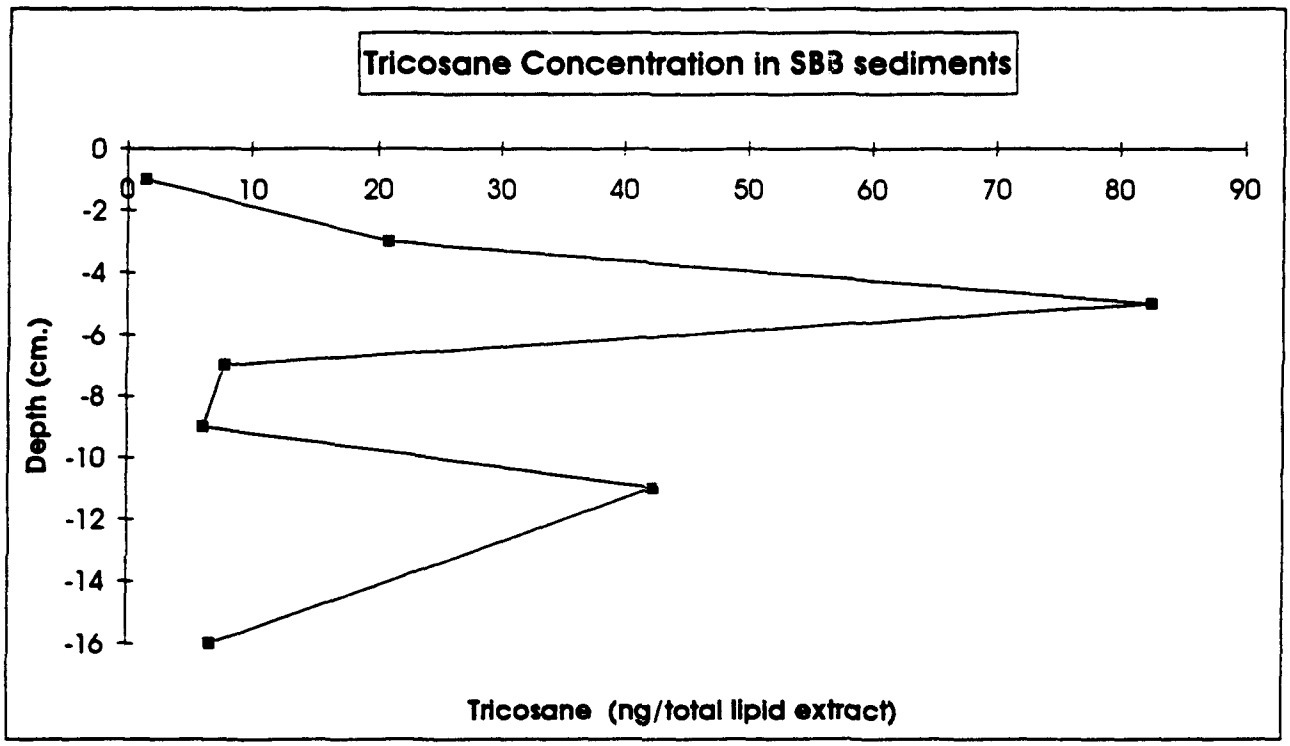

Figure 19. Depth profile for the concentration of tricosane (C23) in the core of Santa Barbara Basin.

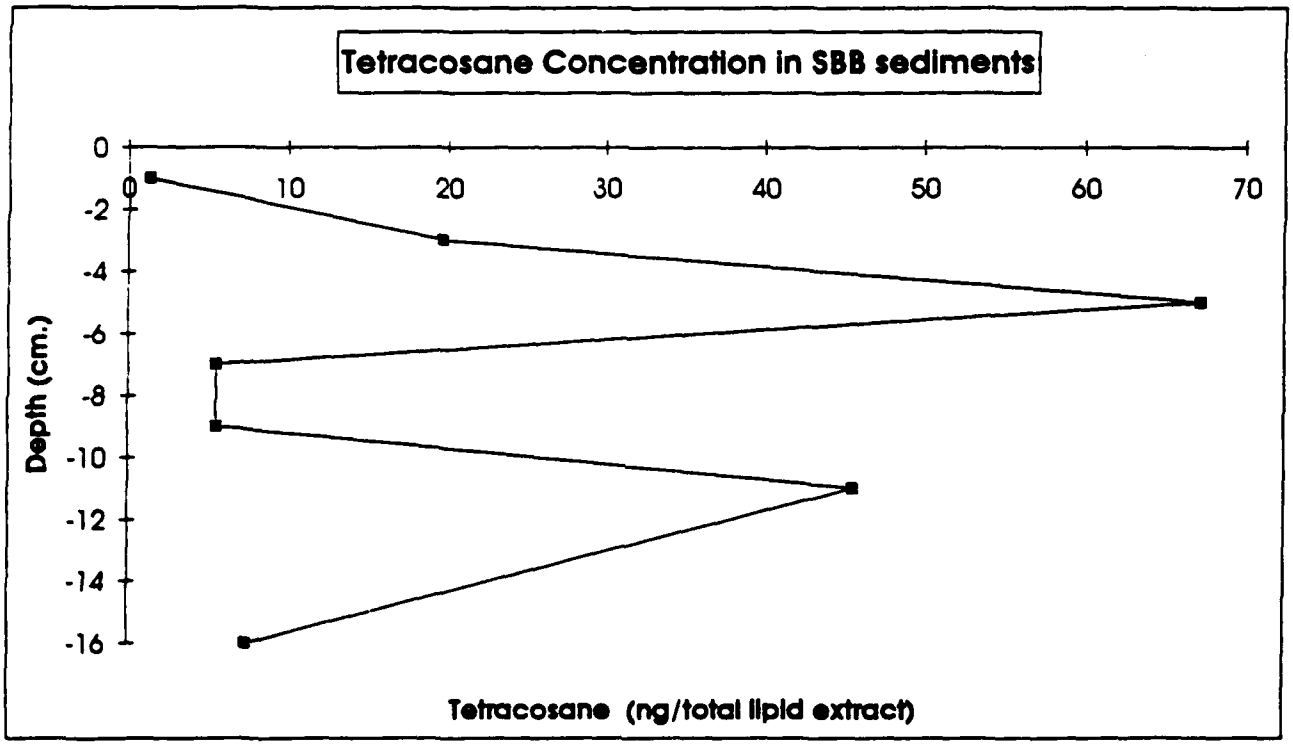

Figure 20. Depth profile for the concentration of tetracosane (C24) in the core of Santa Barbara Basin.

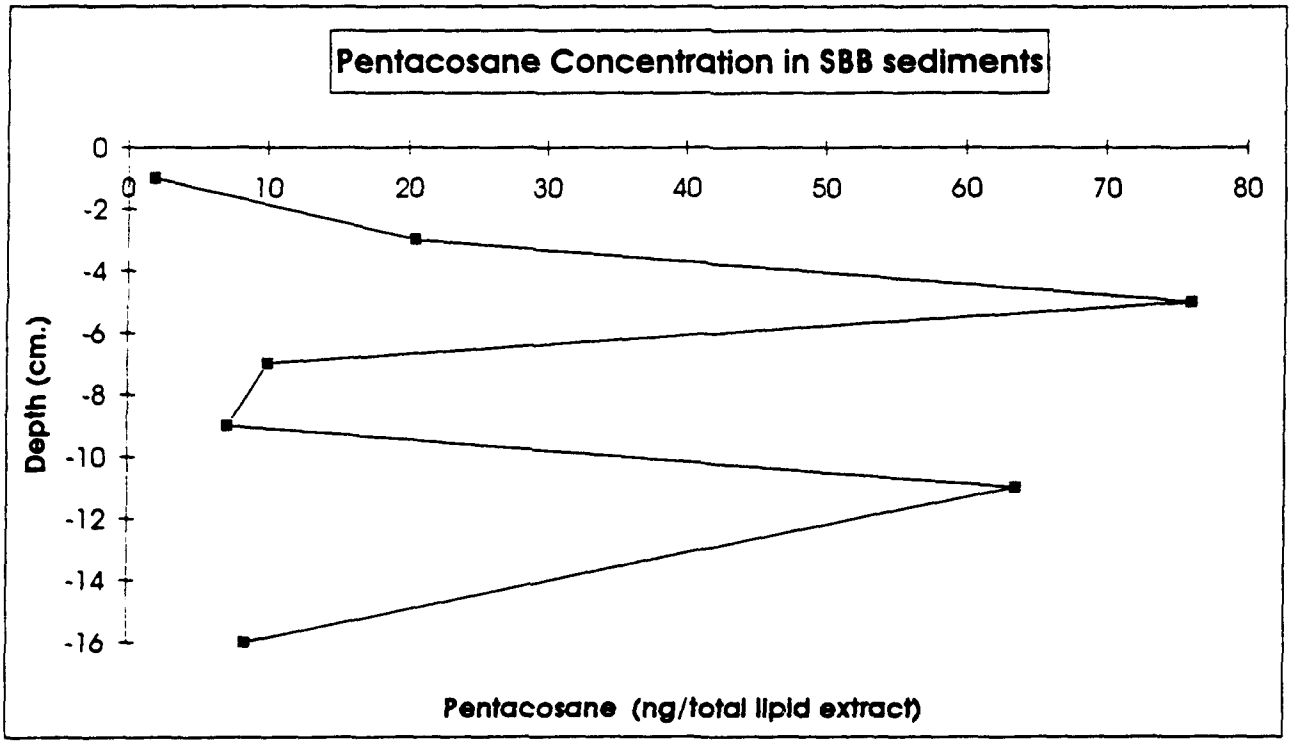

Figure 21. Depth profile for the concentration of pentacosane (C25) in the core of Santa Barbara Basin.

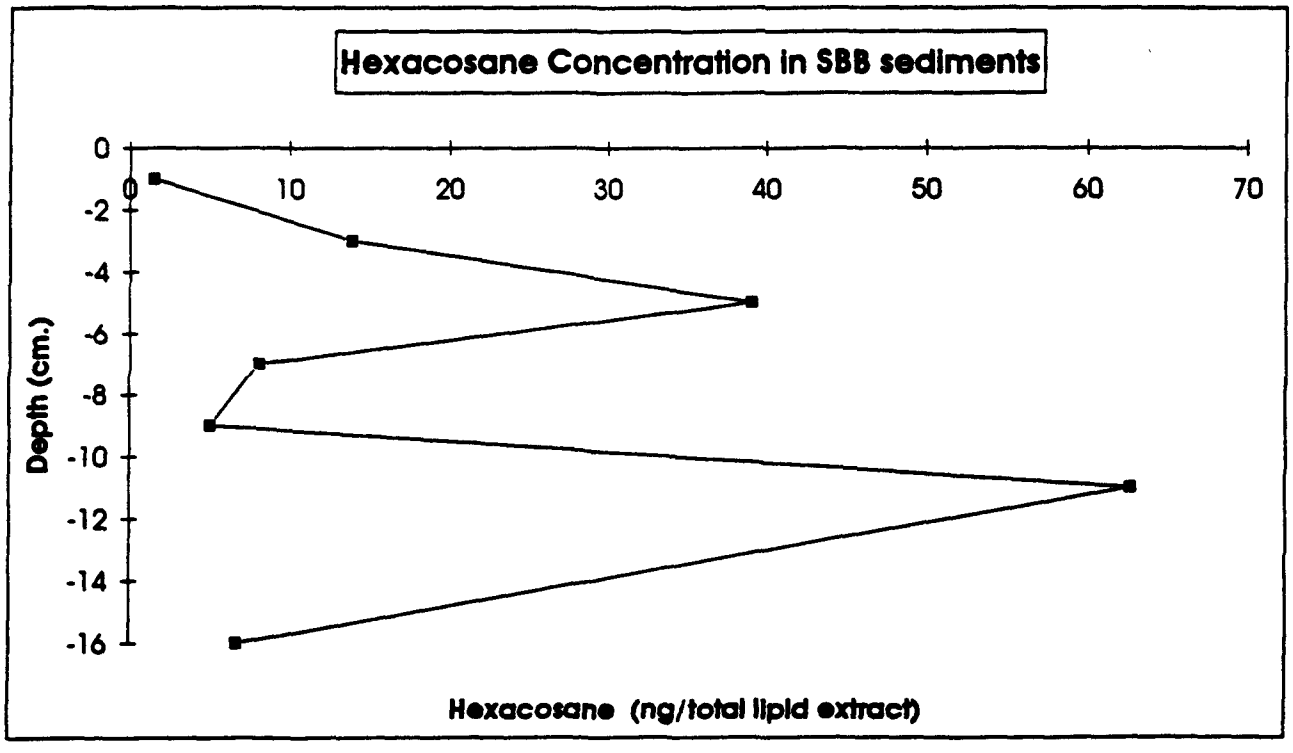

Figure 22. Depth profile for the concentration of hexacosane (C26) in the core of Santa Barbara Basin.

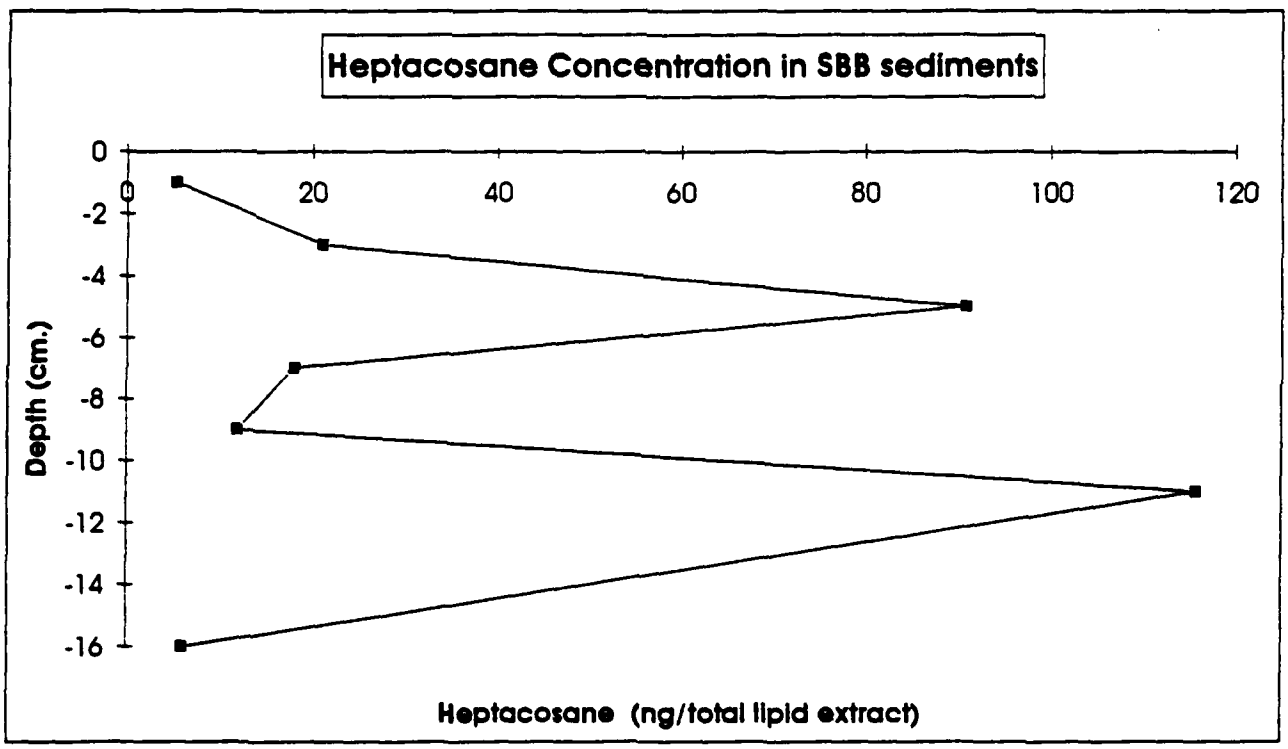

Figure 23. Depth profile for the concentration of heptacosane (C27) in the core of Santa Barbara Basin.

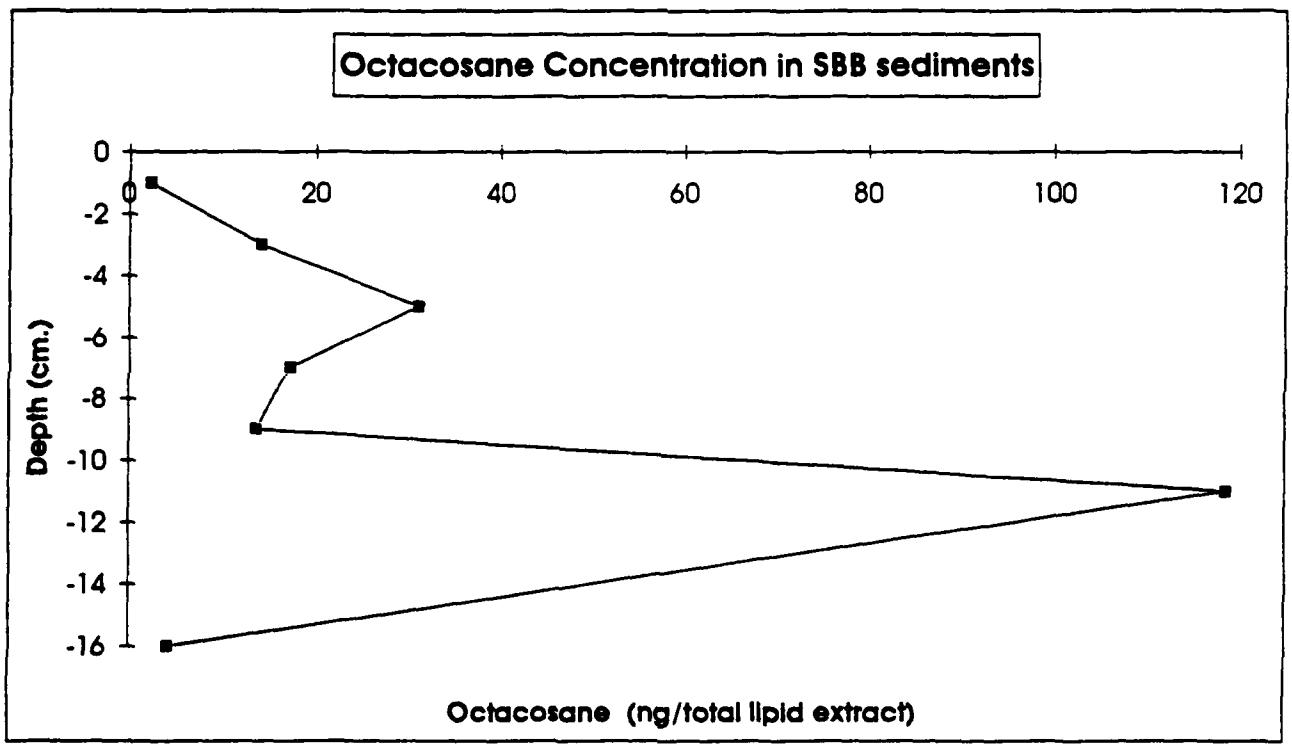

Figure 24. Depth profile for the concentration of octacosane (C28) in the core of Santa Barbara Basin.

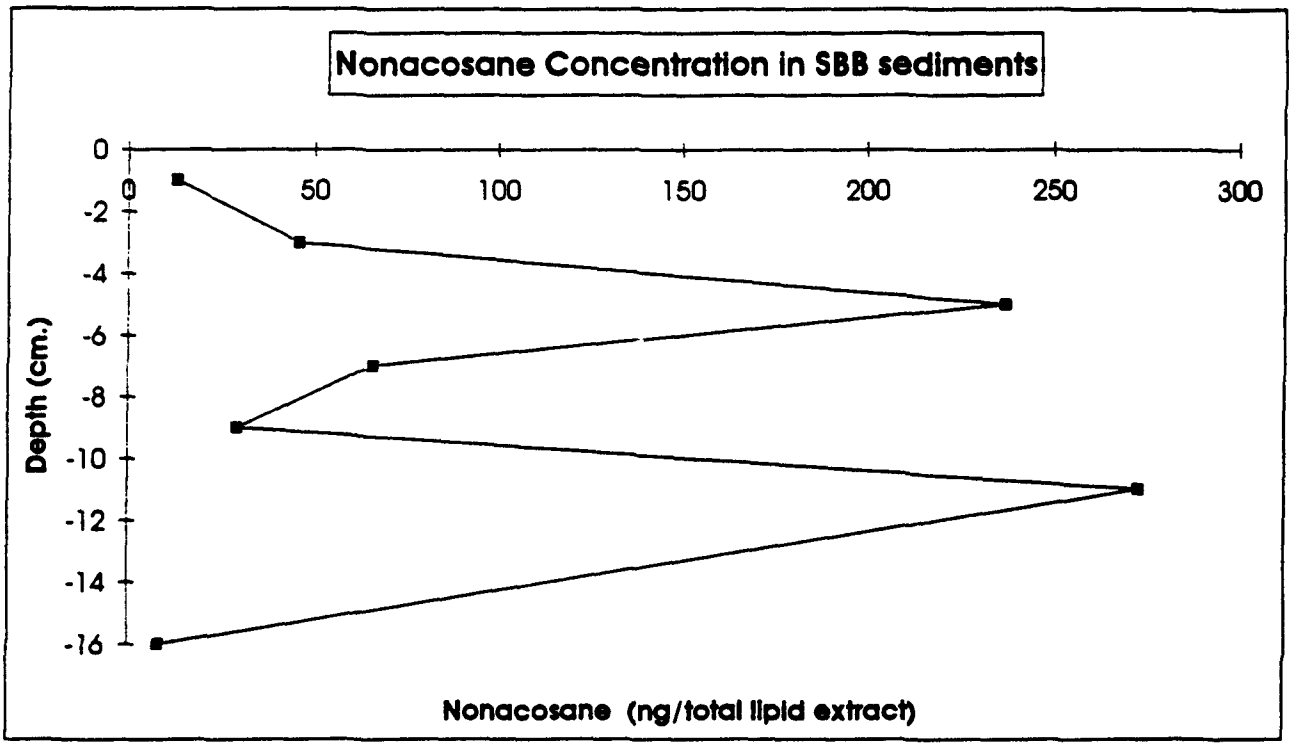

Figure 25. Depth profile for the concentration of nonacosane (C29) in the core of Santa Barbara Basin.

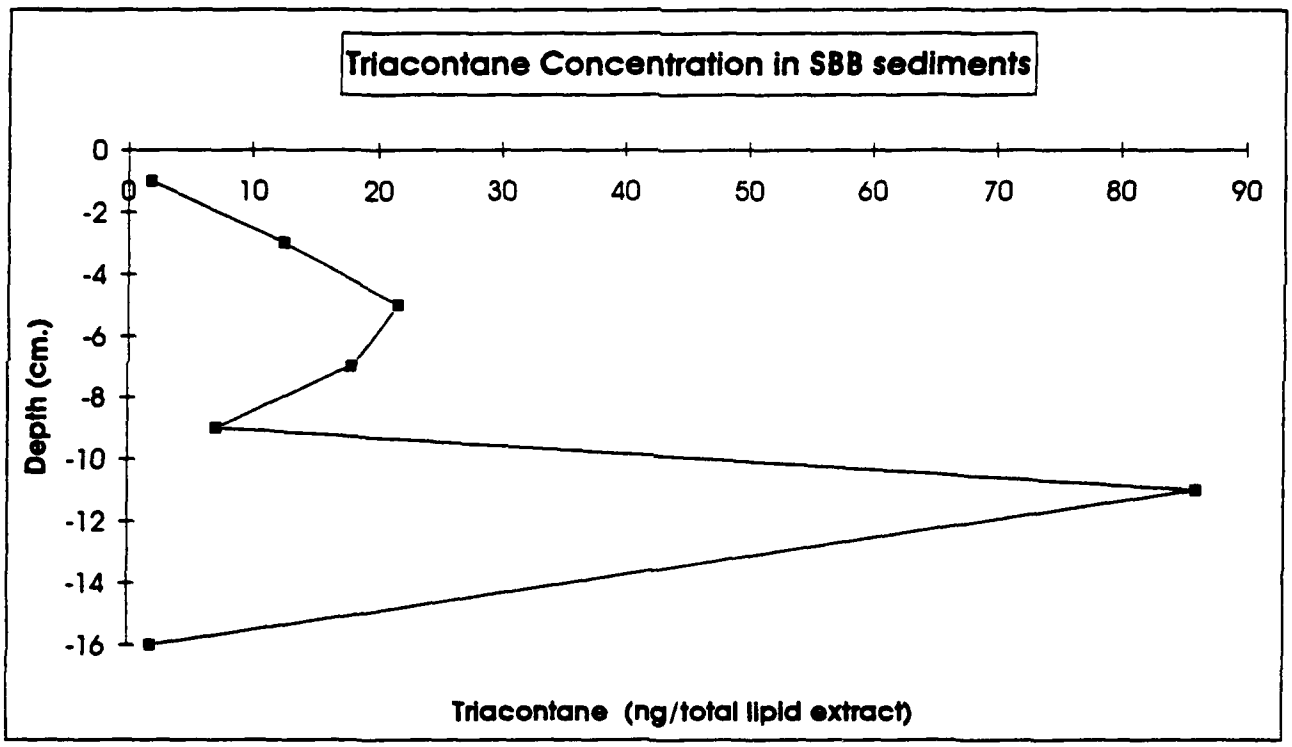

Figure 26. Depth profile for the concentration of dtriacontane (C30) in the core of Santa Barbara Basin.

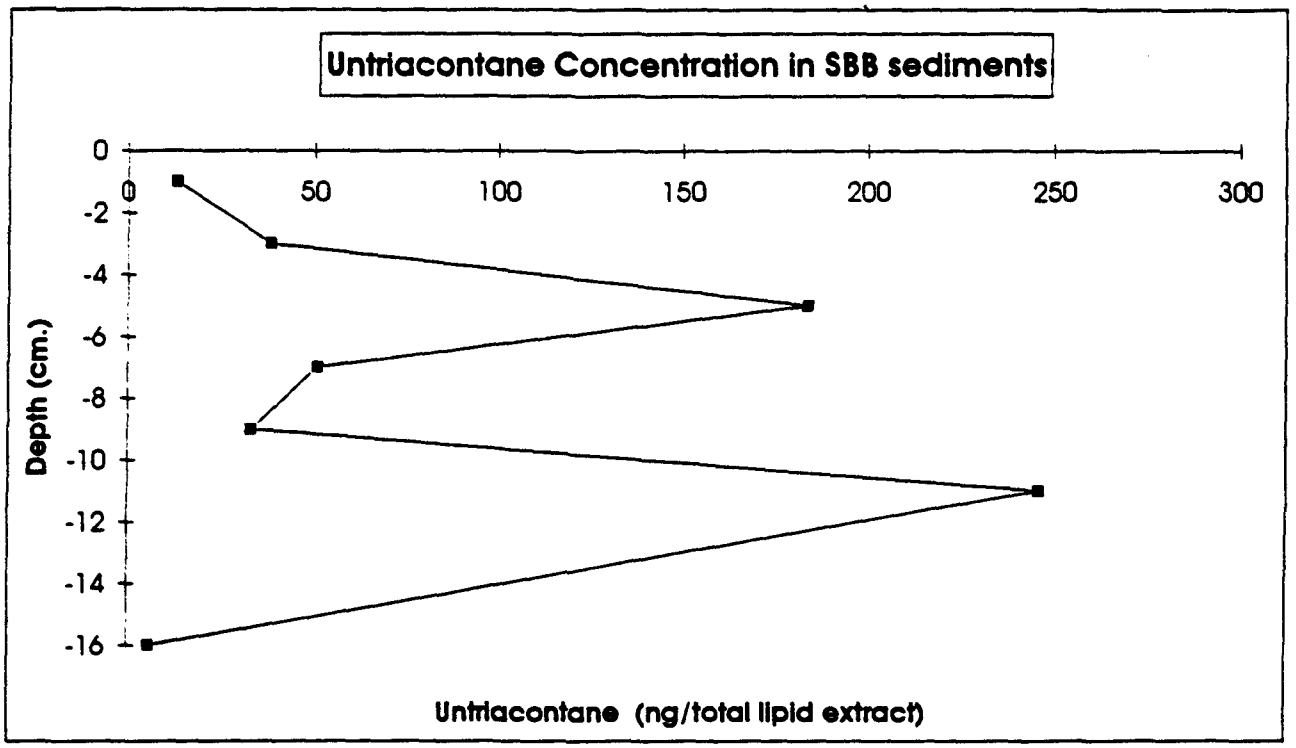

Figure 27. Depth profile for the concentration of untriacontane (C31) in the core of Santa Barbara Basin.

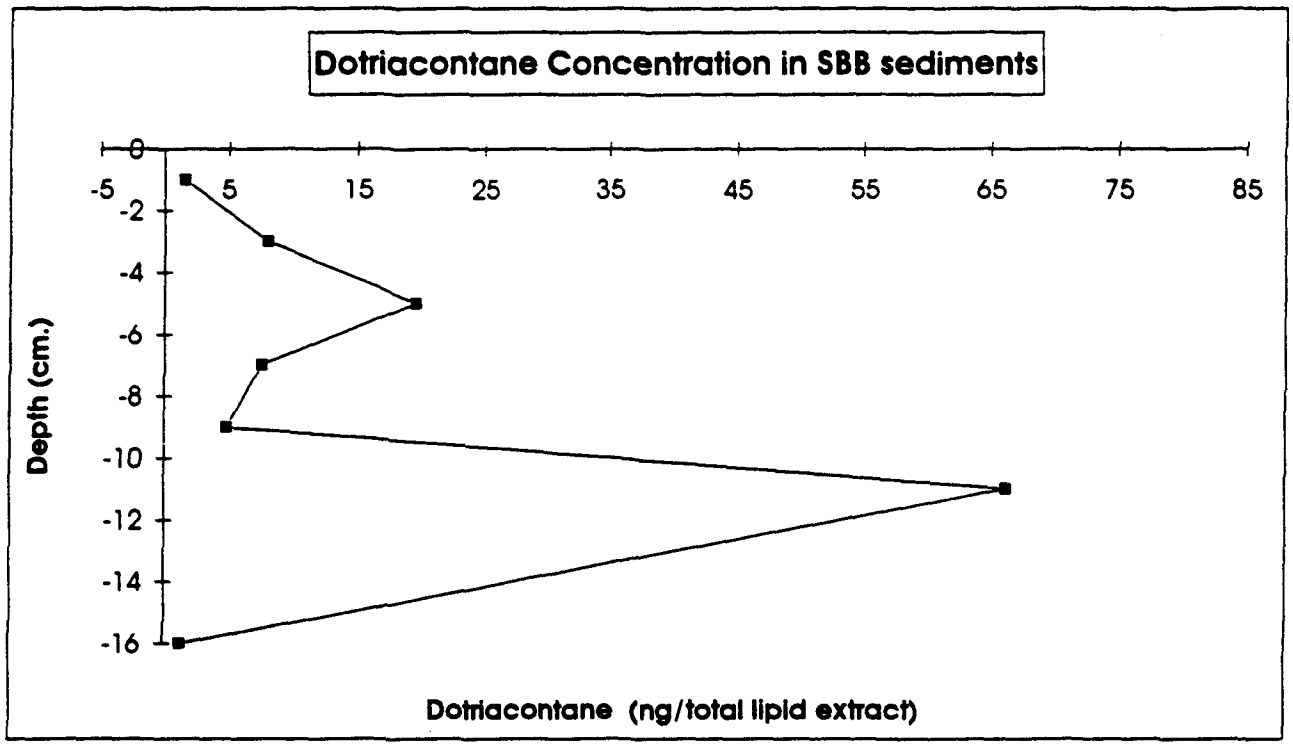

Figure 28. Depth profile for the concentration of dotriacontane (C32) in the core of Santa Barbara Basin.

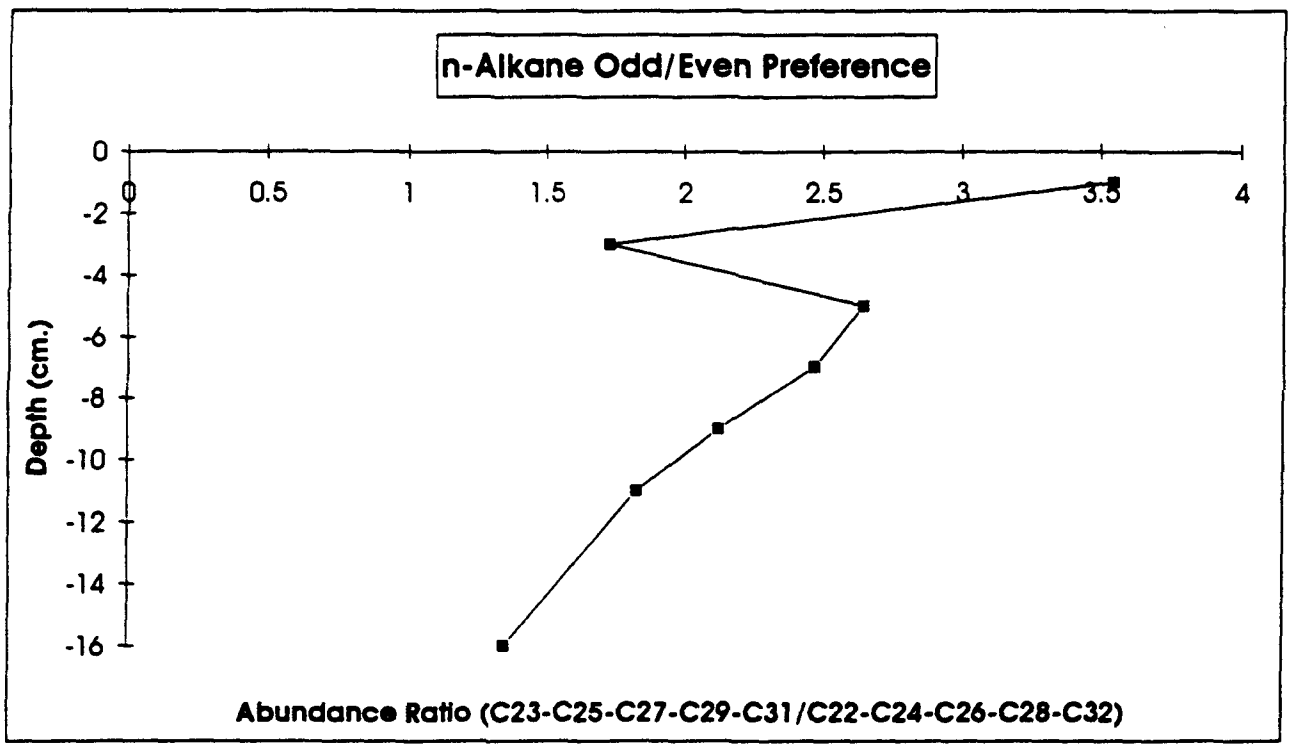

Figure 29. Depth profile for the carbon preference index or n-alakane odd/even preference in the core.

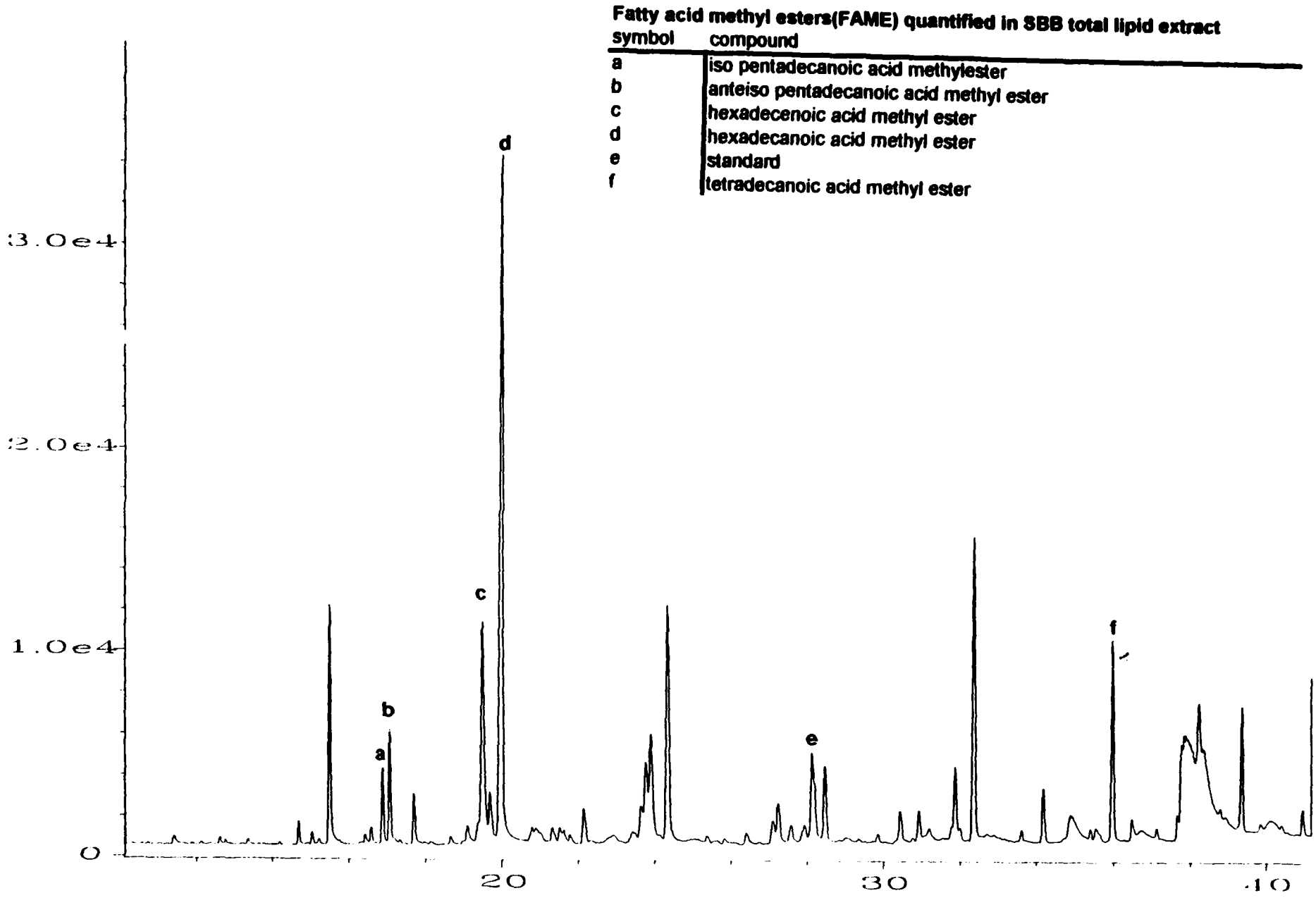

Figure 30. Partial GC chromatogram of the FAME fraction from liquid chromatography of total lip extract neutrals (0-2 cm depth).

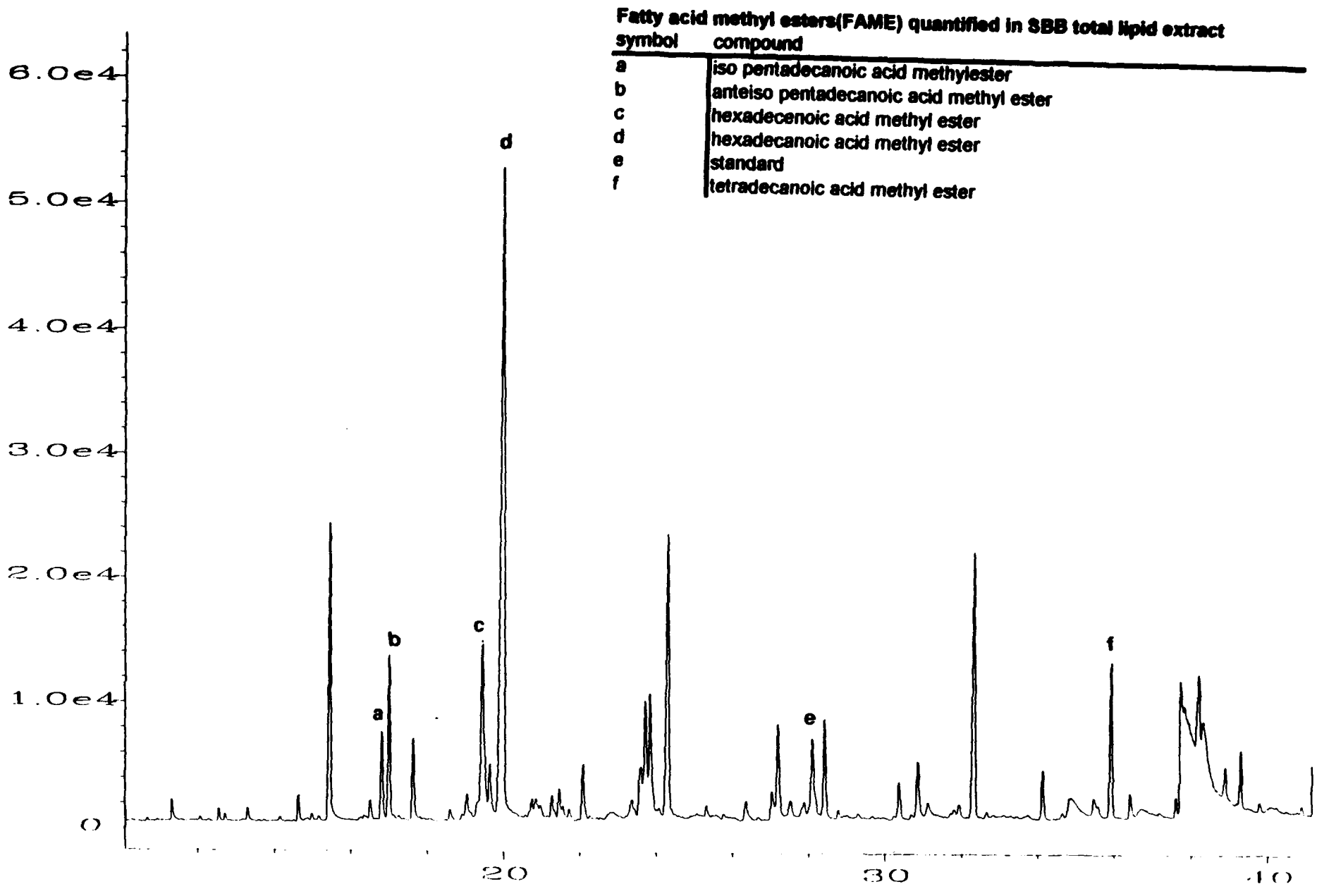

Figure 31. Partial GC chromatogram of the FAME fraction from liquid chromatography of total lip extract neutrals (2-4 cm depth).

Sig. 1 in C:\HPCHEM\1\DATA\FAMES.NV-FO171.D

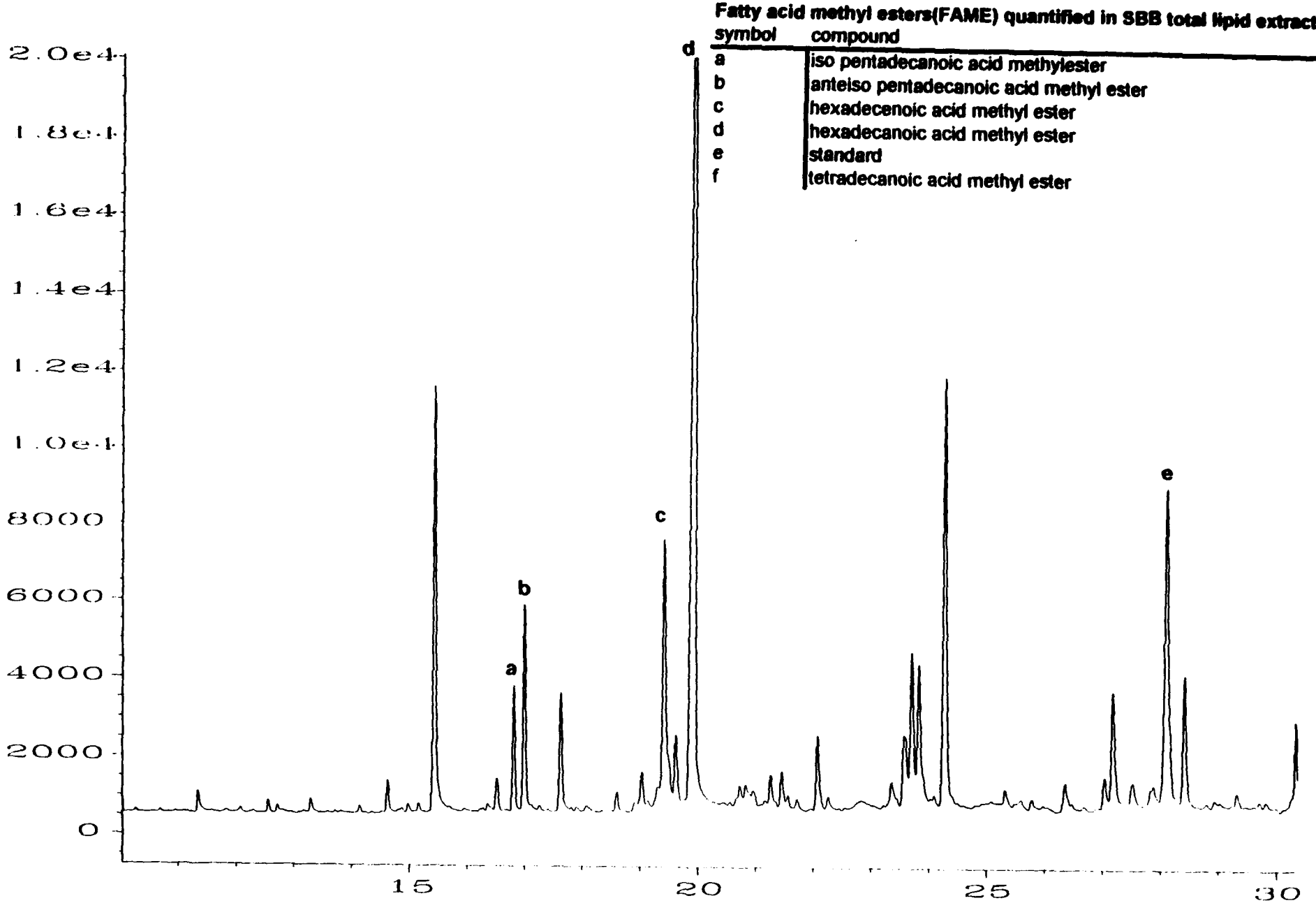

Figure 32. Partial GC chromatogram of the FAME fraction from liquid chromatography of total lip extract neutrals (4-6 cm depth).

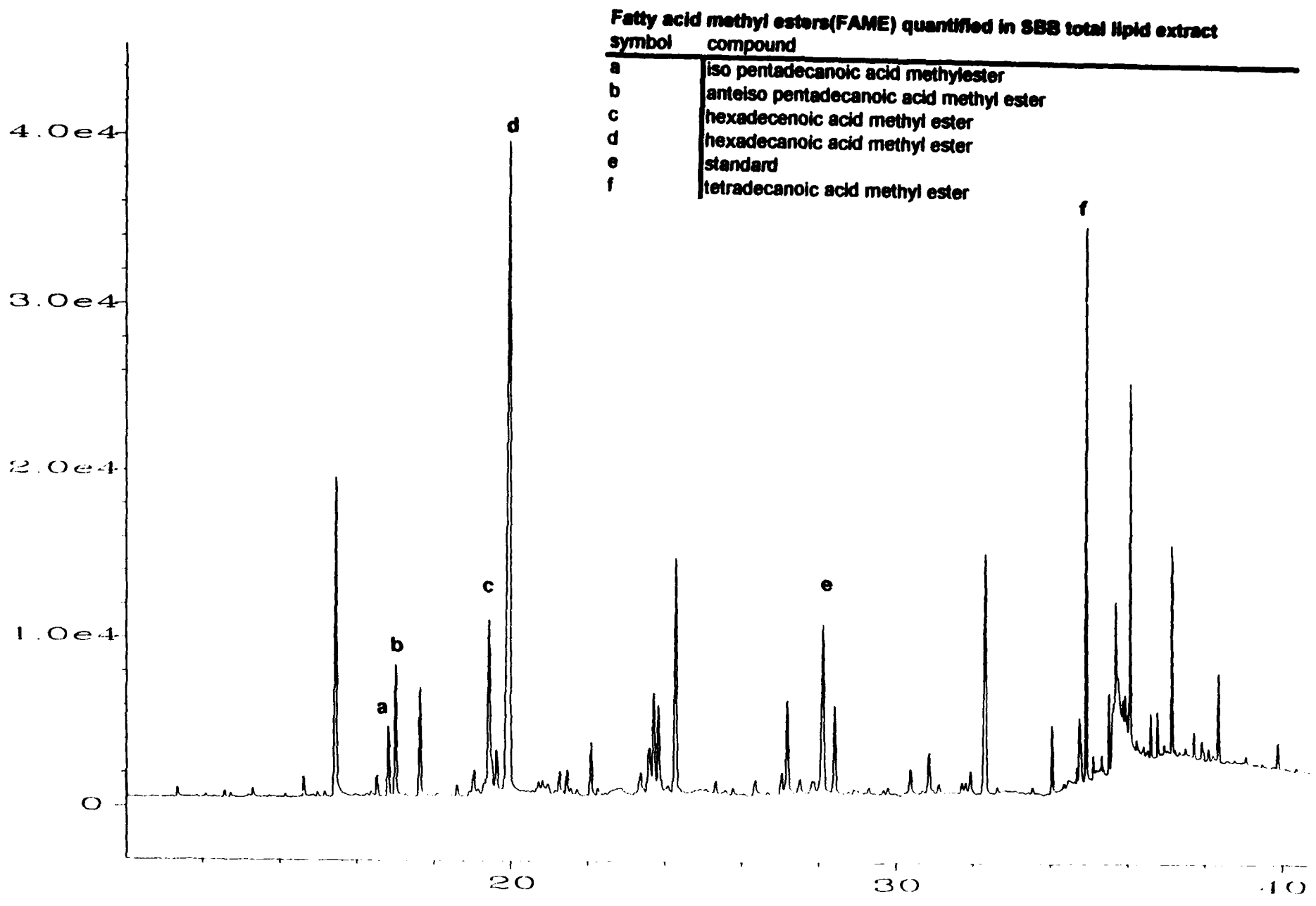

Figure 33. Partial GC chromatogram of the FAME fraction from liquid chromatography of total lip extract neutrals (8-10 cm depth).

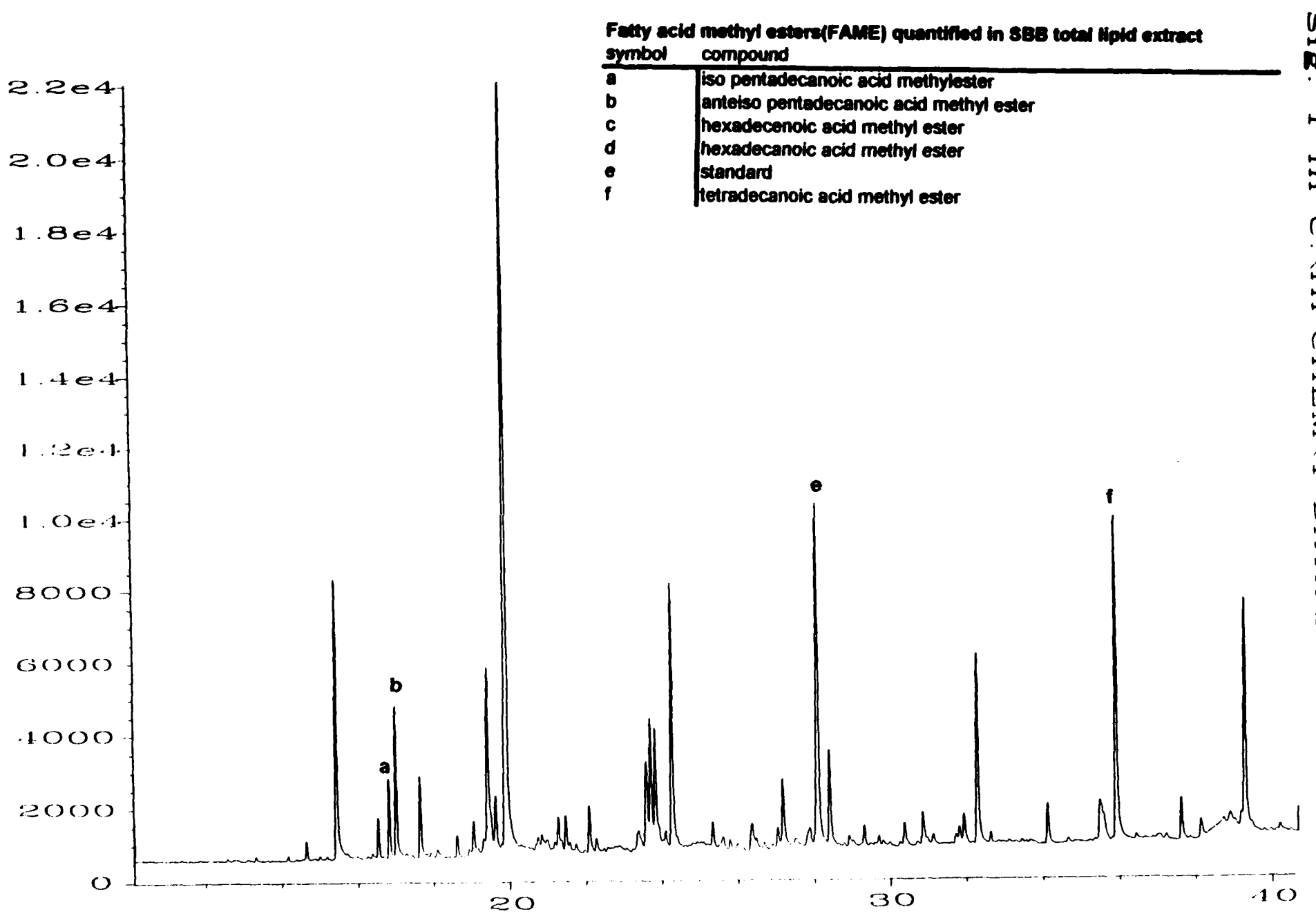

Figure 34. Partial GC chromatogram of the FAME fraction from liquid chromatography of total lip extract neutrals (10-12 cm depth).

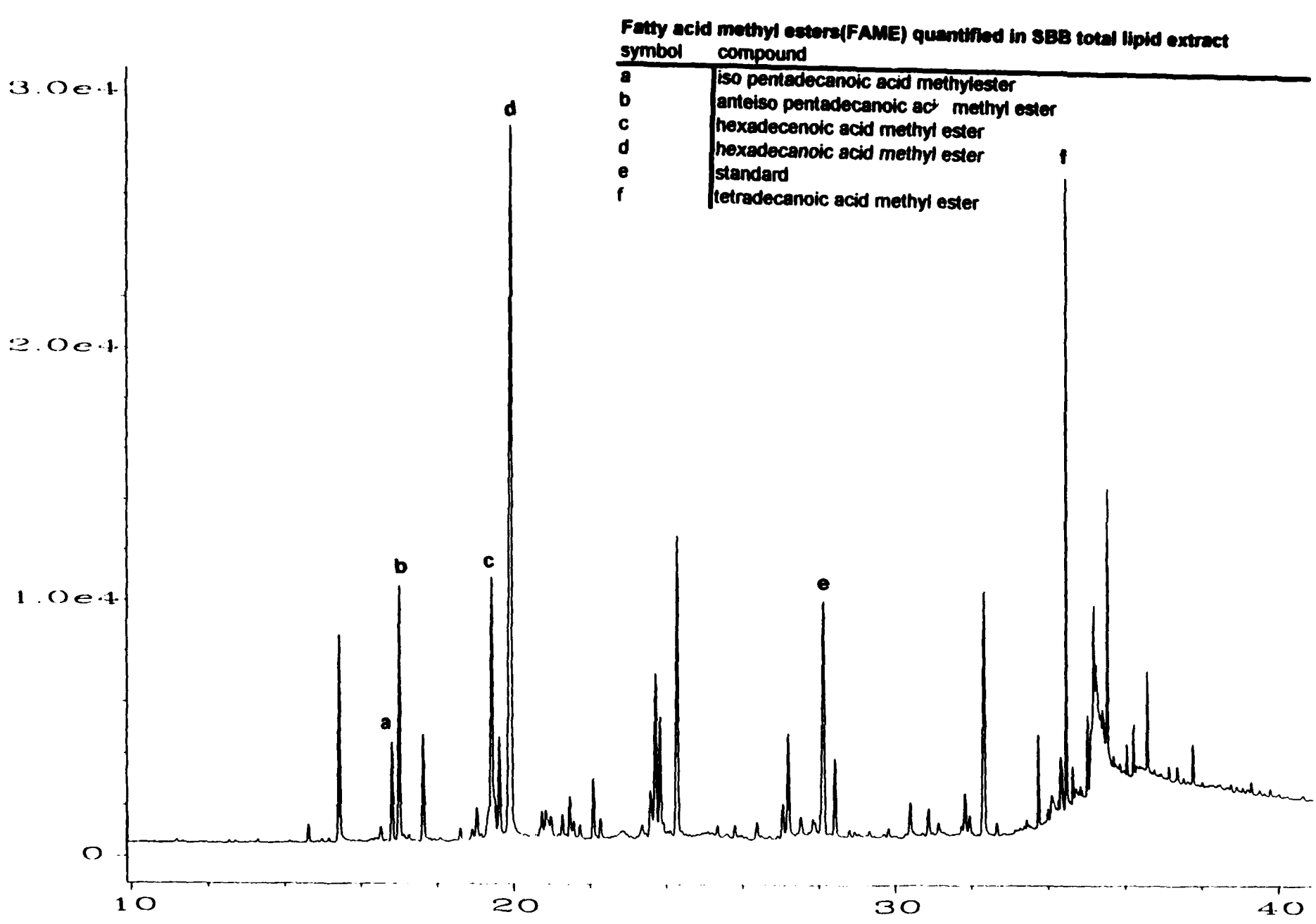

Figure 35. Partial GC chromatogram of the FAME fraction from liquid chromatography of total lip extract neutrals (14-18 cm depth).

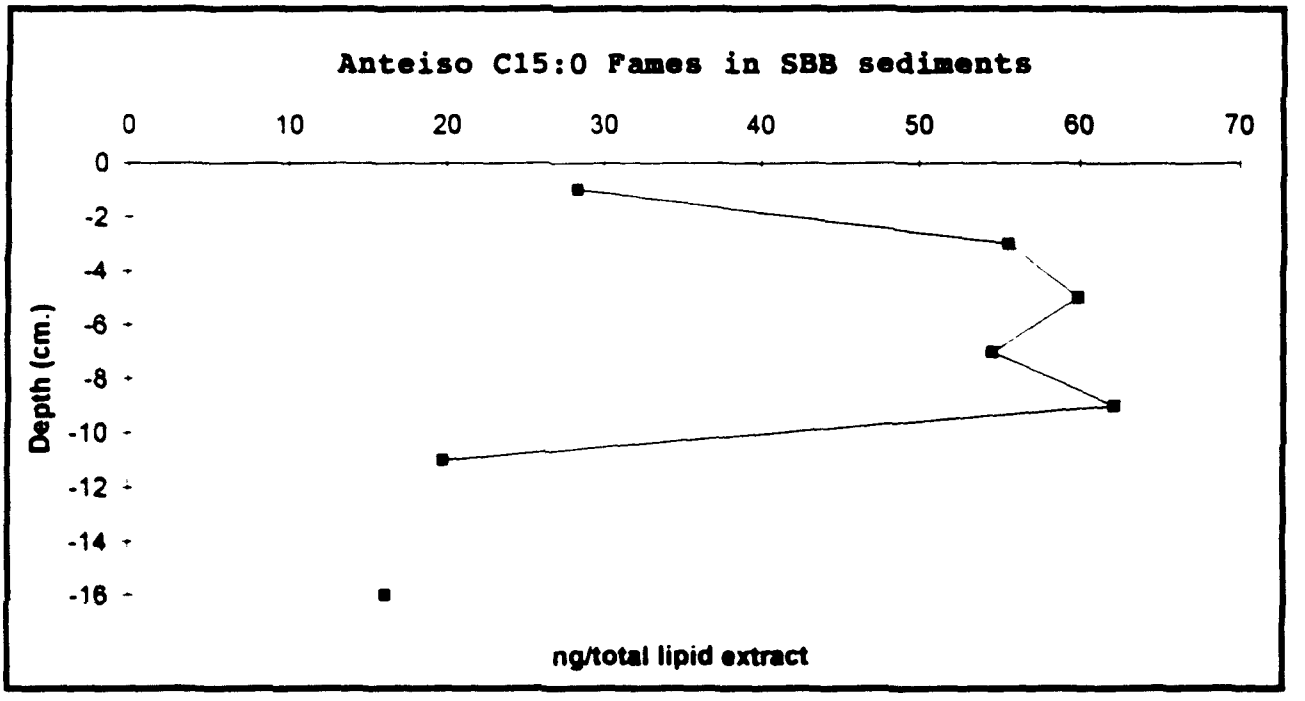

Figure 36. Depth profile of the anteiso C15 FAMEs.

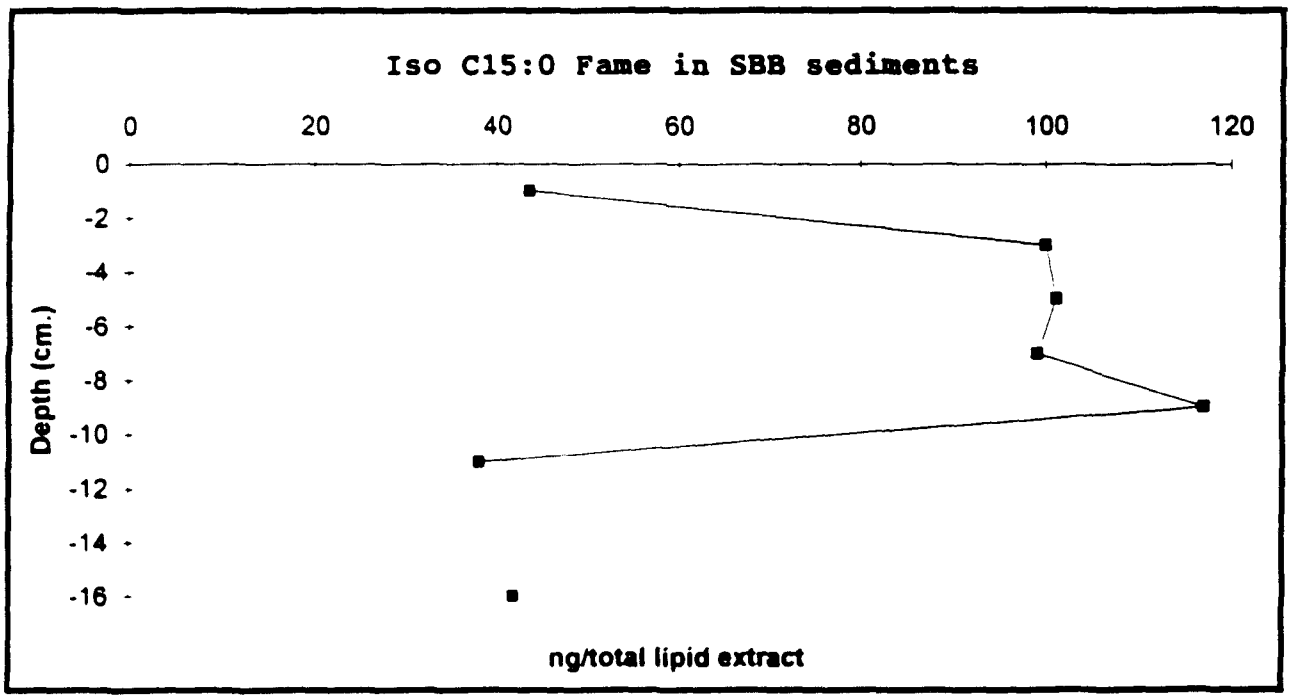

Figure 37. Depth profile of the iso C15 FAMEs.

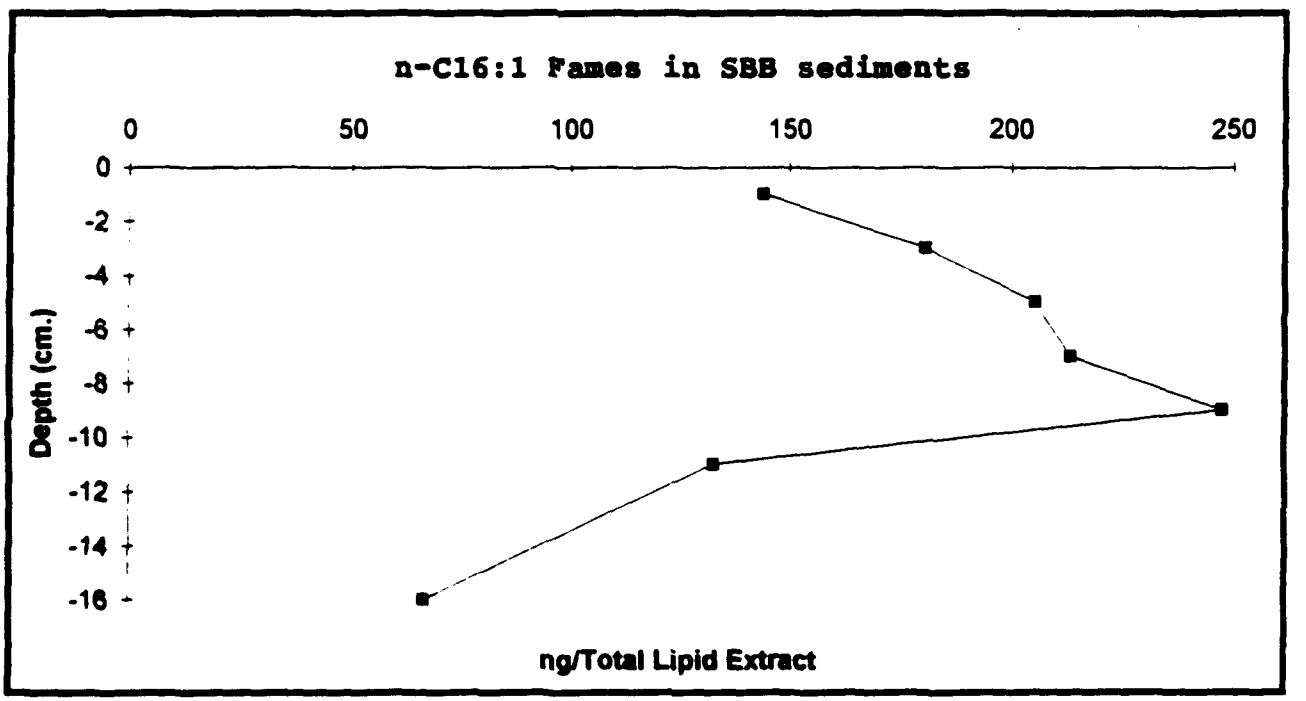

Figure 38. Depth profile of the monunsaturated C16 FAMEs.

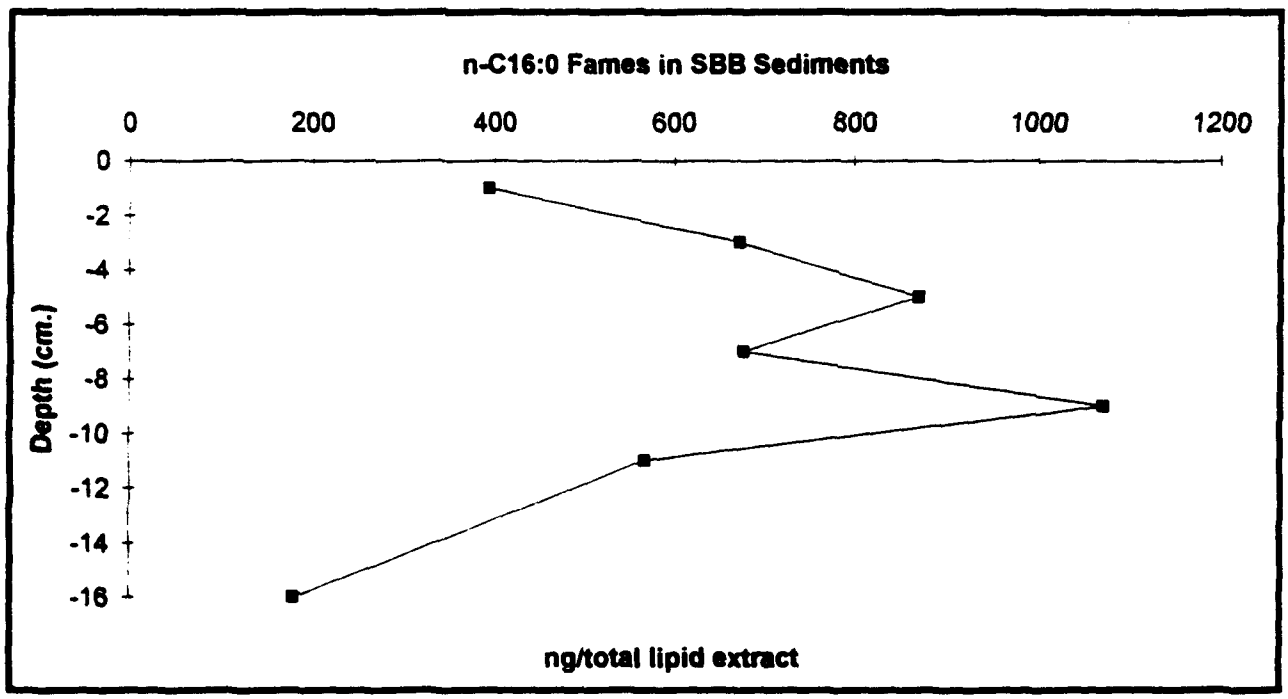

Figure 39. Depth profile of the saturated C16 FAMEs.

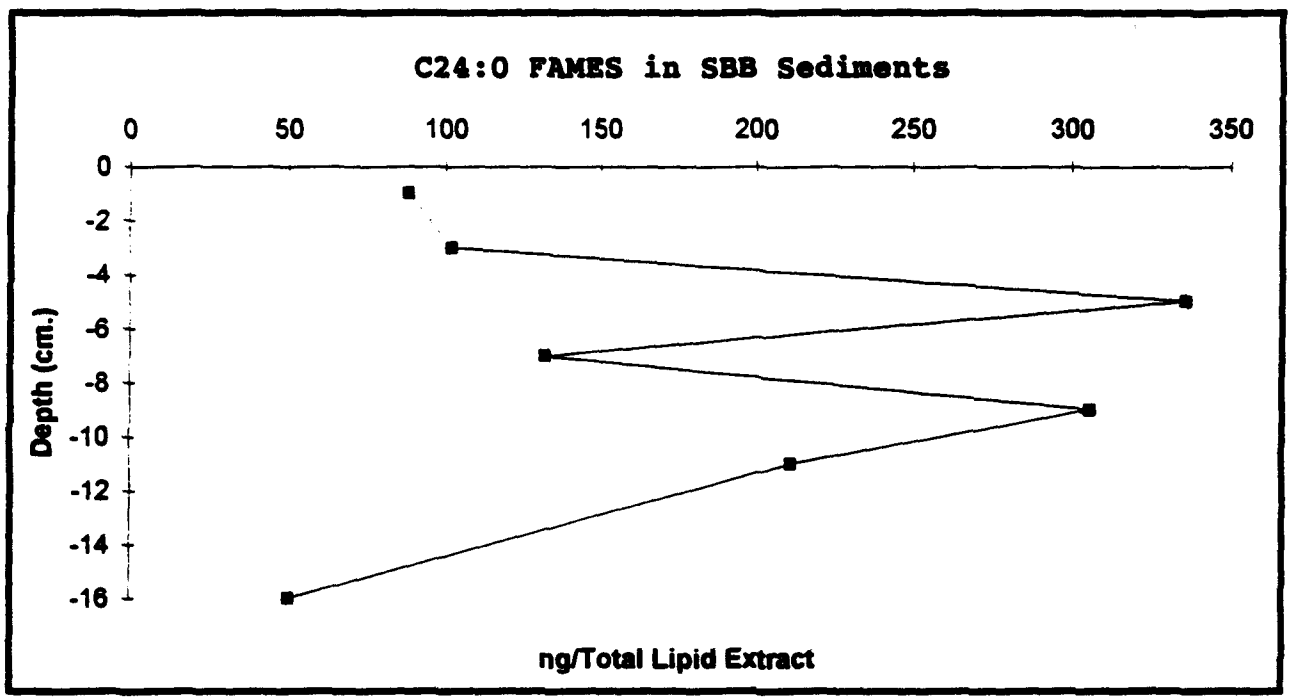

Figure 40. Depth profile of the saturated C24 FAMEs.

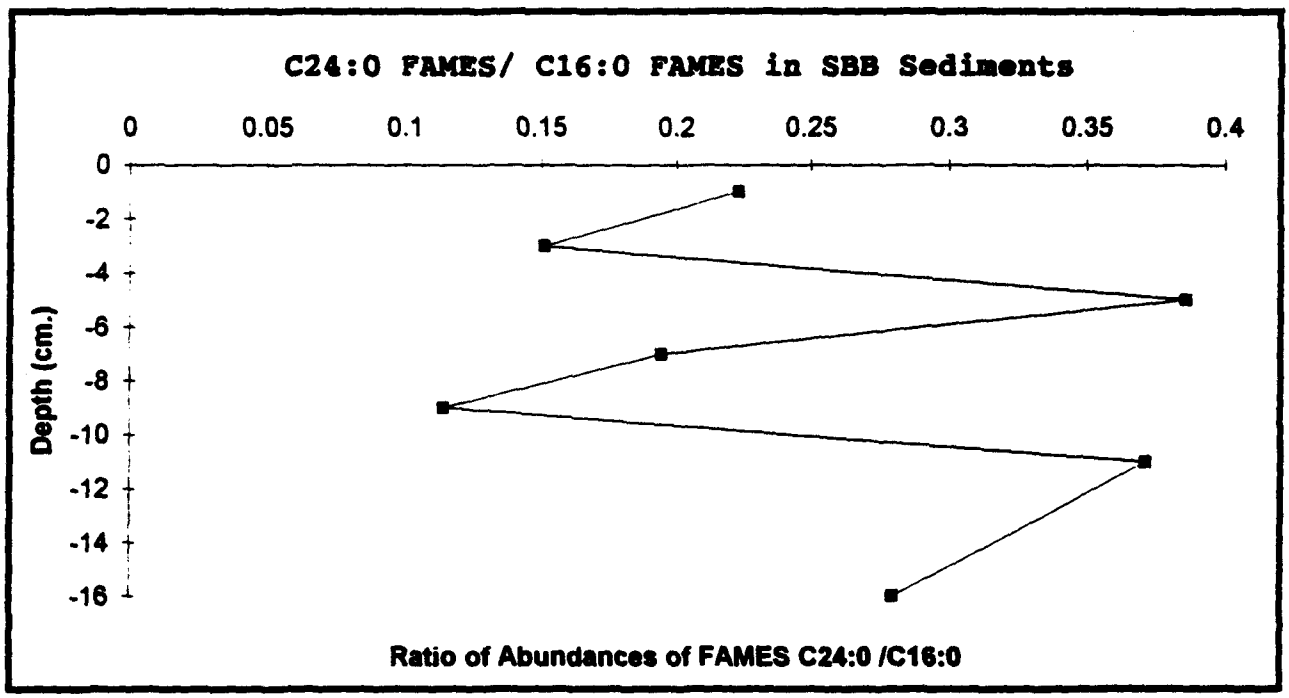

Figure 41. Depth profile of the ratio of saturated C24 FAME to the saturated C16 FAME.

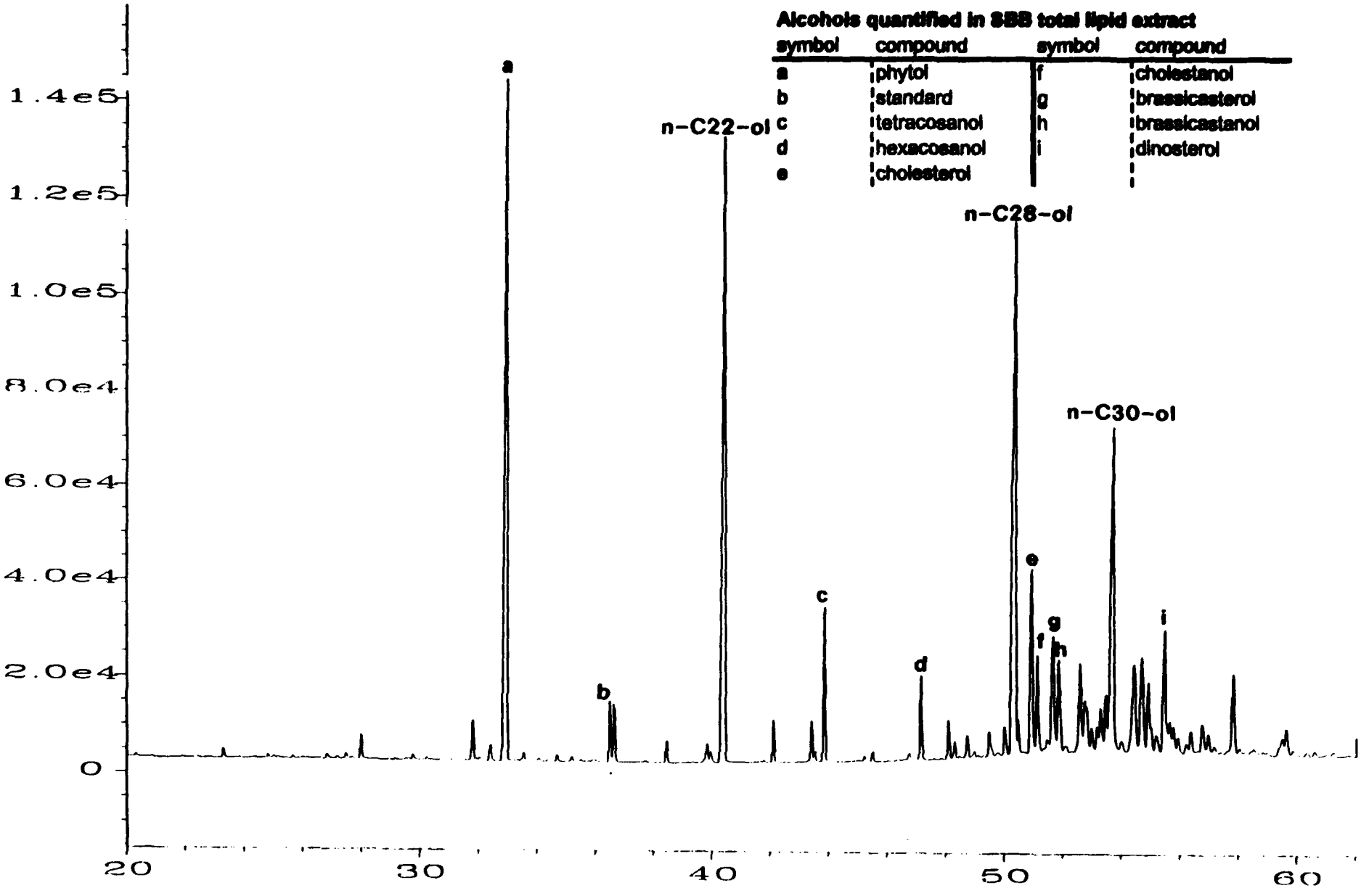

Figure 42. Partial GC chromatogram of the alcohol fraction from liquid chromatography of the total lipid extract neutrals (0-2 cm depth).

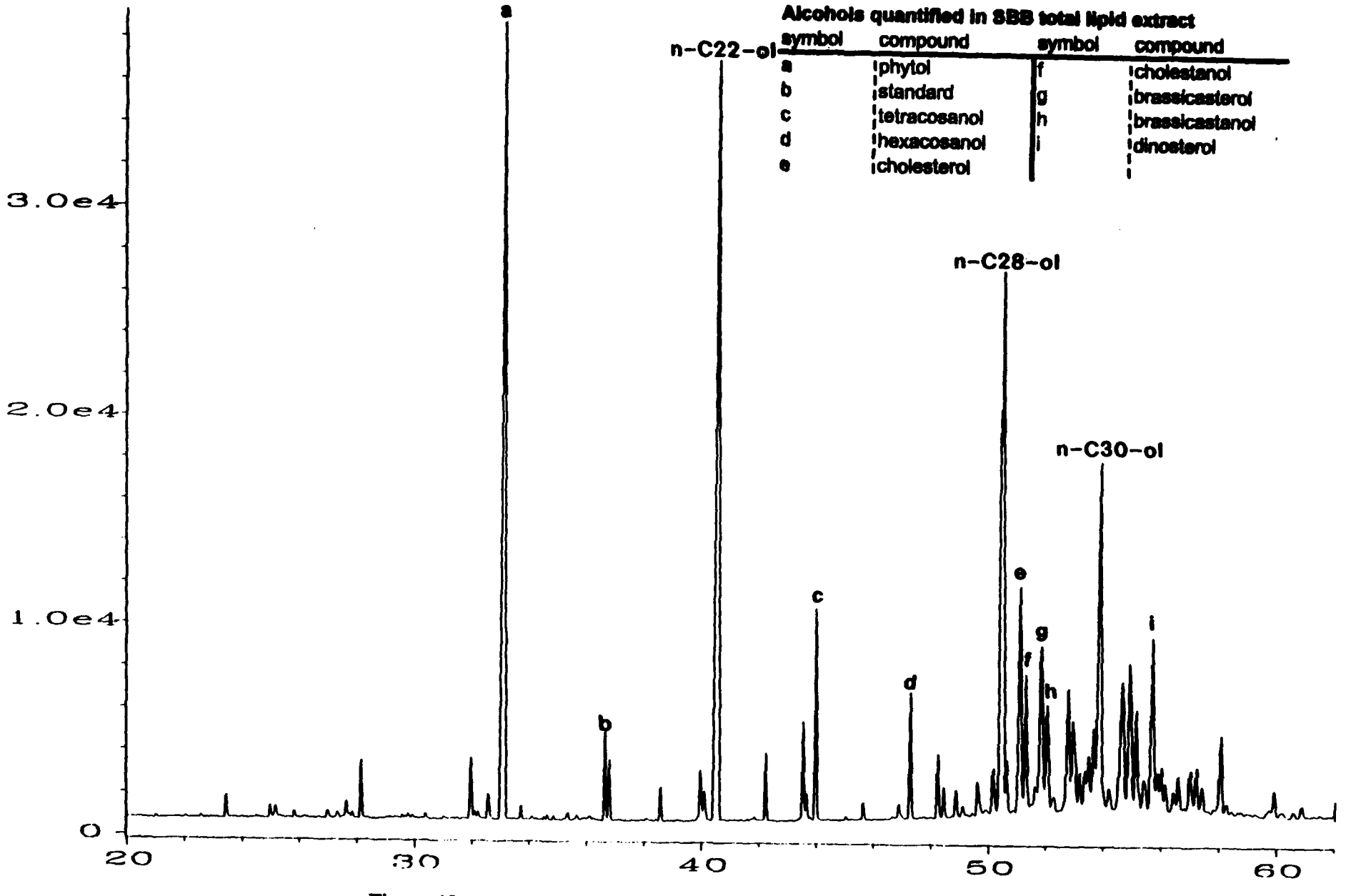

Figure 43. Partial GC chromatogram of the alcohol fraction from liquid chromatography of the total lipid extract neutrals (2-4 cm depth).

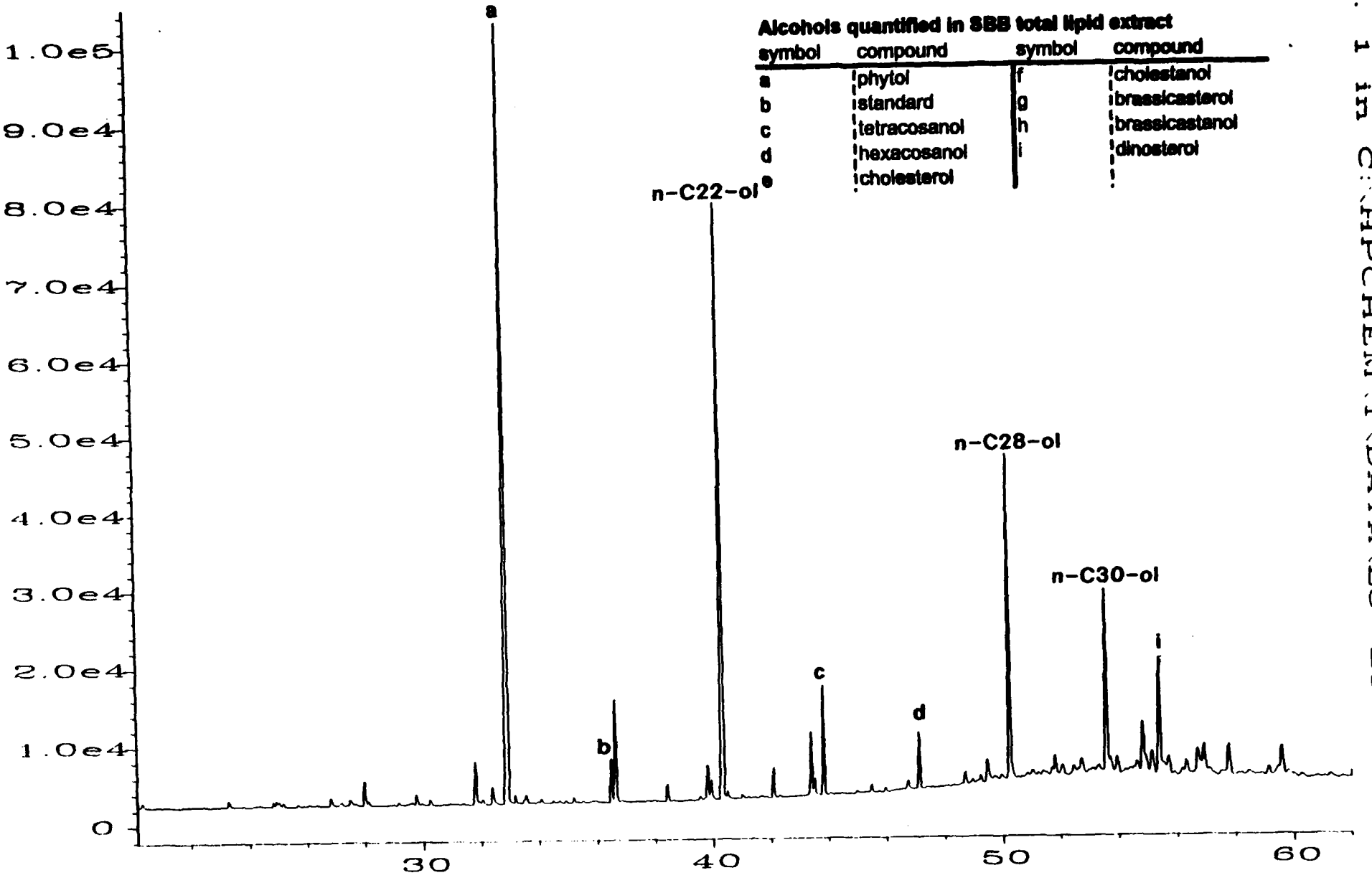

Figure 44. Partial GC chromatogram of the alcohol fraction from liquid chromatography of the total lipid extract neutrals (4-6 cm depth).

Sig. 1 in C:\HPCHEM\1\DATA\L5-L6.NV-FO129.D

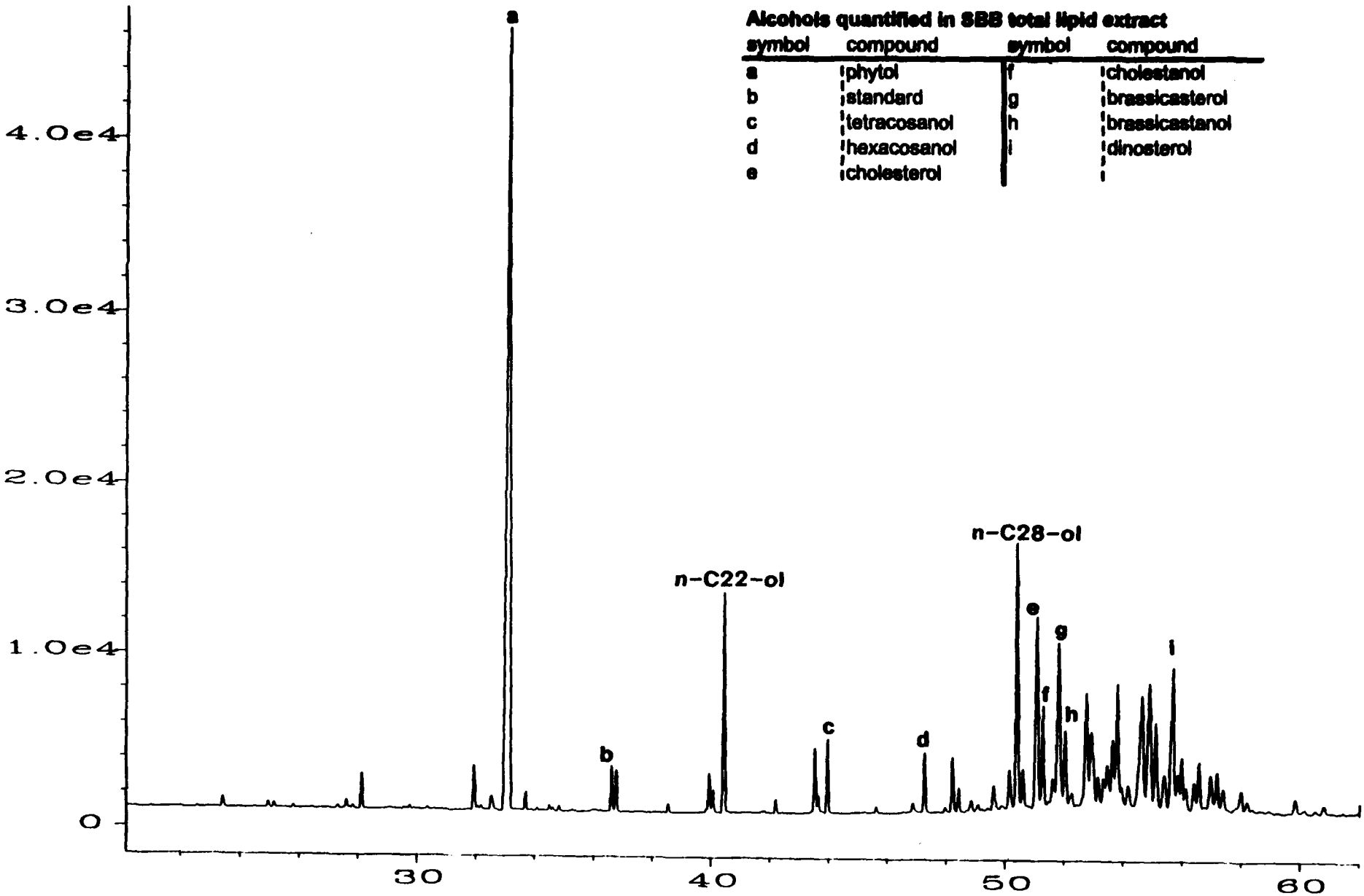

Figure 45. Partial GC chromatogram of the alcohol fraction from liquid chromatography of the total lipid extract neutrals (6-8 cm depth).

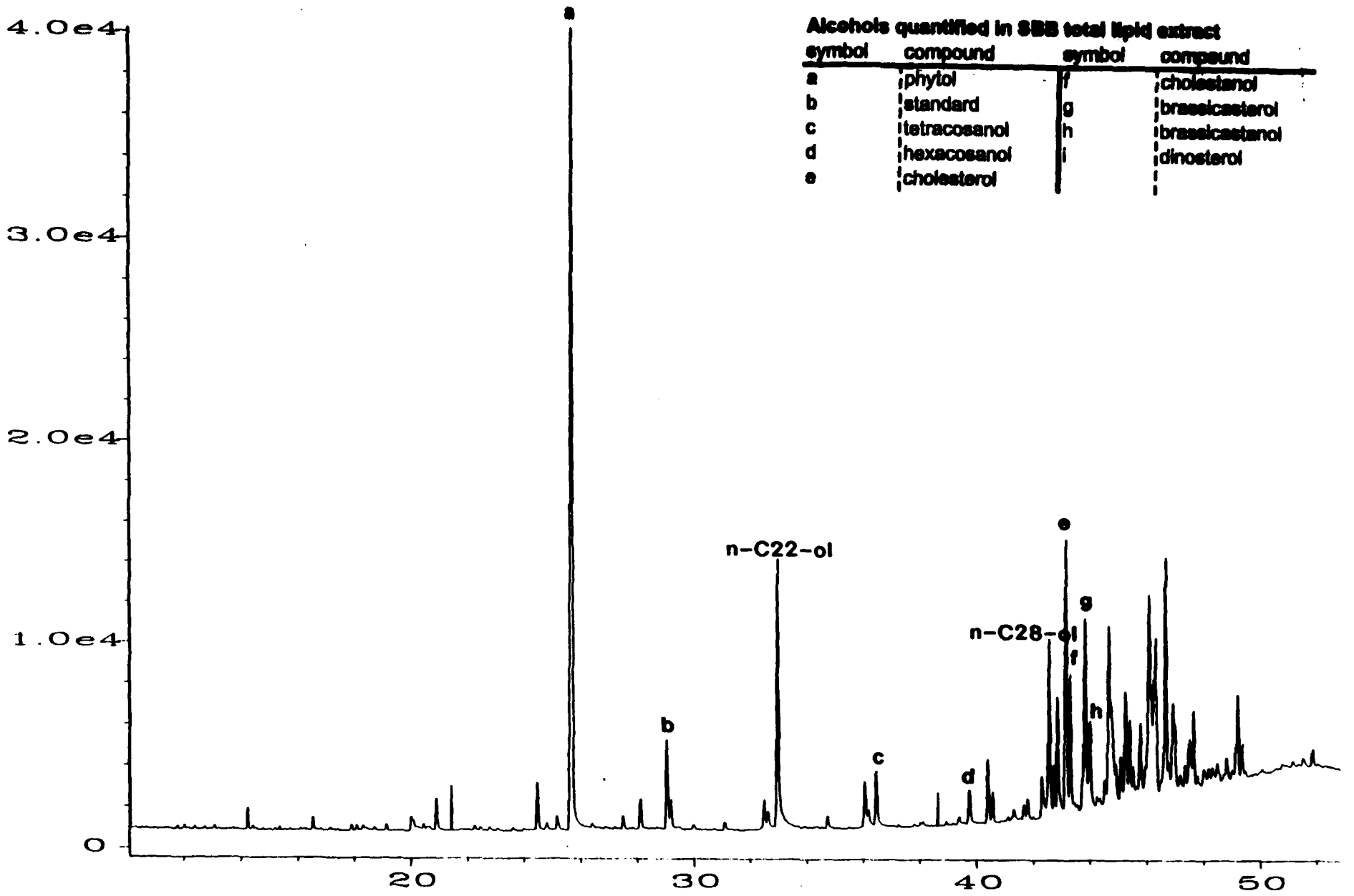

Figure 46. Partial GC chromatogram of the alcohol fraction from liquid chromatography of the total lipid extract neutrals (8-10 cm depth).

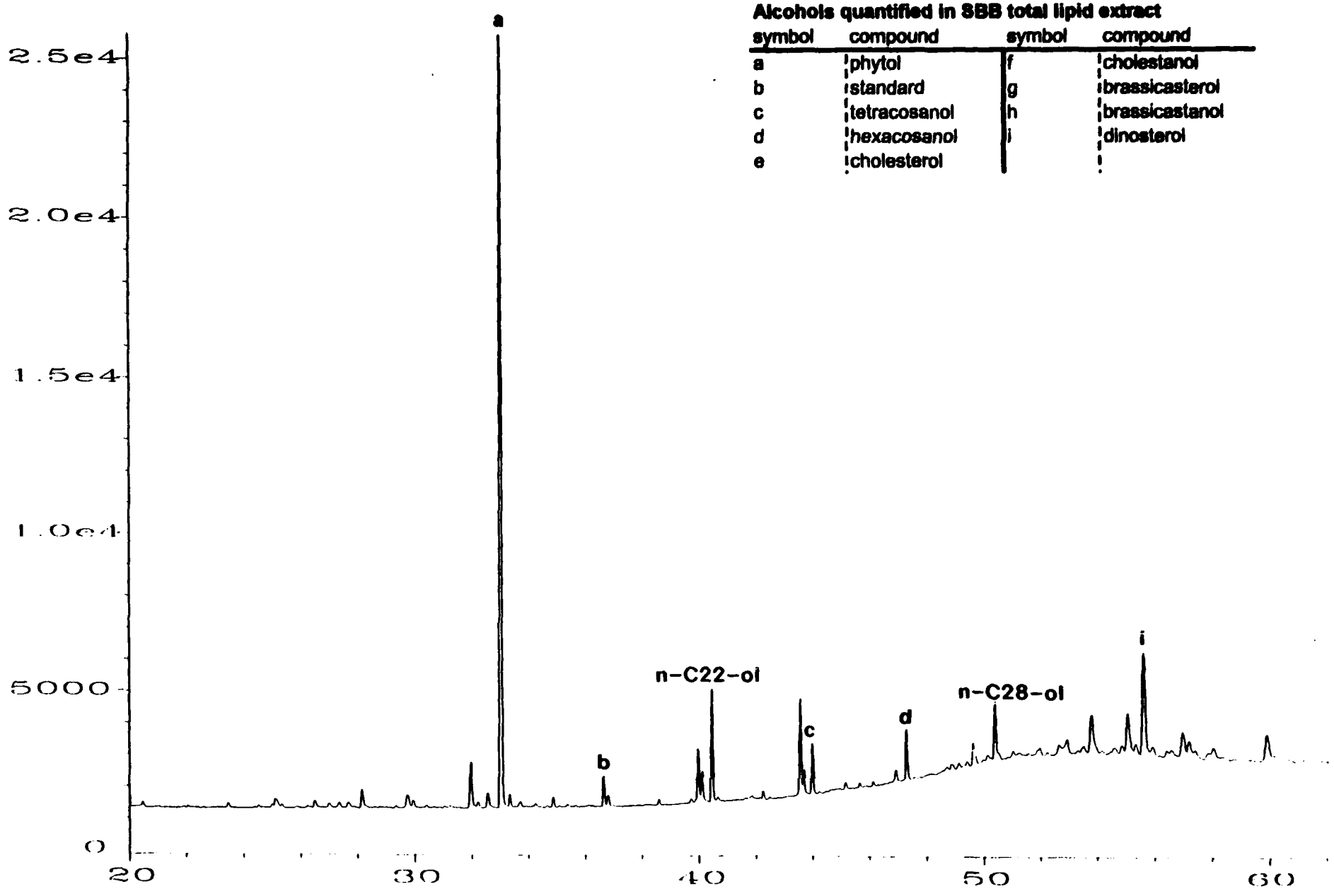

Figure 47. Partial GC chromatogram of the alcohol fraction from liquid chromatography of the total lipid extract neutrals (10-12 cm depth).

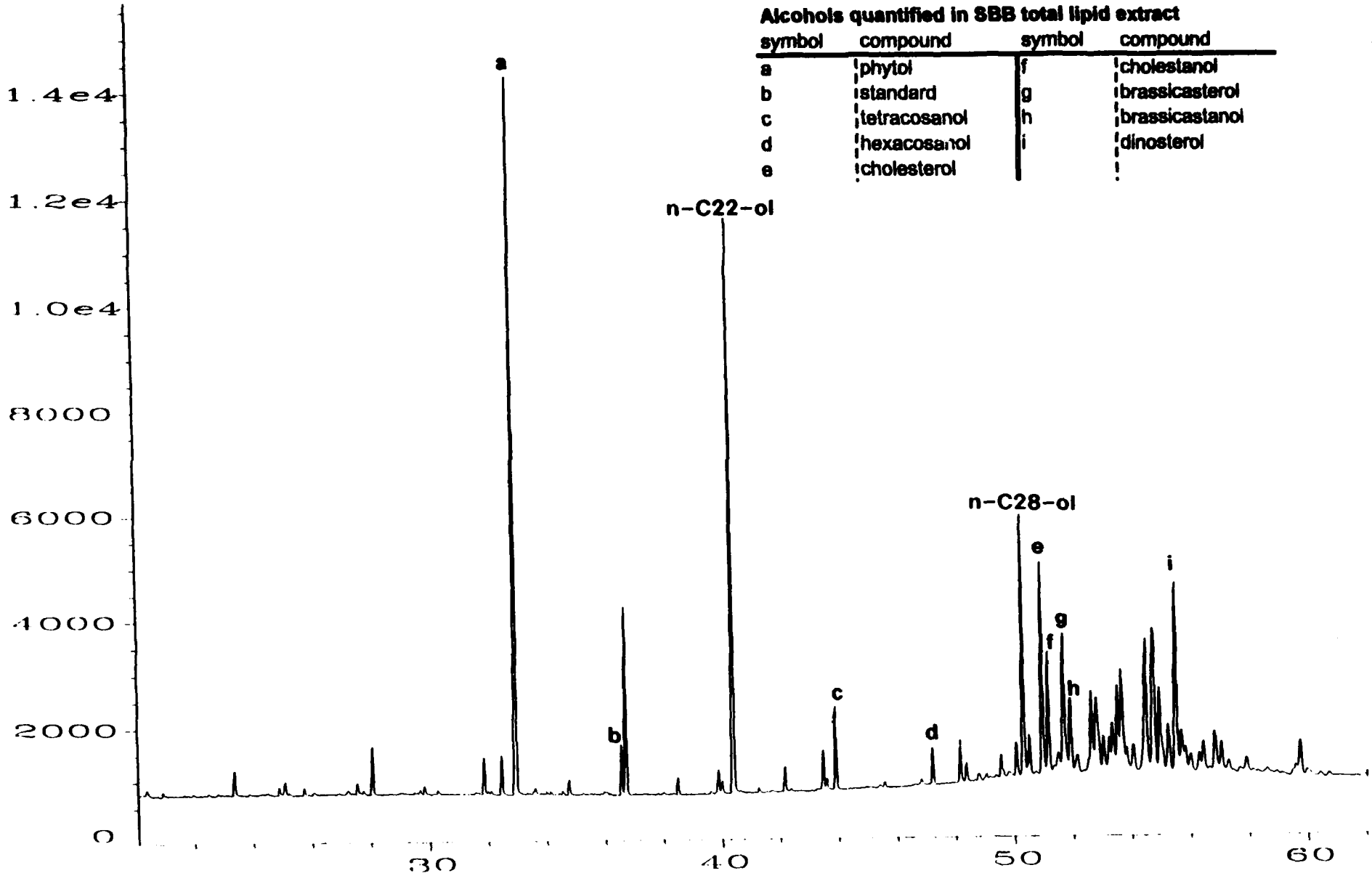

Figure 48. Partial GC chromatogram of the alcohol fraction from liquid chromatography of the total lipid extract neutrals (14-18 cm depth).

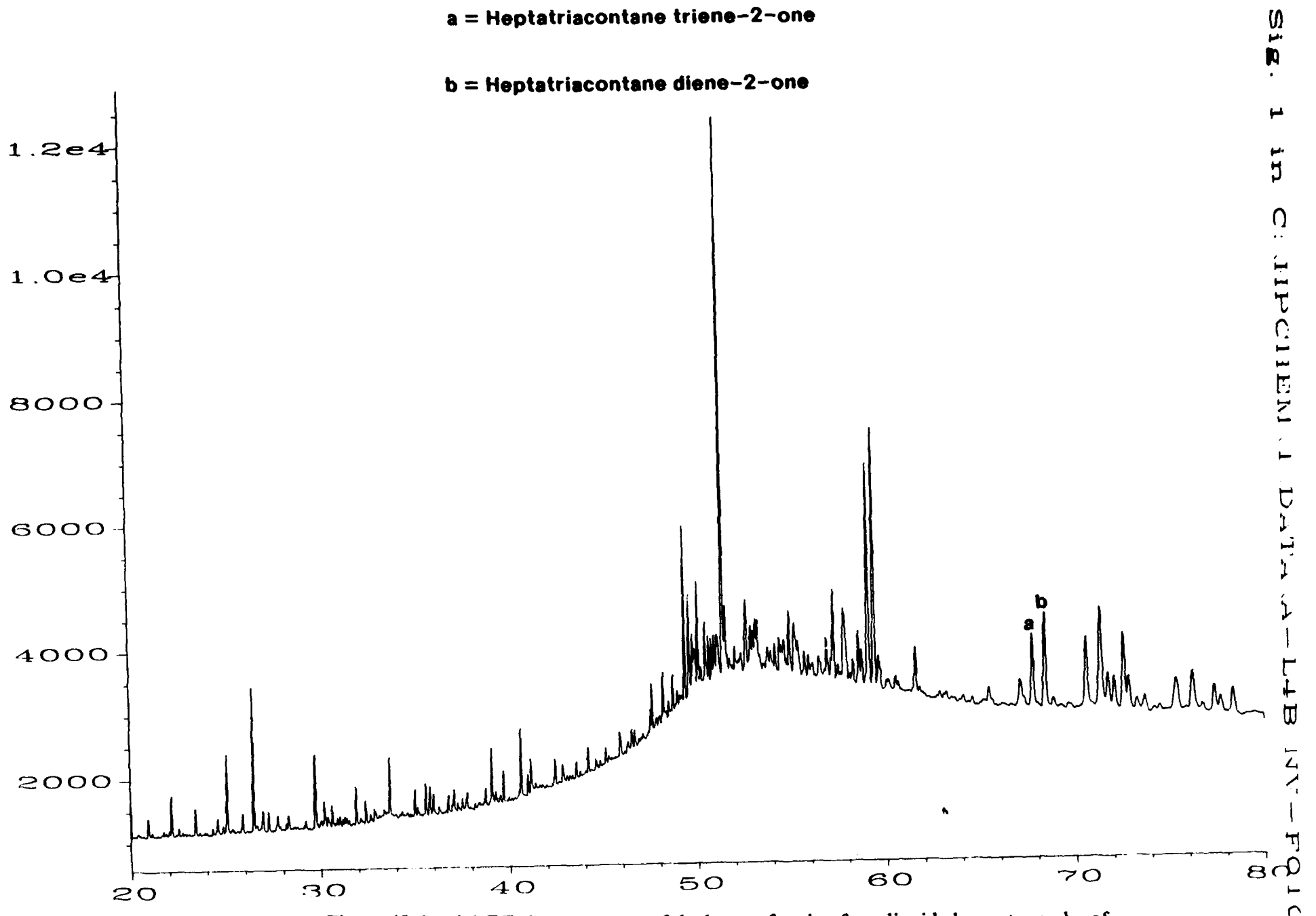

Figure 49. Partial GC chromatogram of the ketone fraction from liquid chromatography of the total lipid extract neutrals (0-2 cm depth).

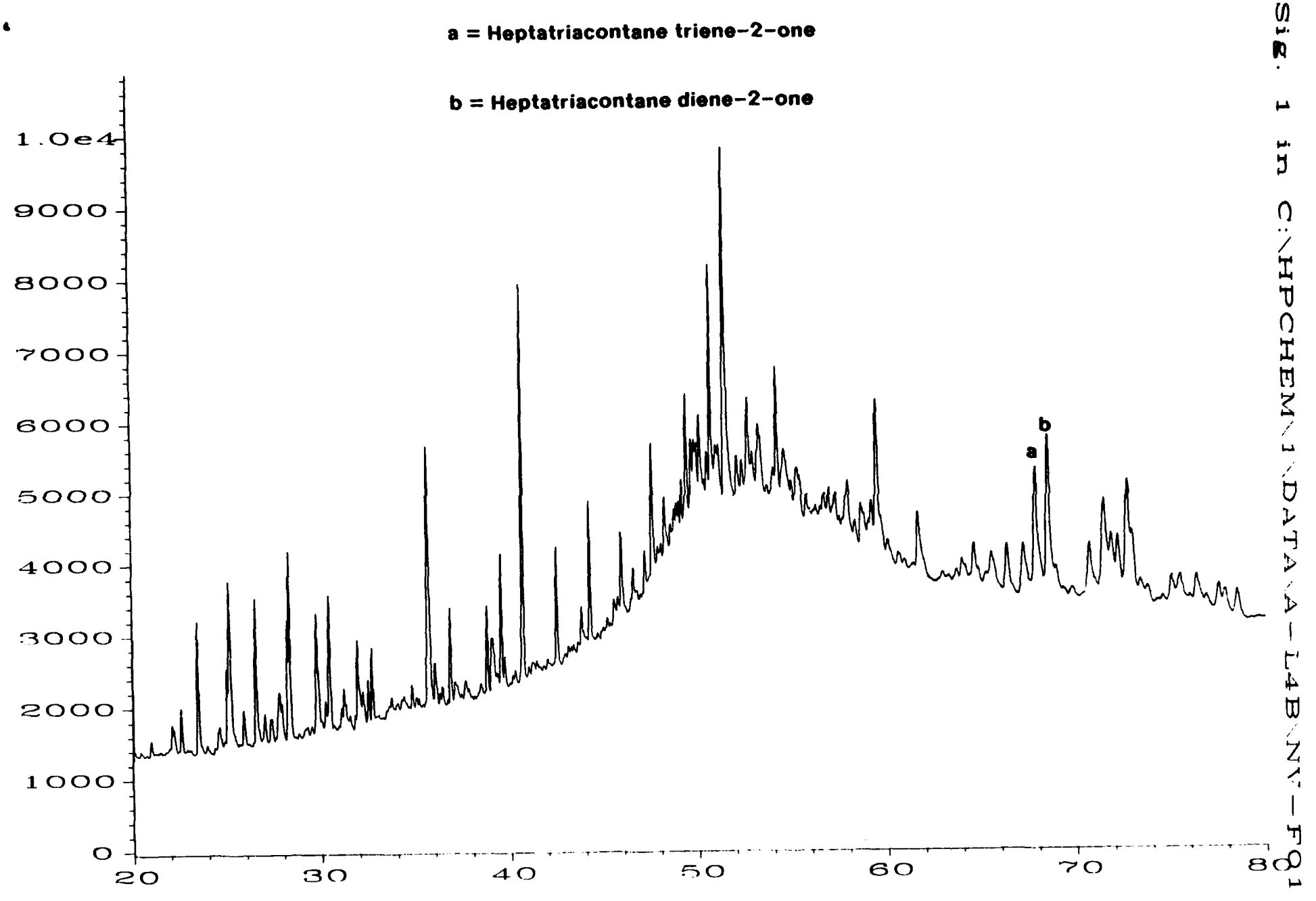

Figure 50. Partial GC chromatogram of the ketone fraction from liquid chromatography of the total lipid extract neutrals (2-4cm depth).

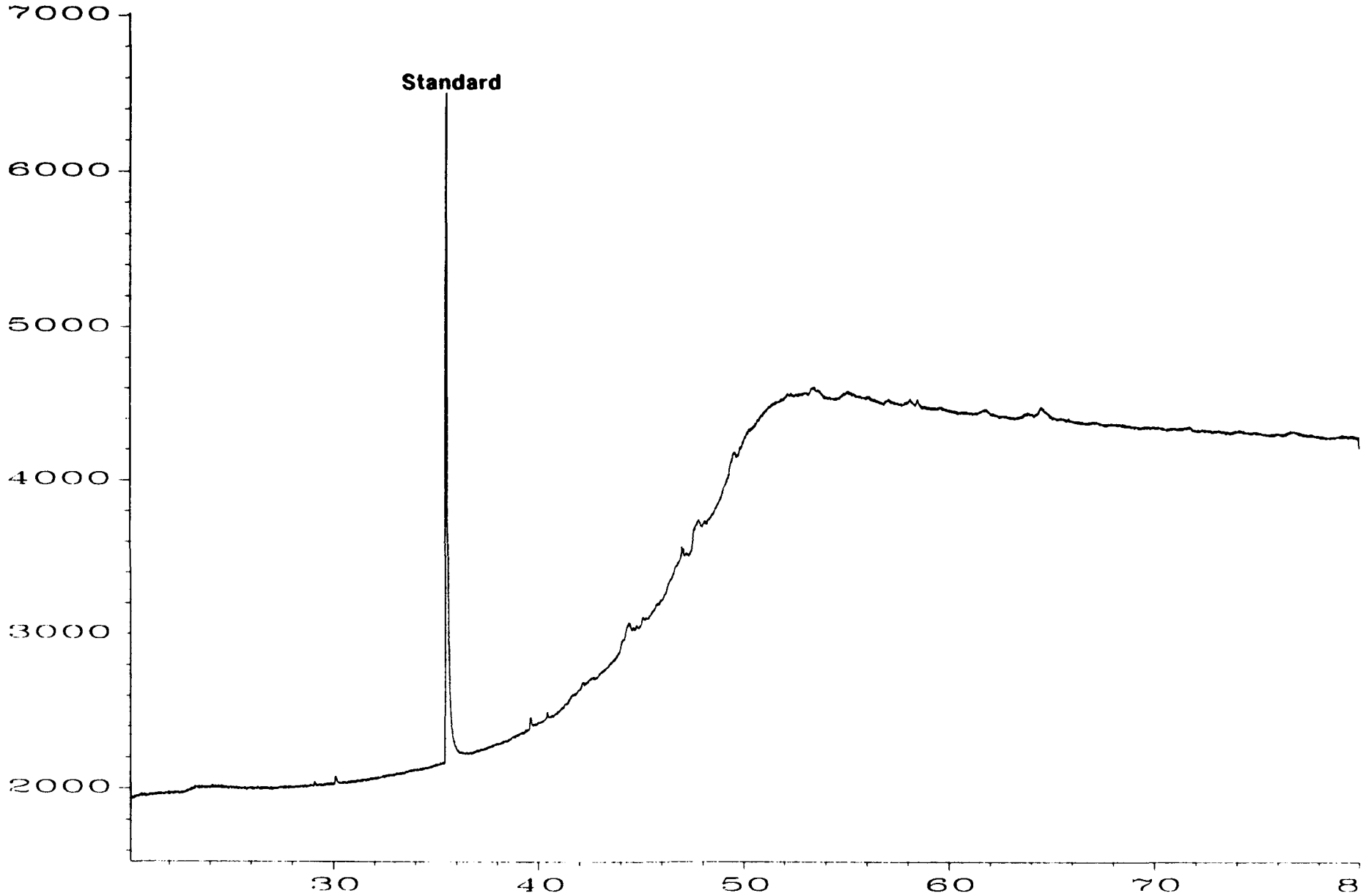

Figure 51. Partial GC chromatogram of the ketone fraction from liquid chromatography of the total lipid extract neutrals (4-6 cm depth).

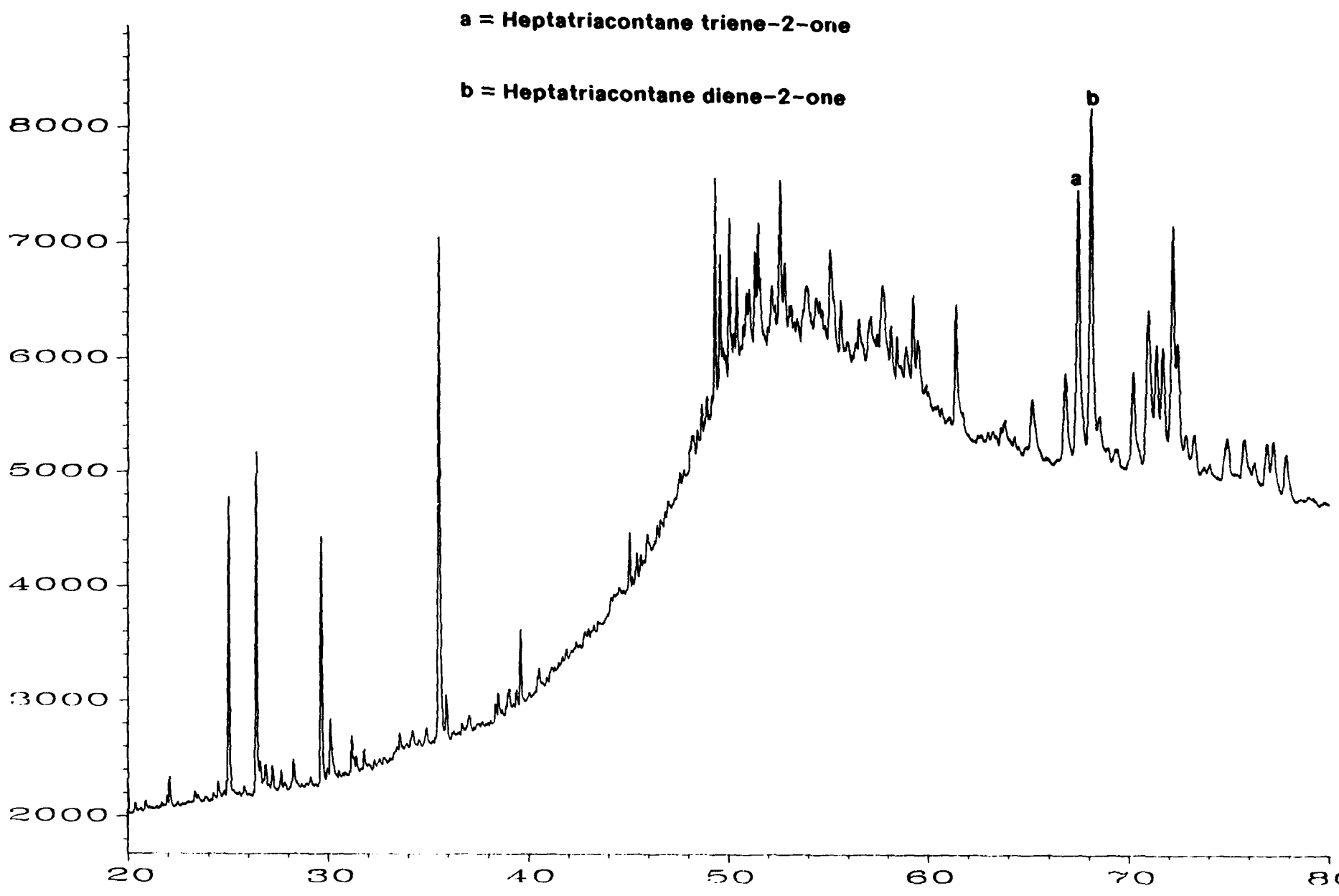

Figure 52. Partial GC chromatogram of the ketone fraction from liquid chromatography of the total lipid extract neutrals (6-8 cm depth).

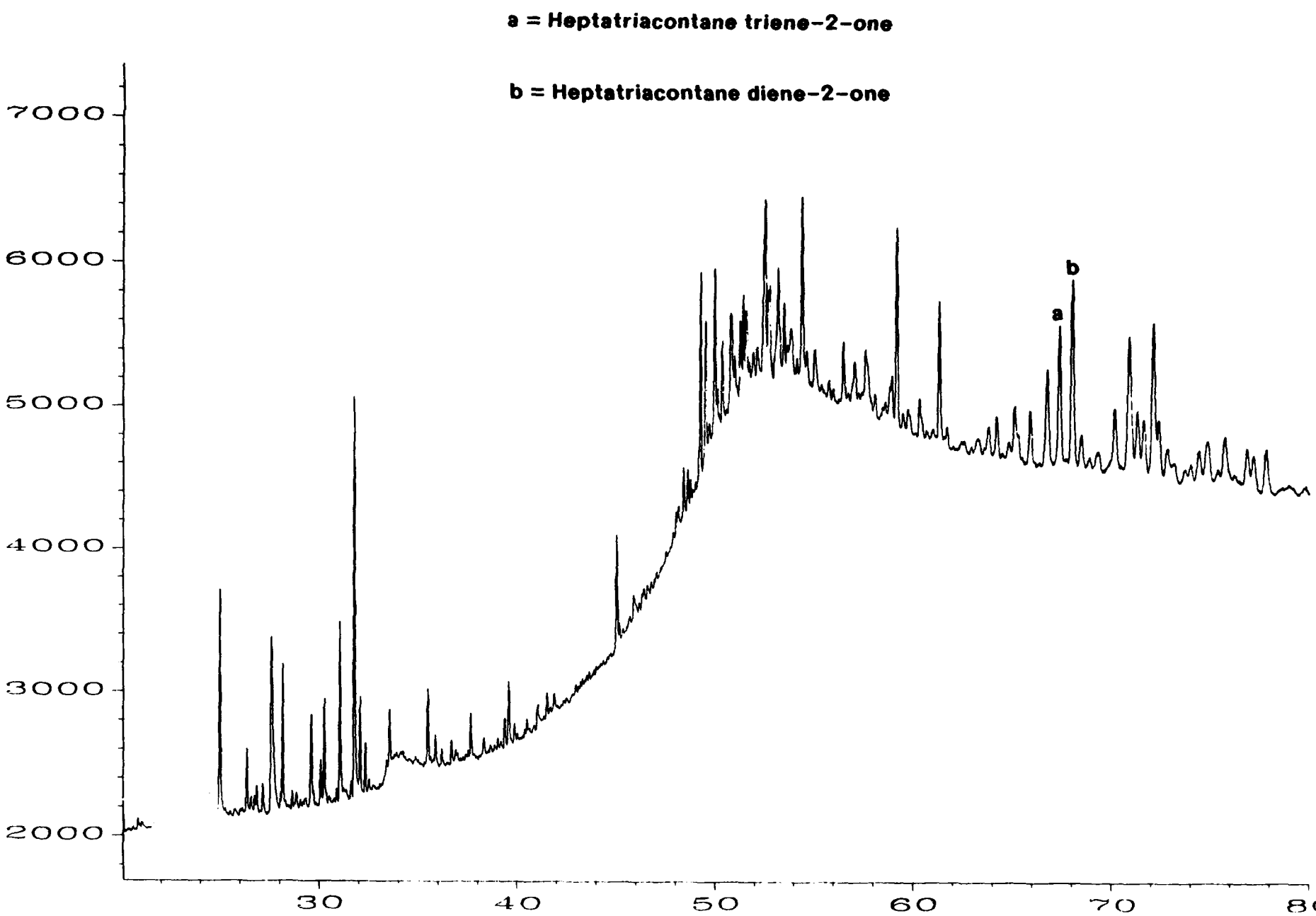

Figure 53. Partial GC chromatogram of the ketone fraction from liquid chromatography of the total lipid extract neutrals (8-10 cm depth).

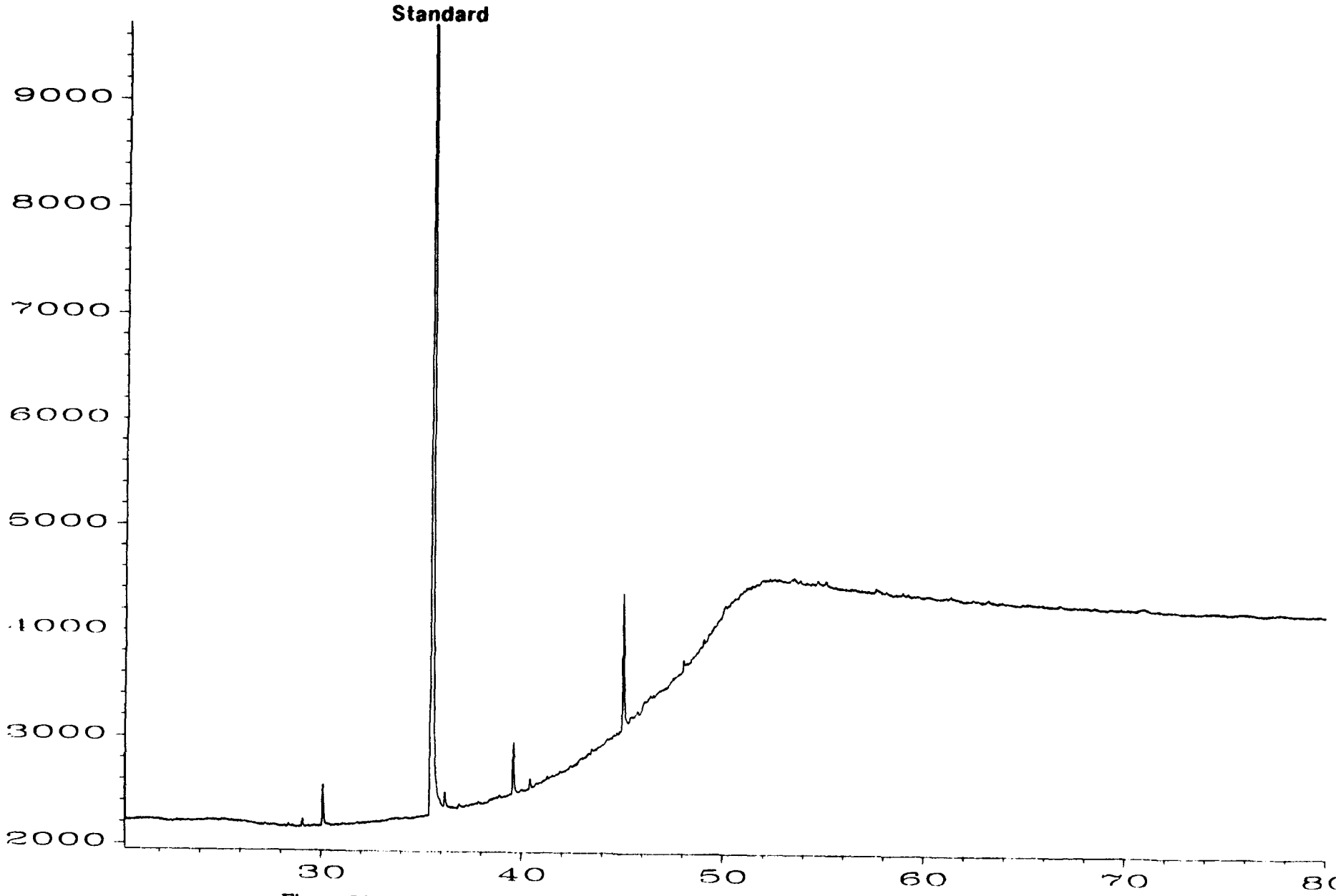

Figure 54. Partial GC chromatogram of the ketone fraction from liquid chromatography of the total lipid extract neutrals (10-12 cm depth).

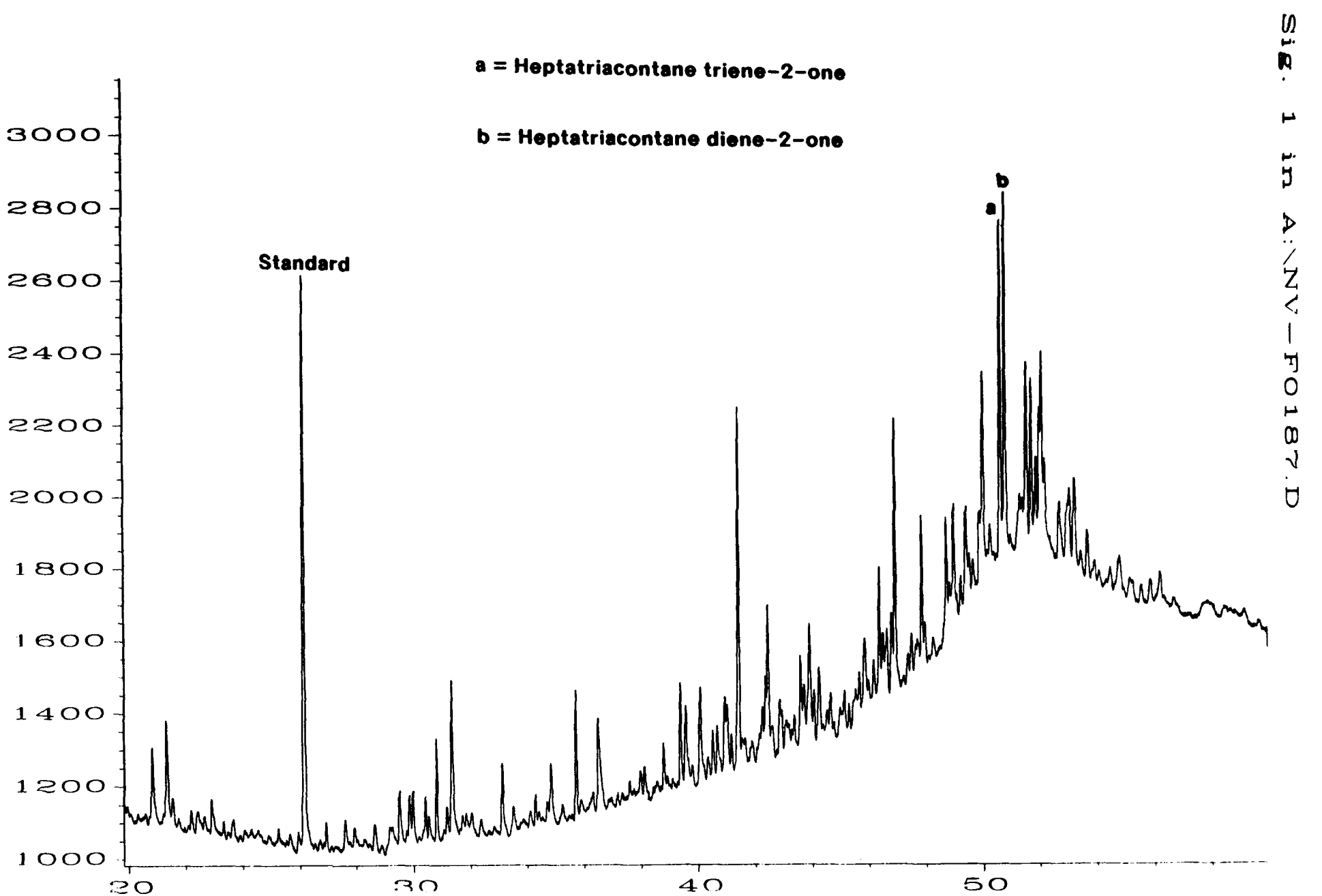

Figure 55. Partial GC chromatogram of the ketone fraction from liquid chromatography of the total lipid extract neutrals (14-18 cm depth).

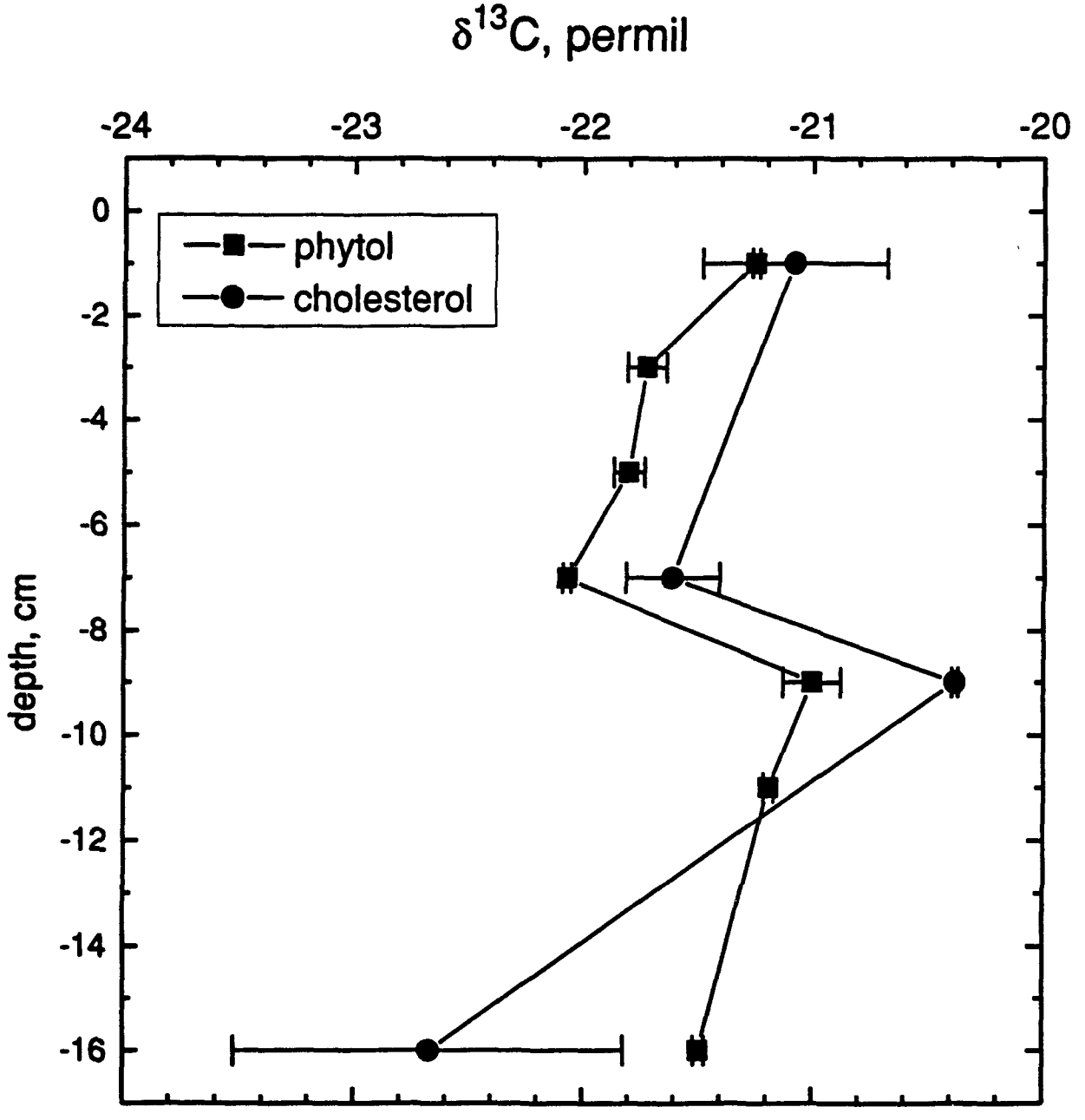

Figure 56. Stable carbon isotopic composition ($\delta\ ^{13}C$) of phytol and cholesterol as a function of depth in the core from Santa Barbara Basin.

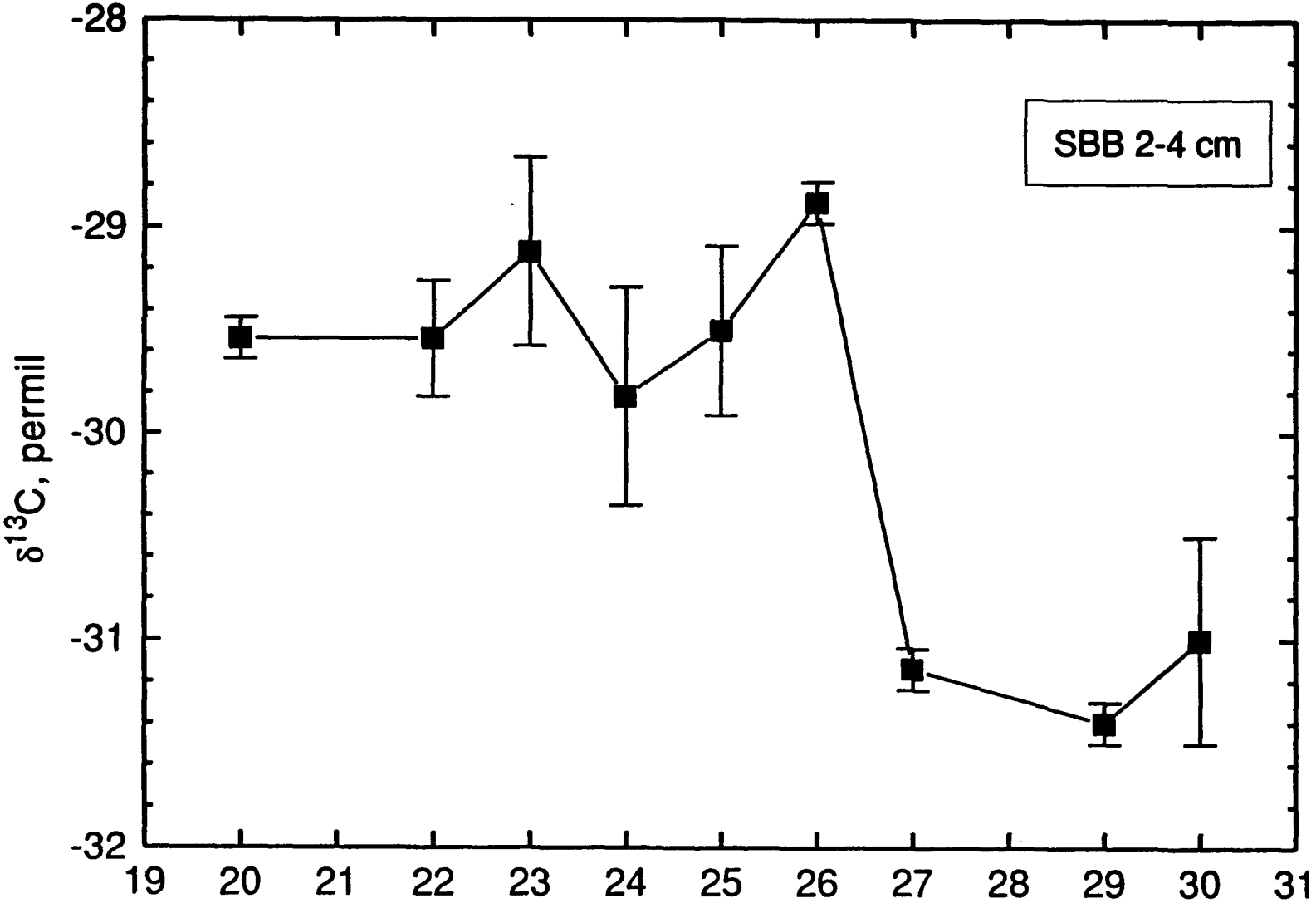

Figure 57. Stable carbon isotopic composition ($\delta\ ^{13}C$) of various n-alkanes from the 2-4 cm depth in the core from Santa Barbara Basin.

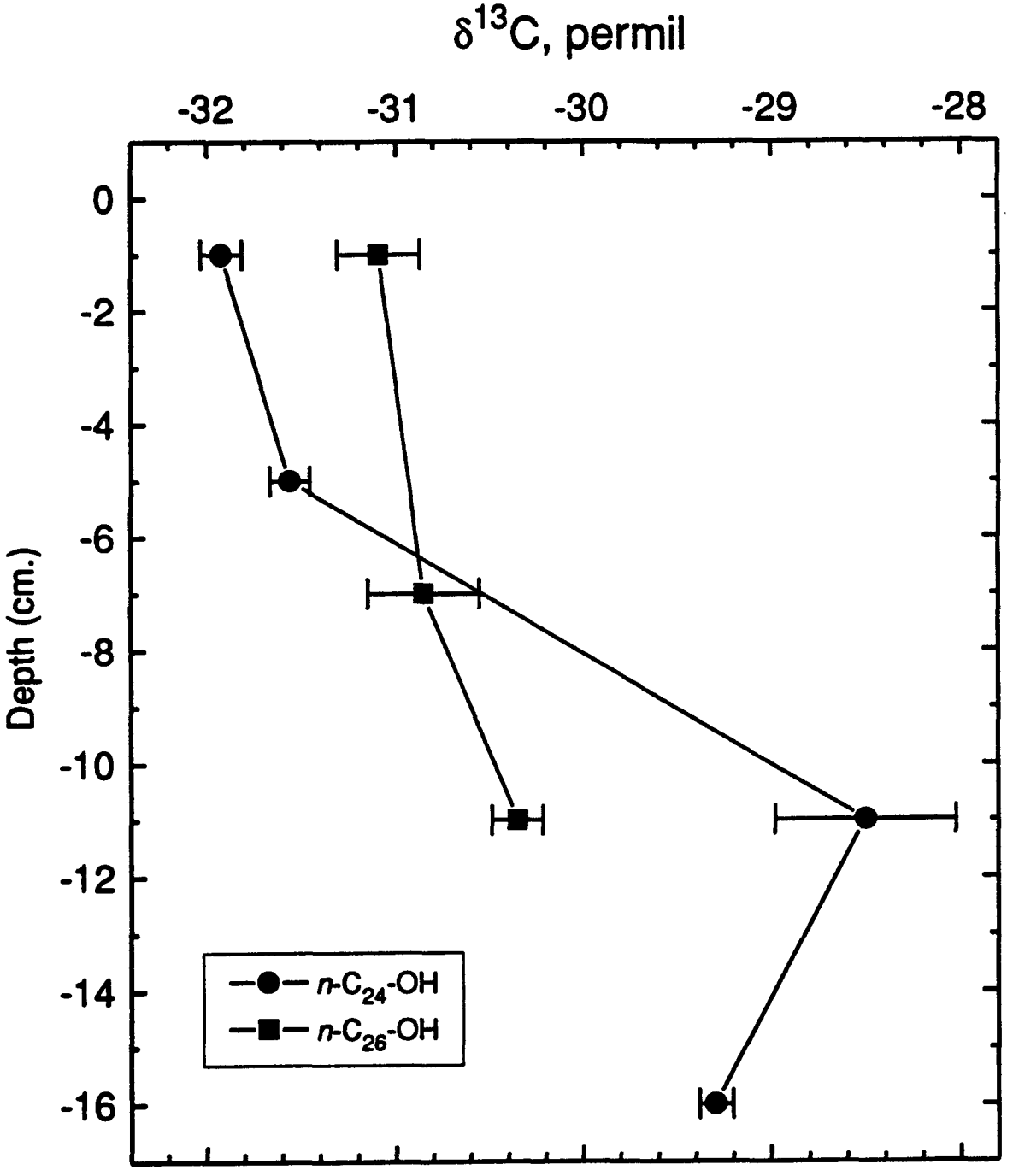

Figure 58. Stable carbon isotopic composition ($\delta^{13}C$) of the alcohols n-C24 and n-C26 as a function of depth in the core from Santa Barbara Basin.

Proposed Mechanism For Sulfurization of Lipids

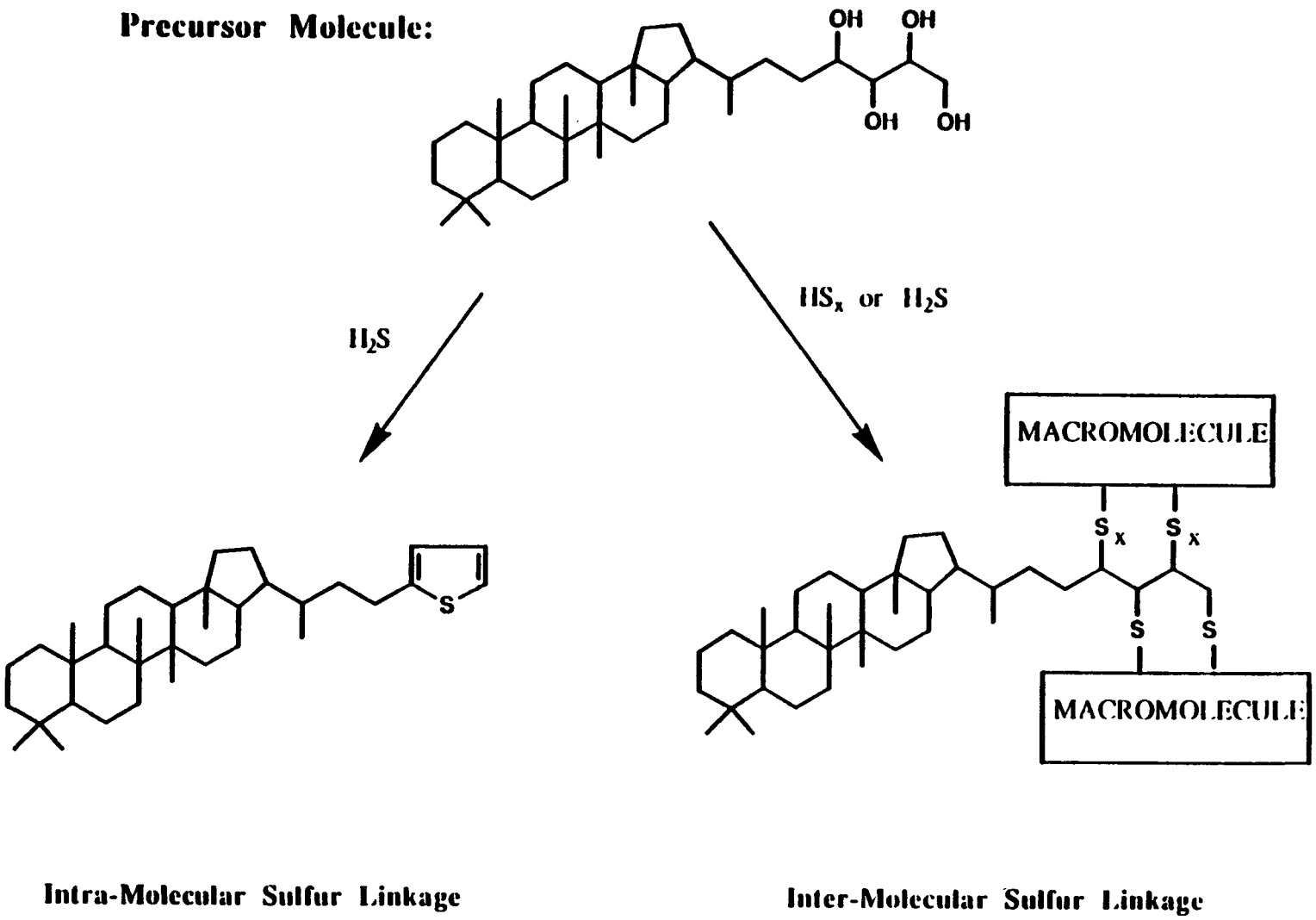

Figure 59. Proposed scheme by Kohnen et al. (1991) showing the relationship between sulfurized lipids found in bituminous shales and oils and the precursor carbon skeleton of hopanetetrol found in modern sediments.

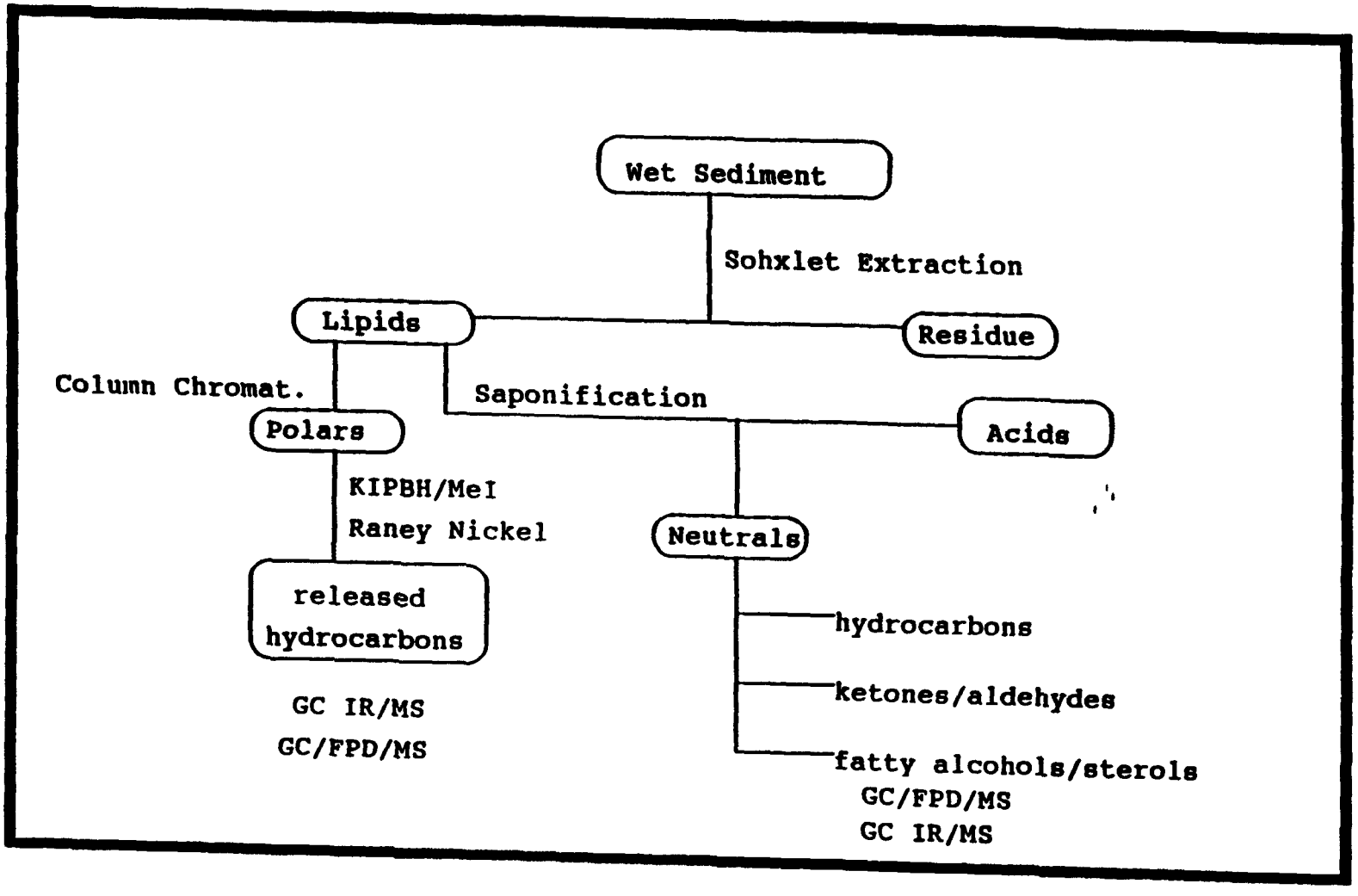

Figure 60. Analytical protocolfor the characterization of sulfur-vulcanized, extractable macromolecular organic matter.

Total Ion Counts From GC/MS of Unhydrogenated, Raney Nickel Cleaved Hydrocarbons

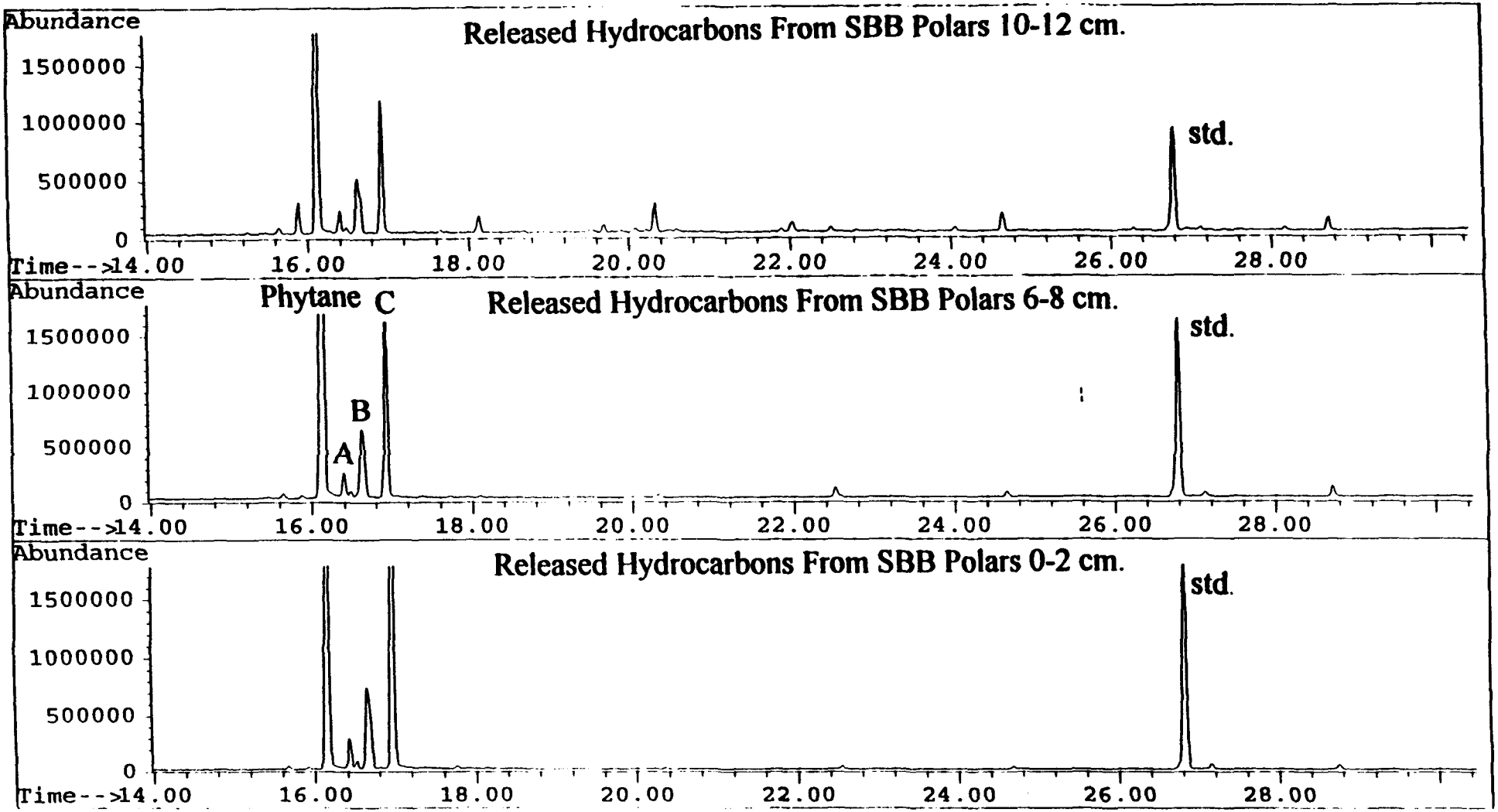

Figure 61. Total ion chromatograms of the hydrocarbons released from the extractable lipids from Santa Barbara Basin sediments by Raney nickel.Phytane plus three groups of phytenes (A,B,C) are labeled for the three sediment depths.

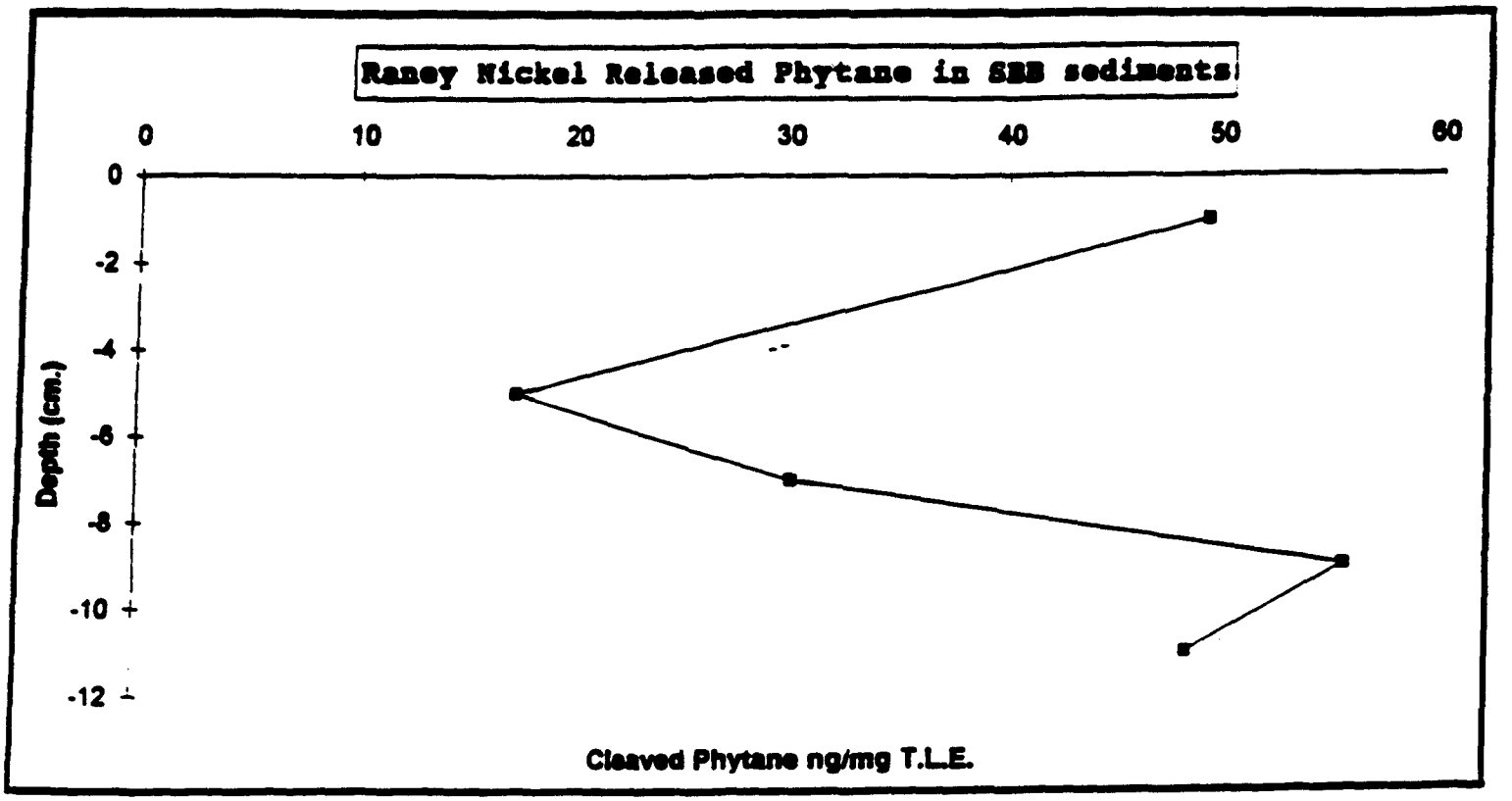

Figure 62. Phytane released from the extractable macromolecular fraction of the TLE in the Santa Barbara Basin sediments.

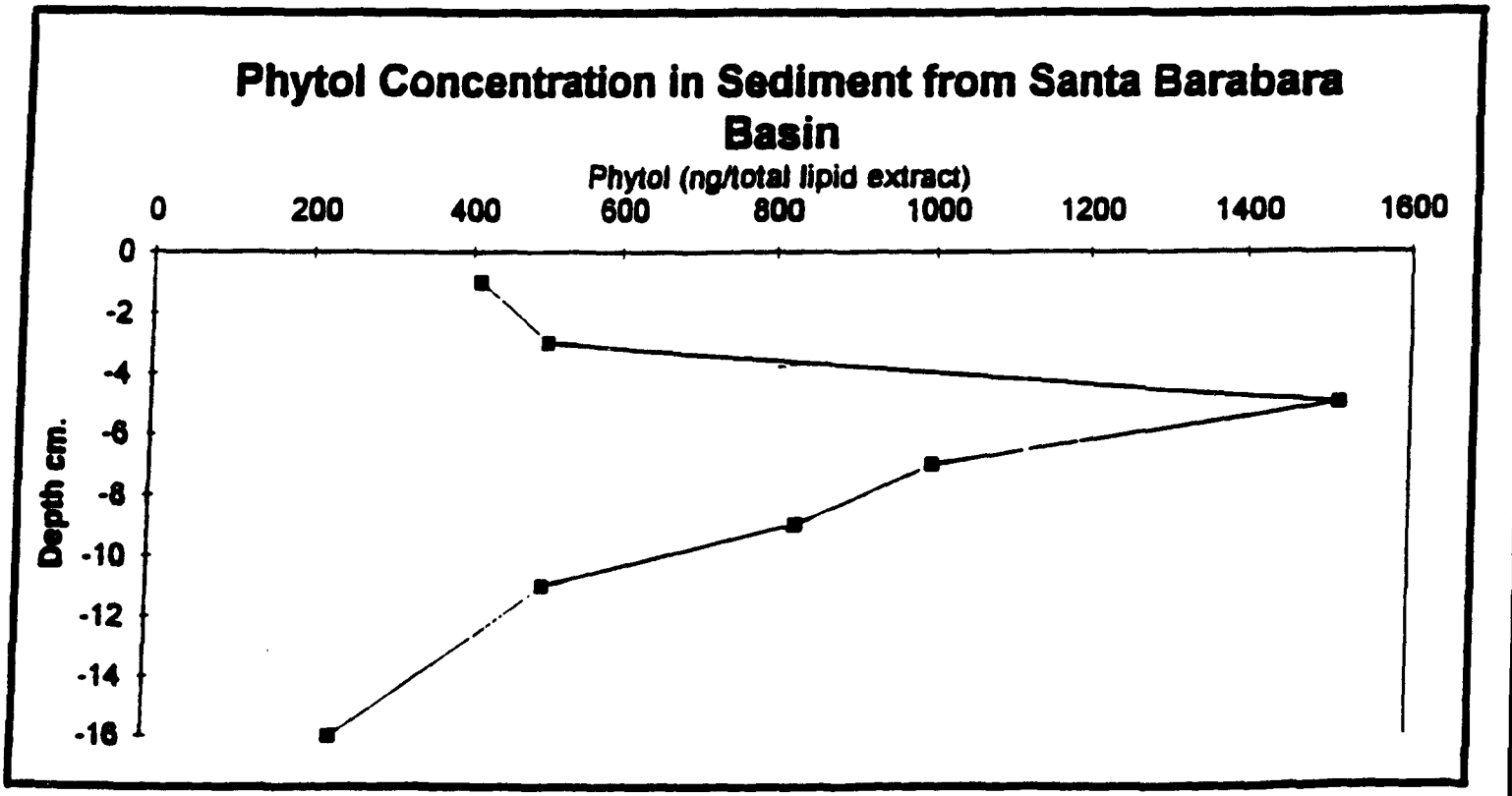

Figure 63. Phytol concentration in the total lipid extract with depth in the Santa Barbara Basin sediments.